ALEXANDRE SANTUCHI DA CUNHA

Study of degradation kinetics of chlorinated phenolic compounds catalyzed by soybean peroxidase

São Paulo

2023

ALEXANDRE SANTUCHI DA CUNHA

Study of degradation kinetics of chlorinated phenolic compounds catalyzed by soybean peroxidase

Corrected Version

Thesis presented to the Polytechnic School of the University of São Paulo to obtain the degree of Doctor of Science.

Concentration area: Chemical Engineering

Advisor: Prof. Dr. Ardson dos Santos Vianna Junior

Co-advisor: Prof. Dr. Enzo Laurenti

São Paulo

2023

Este exemplar foi revisado e corrigido em relação à versão original, sob responsabilidade única do autor e com a anuência de seu orientador.

São Paulo, 31 de janeiro de 2023

Assinatura do autor: Alexandre Santuchi da Cunha

Assinatura do orientador: Cesar de Oliveira Jr.

Catalogação-na-publicação

Cunha, Alexandre Santuchi da
Study of degradation kinetics of chlorinated phenolic compounds catalyzed by soybean peroxidase / A. S. Cunha -- versão corr. -- São Paulo, 2023.
124 p.

Tese (Doutorado) - Escola Politécnica da Universidade de São Paulo. Departamento de Engenharia Química.

1.Degradação Enzimática 2.Enzimas 3.Cinética 4.Peroxidase de Soja 5.Modelagem e Simulação I.Universidade de São Paulo. Escola Politécnica. Departamento de Engenharia Química II.t.

ALEXANDRE SANTUCHI DA CUNHA

Study of degradation kinetics of chlorinated phenolic compounds catalyzed by soybean peroxidase

Corrected Version

Thesis presented to the Polytechnic School of the University of São Paulo to obtain the degree of Doctor of Science.

São Paulo
2023

Name: CUNHA, Alexandre Santuchi da

Title: Study of degradation kinetics of chlorinated phenolic compounds catalyzed by soybean peroxidase

Thesis presented to the Polytechnic School of the University of São Paulo to obtain the degree of Doctor of Science.

Approved in:

Examination Board

Prof. Dr. _____

Institution: _____

Judgment: _____

Prof. Dr. _____

Institution: _____

Judgment: _____

Prof. Dr. _____

Institution: _____

Judgment: _____

Prof. Dr. _____

Institution: _____

Judgment: _____

Prof. Dr. _____

Institution: _____

Judgment: _____

DEDICATION

To my father José Vicente da Cunha (in memoriam)

To my grandmother Maria Paquiela da Cunha (in memoriam)

To my grandmother Marlene Costa Santuchi (in memoriam)

To my mother Dayse Santuchi da Cunha and my brother Vinicius Santuchi da Cunha

ACKNOWLEDGMENTS

First, my sincere and special thanks to my advisor Professor Ardson dos Santos Vianna Junior for the opportunity to carry out my doctorate under his supervision, and for the great experience, learning, and friendship during this time.

Thank you very much to Professor Enzo Laurenti and his family for all the support during my stay in Italy, and also for all the colleagues from the laboratory of the Department of Chemistry of the University of Turin, especially for Monica Rigoletto, who welcomed me very well and made this experience amazing.

Thank you very much to all my colleagues and friends from the Department of Chemical Engineering of the University of São Paulo who were part of this journey. Special thanks to Professor Galo Antonio Carrillo Le Roux for friendship and support. Special thanks to Priscila Marques da Paz and Thamiris Guerra Giacon, who became friends for life.

Thank you very much to all my family and friends for all the love and support. Thanks for my mother Dayse Santuchi da Cunha and my brother Vinicius Santuchi da Cunha, who are always present even from miles away. Special thanks to Sérgio Bassi and Luigi, who are always by my side all the time. You are my reason to carry on.

This study was financed in part by the Coordenação de Aperfeiçoamento de Pessoal de Nível Superior - Brasil (CAPES) - Finance Code 001.

“In theory there is no difference between theory and practice. In practice there is.” (Benjamin Brewster)

ABSTRACT

CUNHA, Alexandre Santuchi da. **Study of degradation kinetics of chlorinated phenolic compounds catalyzed by soybean peroxidase**. 2022. 126 f. Tese (Doutorado) - Departamento de Engenharia Química, Escola Politécnica, Universidade de São Paulo, São Paulo, 2022.

Soybean peroxidase is a Fe(III)-heme enzyme that can be extracted from soybean seed hulls and has the potential to catalyze the oxidation of some substrates in the presence of hydrogen peroxide. In this research, the degradation of 2,4,6-trichlorophenol, triclosan, and bisphenol-A catalyzed by soybean peroxidase is studied. These substrates are potential pollutants in many industrial and urban effluents, and the assimilation of these substances in large quantities can cause serious health problems. However, the products of their degradation usually show less toxicity than the reagents, being in this case a promising and environmentally friendly industrial effluent remediation method. The main objective of this work is to understand enzymatic degradation kinetics through modeling and simulation performed in MATLAB R2015a, and experiments carried out in a Syrris 250 μL microreactor and in batch. Soybean peroxidase was extracted and purified from the soybean seed hulls, to be used in degradation reactions as well as the commercial horseradish peroxidase enzyme. The reaction products were analyzed and quantified through HPLC-UV, and toxicological tests on the reaction mixture both before and after the reaction were also carried out. Different assumptions for the kinetic model were evaluated, and the simulations were compared to experimental data. The results showed the potential of the soybean peroxidase enzyme in degrading chlorinated phenolic components even in a reaction medium with more than one substrate, and that the modified bi-bi ping-pong model can satisfactorily represent the experimental data set. Therefore, a better comprehension of the reaction mechanism can be achieved, contributing to a more accurate reactor project and process simulation of enzymatic reactions.

Keywords: Enzymatic Degradation. Enzymes. Kinetics. Soybean Peroxidase (SBP). Modeling and Simulation.

RESUMO

CUNHA, Alexandre Santuchi da. **Study of degradation kinetics of chlorinated phenolic compounds catalyzed by soybean peroxidase**. 2022. 126 f. Tese (Doutorado) - Departamento de Engenharia Química, Escola Politécnica, Universidade de São Paulo, São Paulo, 2022.

A peroxidase de soja é uma enzima Fe(III)-heme que pode ser extraída da casca da semente de soja e tem o potencial de catalisar a oxidação de alguns substratos na presença de peróxido de hidrogênio. Nesta pesquisa, estuda-se a degradação do 2,4,6-triclorofenol, triclosan e bisfenol-A catalisada pela peroxidase de soja. Esses substratos são potenciais poluentes em muitos efluentes industriais e urbanos, e a assimilação dessas substâncias em grandes quantidades pode causar sérios problemas à saúde. No entanto, os produtos de suas degradações geralmente apresentam menor toxicidade do que os reagentes, sendo neste caso um método de remediação de efluentes industriais promissor e ecologicamente correto. O objetivo principal deste trabalho é compreender a cinética de degradação enzimática por meio de modelagem e simulação realizada em MATLAB R2015a, e experimentos conduzidos em um microrreator Syrris de 250 μL e em batelada. A peroxidase de soja foi extraída e purificada a partir da casca da semente de soja, para ser utilizada em reações de degradação assim como a enzima peroxidase de rábano comercial. Os produtos da reação foram analisados e quantificados por HPLC-UV, e também foram realizados testes toxicológicos antes e depois da reação. Diferentes hipóteses para o modelo cinético foram avaliadas e as simulações foram comparadas com dados experimentais. Os resultados mostraram o potencial da enzima peroxidase de soja em degradar componentes fenólicos clorados mesmo em um meio reacional com mais de um substrato, e que o modelo bi-bi ping-pong modificado pode representar satisfatoriamente o conjunto de dados experimentais. Assim, o mecanismo de reação pode ser melhor compreendido, contribuindo para um projeto de reator mais preciso e simulação de processos de reações enzimáticas.

Palavras-chave: Degradação Enzimática. Enzimas. Cinética. Peroxidase de Soja. Modelagem e Simulação.

LIST OF FIGURES

LIST OF TABLES

List of Abbreviations and Acronyms

Acronym	Description
4-AAP	4-Aminoantipyrine
APX	Ascorbate Peroxidase
BDF	Backward Differentiation Formula
BPA	Bisphenol A
DAE	Differential-Algebraic Equations
DMAB	3-(dimethylamino)benzoic acid
EDC	Endocrine Disrupting Compound
His	Histidine
HPLC	High-Performance Liquid Chromatography
HRP	Horseradish Peroxidase
LiP	Lignin Peroxidase
MBTH	3-methyl-2-benzothiazolinone hydrazone
Met	Methionine
MnP	Manganese Peroxidase
ODE	Ordinary Differential Equation
OF	Objective Function
PEG	Polyethylene glycol
RMSE	Root Mean Square Error
SBP	Soybean Peroxidase
SEM	Scanning Electron Microscope
TCP	2,4,6-Triclorophenol
TCS	Triclosan
Trp	Tryptophan
WLS	Weighted Least Squares

LIST OF SYMBOLS

Symbol	Description
A	Substrate 1
B	Substrate 2
CpI	Compound I; First enzyme oxidized intermediate
CpII	Compound II; Second enzyme oxidized intermediate
CpIII	Compound III; Third enzyme oxidized intermediate
$CpI \cdot H_2O_2$	Compound I complex with H_2O_2
E	Enzyme
E·A	Enzyme complex with substrate A
E-P	Modified form of the enzyme
E-P·B	Enzyme modified form complex with substrate B
E·S	Enzyme-substrate complex
G	Gibbs free energy
k_i	Kinetic constant of direct reaction i
k_{-i}	Kinetic constant of reverse reaction $-i$
k_{cat}	Catalytic constant
K_M	Apparent equilibrium constant
K_s	Turnover number of an enzyme
L	Pathlength
m	Number of experiments
n	Number of experimental points
p	Number of model parameters
P	Product
P-670	Inactive form of enzyme called verdohemoprotein
Q	Product

To be continued

Continuation

Symbol	Description
R^2	Coefficient of determination
$R^2_{adjusted}$	Adjusted coefficient of determination
RZ	Reinheitszahl
S	Substrate
$t_{residence}$	Residence time
u_i	Experimental data
$\overline{u}_i$	Average of experimental data
$\widehat{u}_i$	Value predicted by the model
v	Reaction rate
v_{max}	Maximum reaction rate
ε	Molar absorptivity
λ	Wavelength
σ	Standard deviation

SUMMARY

CHAPTER 1
INTRODUCTION

1.1 CONTEXTUALIZATION

Chemical processes are designed to economically produce a particular product from a variety of raw materials and through successive processing steps. The chemical processing step is considered the main part of the process and is responsible for its success or failure (LEVENSPIEL, 1999). They also take into account the design of reactors and reaction systems, which can become quite complex and create a challenging scenario for process modeling. Chemical kinetics and reactor design are the heart of almost all industrial chemicals, and it is mainly their knowledge that distinguishes the chemical engineer from other engineers (FOGLER, 2016).

Chemical reaction engineering principles can be applied in many areas, both laboratory and industrial scales, such as waste treatment, microelectronics, nanoparticles, and living systems, in addition to the more traditional areas of chemical, petrochemical, and pharmaceutical manufacturing (FOGLER, 2016). Like conventional reactors, microreactors are equipment that allow chemical reactions to occur, but in micrometer dimensions. Currently, these technologies have been the target of increasing studies due to their application in several areas such as biological, chemical, pharmaceutical, and environmental (LAURENTI; VIANNA JR, 2016).

Among these areas of study, the environmental area has been the main focus, due to the impacts of industries and the consequent concerns about sustainability issues nowadays. Environmental degradation caused by the action of industries occurs because of several pollutants constantly generated, such as compounds with amines and phenols in their structure. Some chemical methods, such as advanced oxidation techniques, have been adopted for treating such effluents, but they have limited success for commercial scales. One possible alternative is the use of enzymes as catalysts in the degradation reactions of these compounds, mainly due to their specificity. One of the advantages of this type of bioremediation is the possibility to perform it at a low cost compared to conventional techniques (COSTA et al., 2020).

1.2 MOTIVATION

Enzymes can be defined as organic substances that act as biological catalysts, decreasing the activation energy of a chemical reaction under mild environmental conditions and with high efficiency. They can be obtained from renewable resources, which is an advantage over traditional chemical catalysts. They act specifically on a substrate or a group of substrates, so they can be used to modify specific components. Many authors state that soybean peroxidase (SBP, E.C. 1.11.1.7) shows a good potential in the degradation of organic pollutants (NISSUM et al., 2001; AL-ANSARI et al., 2011; STEEVENSZ et al., 2014).

SBP is a Fe(III)-heme enzyme that belongs to the oxidoreductase family, which oxidizes organic substrates using hydrogen peroxide as an electron acceptor. It can be harvested from soybean seed hulls, which can be processed in a sustainable and low-cost way (STEEVENSZ et al., 2014; CALZA et al., 2016; TOLARDO et al., 2019). The advantages of SBP compared to other enzymes are: it is cheaper than other enzymes used for the same application since it is a byproduct of the soybean processing industry; it is easier to obtain since a complex purification process is not required; it can operate at relatively high temperatures and over a wide pH range; it is less susceptible to irreversible inactivation by hydrogen peroxide and chemical or thermal denaturation; it is the most effective peroxidase (AL-ANSARI et al., 2011).

Substances such as 2,4,6-trichlorophenol (TCP), triclosan (TCS) and bisphenol A (BPA) can commonly appear as persistent pollutants in many industrial and urban effluents, recalcitrant to the common environmental degradation processes. TCP is used as antiseptics and pesticides in general (fungicides, herbicides, insecticides), and its consumption has been linked to lymphomas, leukemia, and liver cancer (GOWDA et al., 1985). TCS is a fungicidal and bactericidal agent which is part of the composition of soaps, toothpaste, deodorants, and medical skin creams. Consumption of TCS can contribute to the development of bacterial resistance and cause health problems (LI et al., 2016). BPA is a synthetic organic compound used in the manufacture of products like plastic food packaging, bottles, dental materials, and lacquers. Consumption of BPA can cause health problems such as testicular, prostate, and breast cancers and alteration of immune functions (YAMADA et al., 2010). However, the products of their degradation usually show less toxicity than the reagents, so the use of SBP can be a very promising and environmentally friendly industrial effluent remediation method. The ability of SBP was previously studied for the degradation of TCP (CALZA et al., 2014), TCS (LI et al., 2016), and BPA (KOBAYASHI et al., 1998; CAZA et al., 1999; WATANABE et al., 2011;

JIANG; ZHENG, 2013).

The reactions can be carried out in a microreactor, a suitable equipment for fast reactions such as those catalyzed by enzymes, which can be 10^3 to 10^{17} times faster than uncatalyzed reactions (FOGLER, 2016). They have similar functions compared to the conventional reactors but in micrometric dimensions. They have been used in studies in several areas such as biological, chemical and pharmaceutical. The main advantages of the use of microreactors are the strict control of the reaction conditions, safety in operation, improved mass and heat transfer, and energy efficiency (LAURENTI; VIANNA JR, 2016).

1.3 OBJECTIVES

The general objective of this thesis is to understand through modeling and experiments the enzymatic degradation kinetics using the enzyme SBP in the presence of hydrogen peroxide. One of the objectives is to carry out the procedures for extracting and purifying the SBP enzyme from soybean seed hulls. Then, another objective is to use the SBP enzyme produced as well as the commercial horseradish peroxidase (HRP) enzyme for degradation reactions of three different pollutants: TCP, TCS, and BPA. The degradations are studied both individually and in a mixture, aiming to evaluate the possible competition between the substrates. The reactions are performed both in batch and in the microreactor, and a specific objective is to show the effectiveness of this equipment in the reproducibility and repeatability of data obtained under different conditions. The reaction products are analyzed and quantified by HPLC-UV techniques. Finally, toxicological tests on the reaction mixture both before and after the reaction are also performed, to evaluate the environmental impact of the enzymatic treatment.

Currently, there is a lack in the literature of works with an approach more focused on the mathematical modeling of enzymatic degradation processes, and this is another major objective of this work. Then, the work aims to develop a model to satisfactorily represent the experimental data set obtained by several laboratory tests, and also to apply process optimization strategies and parameter estimation using computational tools.

Thus, this thesis is developed through computational activities, implementation models in MATLAB, as well as laboratory activities, which are performed in the laboratories of the Department of Chemical Engineering, Polytechnic School, University of São Paulo, and the Department of Chemistry, University of Turin.

1.4 CONTRIBUTIONS OF THIS THESIS

This doctoral thesis aims to contribute to the technical-scientific literature regarding the theme of "enzymatic degradation of industrial pollutants using soybean peroxidase", and its main contributions are:

- To carry out enzymatic degradation experiments in a microreactor, highlighting the importance of this equipment in the study of fast kinetics, conducting reactions under different conditions using the organic pollutants TCP and TCS and the commercial enzyme HRP;
- To carry out enzymatic degradation experiments in batch, under different reaction conditions, of the organic pollutants TCP, TCS, and BPA, both individually and in a mixture to evaluate the possible competition between the pollutants, using the produced SBP and the commercial HRP enzymes;
- To obtain a mathematical model that describes the process satisfactorily to be used for the simulation and parameter estimation of the enzymatic reactions proposed. There is a lack of studies in the literature with a strict mathematical approach to this subject.

1.5 THESIS STRUCTURE

In addition to this introduction, which presents an overall contextualization, motivation, objectives, and contributions of this work, this doctoral thesis is composed of other chapters and it is organized as follows:

Chapter 2: The fundamentals used throughout this work are presented, including concepts about enzymes, enzymes used in the removal of organic pollutants, the enzyme soybean peroxidase, chlorinated phenolic compounds, enzymatic kinetics and mechanism of peroxidases, as well as a brief background on modeling and simulation of processes and parameter estimation.

Chapter 3: A literature review of the processes involving enzymatic degradation and its specific approaches is performed, focusing mainly on the application of SBP for chlorophenols degradation, based on the main studies published on the proposed theme.

Chapter 4: The methodology used in this thesis is presented, including the development of the mathematical modeling of the kinetic reactions involving peroxidases, as well as the experimental procedures to be performed.

Chapter 5: The experimental results and the discussion are presented.

Chapter 6: The modeling and simulation results and the discussion are presented.

Chapter 7: The conclusions obtained and future works are presented.

Finally, all the bibliographic references consulted and cited throughout this thesis are presented, as well as the annexes.

This doctoral thesis was developed in the Postgraduate Program in Chemical Engineering of the Polytechnic School of the University of São Paulo, and it is part of the research area of Chemical Reaction Engineering, specifically in the line of Modeling and Simulation.

CHAPTER 2
FUNDAMENTALS

2.1 ENZYMES

Enzymes are organic substances considered biological catalysts because they have the function of increasing the velocity of a chemical reaction. In some cases, they are responsible for the generation of highly reactive free radicals that undergo a complex series of spontaneous cleavage reactions (VOET; VOET, 2011). They consist of proteins with high molecular weight and act on specific substrates to transform them chemically at a greatly accelerated rate, usually 10^3 to 10^{17} times faster than the uncatalyzed reaction rate. Without them, essential biological reactions would not feasibly take place to sustain life (FOGLER, 2016).

Enzymes are usually present in small quantities and are not consumed during the reaction, providing an alternate pathway for the reaction to occur. As well as chemical catalysts, they act by lowering the activation energy of the reaction, binding the transition state of the catalyzed reaction in preference to the substrate, as shown in Figure 2.1 (VOET; VOET, 2011). In this figure, G is the Gibbs free energy, A and B are the reagents, and P and Q are the products.

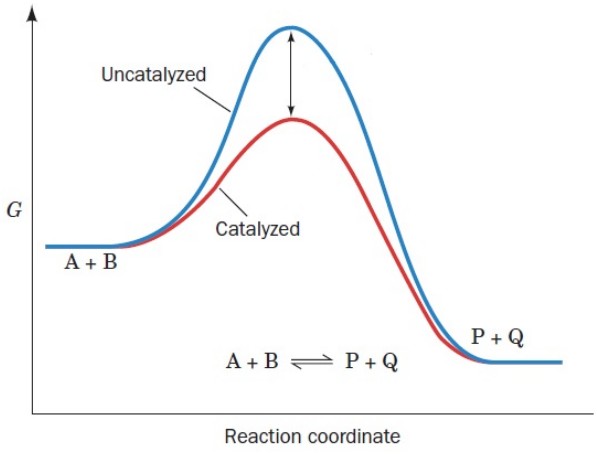

Figure 2.1 – The effect of a catalyst on the transition state diagram of a reaction.
Source: Voet and Voet (2011).

These biological catalysts are extremely versatile, carrying out such diverse reactions as hydrolysis, polymerization, functional group transfer, oxidation–reduction, dehydration, and isomerization. They are complex molecular machines that operate through a great diversity of mechanisms. Some enzymes act on only a single substrate molecule and others act on two or more different substrate molecules structurally related. Some enzymes form covalently bound intermediate complexes with their substrates, and others do not (VOET; VOET, 2011).

One of the advantages of using enzymes over traditional chemical catalysts is that they are obtained from renewable resources, that is, they are not easily depleted because they can be restored by natural processes. They operate in moderate temperature and pH conditions, usually resulting in excellent selectivity for both reagents and products, avoiding adding impurities, and reducing environmental impact. Enzymatic technology offers great potential to improve industrial performance and reduce cost, and significant savings in resources such as energy and water, bringing benefits to industry and the environment (CHERRY; FIDANTSEF, 2003).

The main particular feature of enzymatic reactions compared to other catalyzed reactions is the formation of an enzyme–substrate complex, which can be illustrated by the lock-and-key model, suggested by Emil Fischer in 1894, and the induced fit model, both shown in Figure 2.2. The first one has been preferred for many years, but it is not the most useful model and can be considered obsolete. The lock is believed to undergo some adjustment as the key reaches it, allowing the interaction between enzyme (E) and substrate (S) to form different product forms (P_1 and P_2). In the induced fit model both enzyme and substrate molecules are distorted, making the molecule more susceptible to rearrangement or attachment (FOGLER, 2016).

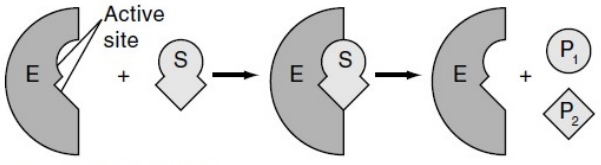

(a) Lock-and-key model.

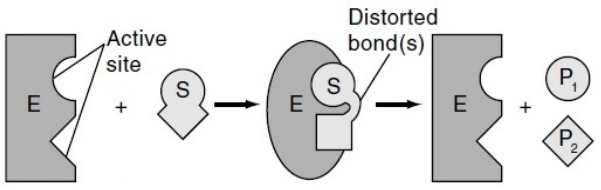

(b) Induced fit model.

Figure 2.2 – Enzyme–substrate interactions.
Source: Fogler (2016).

Enzymatic activity can be modulated through substances called enzyme inhibitors. Inhibitors are molecular agents that interfere with enzyme catalysis, slowing or stopping reactions. Their study may provide important information about enzymatic mechanisms and also define metabolic pathways. Enzymatic inhibition may be irreversible or reversible, and the three most common types of reversible inhibition are competitive, uncompetitive, and noncompetitive. A competitive inhibitor is usually a substrate-like molecule substance that competes for the same site on the enzyme. An uncompetitive inhibitor deactivates the enzyme-substrate complex, usually by binding to both the substrate and the enzyme molecules in the complex. Non-competitive inhibition is also known as mixed inhibition and occurs with enzymes containing at least two different types of sites. The substrate binds only to one type of site and the inhibitor binds only to the other to render the enzyme inactive (FOGLER, 2016).

Enzymatic systems fall into two traditional categories of processes, both chemical and biological, as they involve chemical reactions and catalytic and biological action. Because they have a highly species-specific action and compound class, enzymatic processes can be applied to specific environmental hazards. They are commonly used for the treatment of wastewater, which presents in its composition aromatic contaminants, and may undergo a degradation process (ANJANEYULU et al., 2005). This will be the main subject of the next section.

2.2 ENZYMES USED FOR THE REMOVAL OF ORGANIC POLLUTANTS

Removal of undesirable components from water can be classified into physical, chemical, and biological treatments. The physical processes include unit operations such as solid-liquid separations, screening, mixing, and adsorption. The chemical ones comprehend flocculants, chemical precipitation, oxidation, and advanced oxidation processes. The biological ones, in turn, involve biological oxidation, denitrification, anaerobic oxidation, and activated sludge process (TCHOBANOGLOUS et al., 2014). However, these treatments are not suitable for some recalcitrant effluents, such as aromatic and other complex molecules, then the enzymatic reactions should be used in these special cases (HUSAIN, 2010).

Sharma et al. (2018) presented a review on enzyme-based technologies for bioremediation, which covers all the treatments of soil and water polluted with hazardous environmental pollutants using enzymes. These technologies include genetic engineering, enzyme immobilization, and nanoenzymes. In the context of bioremediation, useful enzymes belong to oxidoreductases and hydrolases and their subdivisions, as shown in Table 2.1.

Table 2.1 – Enzymes used in bioremediation and their functions.

Enzyme classification	Examples	Functions
Oxidoreductases	Oxygenases	Catalyze oxidation of aromatic compounds by incorporating one or two atoms of oxygen.
	Laccases	Cleave ring present in aromatic compounds and reduce one molecule of oxygen in the water and produce free radicals.
	Peroxidases	Catalyze oxidation reaction in the presence of peroxides, such as hydrogen peroxide (H_2O_2), and generate reactive free radicals after oxidation of organic compounds.
Hydrolases	Lipases	Break triglycerol into glycerol and fatty acid; widely used for wastewater treatment, polyaromatic hydrocarbon degradation, etc.
	Cellulases	Break down complex cellulosic materials into simple sugars; commonly used in the treatment of agricultural residues such as cotton waste and rice straw.
	Carboxylesterases	Catalyze hydrolysis of carboxyl ester bond present in synthetic pesticides such as organophosphates.
	Phosphotriesterases	Catalyze hydrolysis of phosphotriesters, the main components of organophosphorus compounds used worldwide in pesticides.
	Haloalkane dehalogenases	Used for biodegradation of halogenated aliphatic compounds.

Source: Sharma et al. (2018).

2.2.1 Peroxidases

As the focus of this work is on enzymatic degradation using SBP, only peroxidase-type enzymes are focused here. The heme-containing peroxidases, in general, can be divided into two groups: one group found only in animals and the other group found in fungi, bacteria, and plants. The second one is further divided into 3 classes (SHARMA et al., 2018):

- **Class I**: intracellular enzymes including cytochrome-C peroxidase produced by yeast, ascorbate peroxidase (APX) produced by some species of plants, and bacterial catalase peroxidases.

- **Class II**: secreted fungal enzymes including lignin peroxidase (LiP) and manganese peroxidase (MnP).
- **Class III**: plant secreted peroxides such as soybean peroxidase (SBP) from soybean seed hulls and horseradish peroxidases (HRP) from horseradish plants.

Peroxidases in the presence of H_2O_2 catalyze the dehydrogenation of compounds such as phenols and amines following a modified bi-bi Ping-Pong mechanism, also known as the peroxidase mechanism (AL-ANSARI et al., 2011). This mechanism is covered in more detail in section 2.4.3. Although the peroxidases have been proposed for applications in several fields, few industrial processes utilize peroxidases. The commercial applications of these enzymes are limited to diagnosis and research (CUNHA et al., 2021). Unfortunately, the economic feasibility of peroxidase-based processes has not been always assessed (TORRES; AYALA, 2010). In this context, in recent years SBP has been the focus of research, due to its great availability and other factors discussed in the next subsection.

2.2.2 Soybean Peroxidase

SBP (Enzyme Classification 1.11.1.7) is an enzyme that can be extracted from the hull of the seed *Glycine max* (Protein Database ID: 1FHF) (HENRIKSEN, 2001; GILLIKIN; GRAHAM, 1991). This enzyme can be applied in wastewater treatments containing phenolic compounds, which are present in various industries (STEEVENSZ et al., 2014). Kamal and Behere (2002) published the three-dimensional crystal structure of SBP, as shown in Figure 2.3:

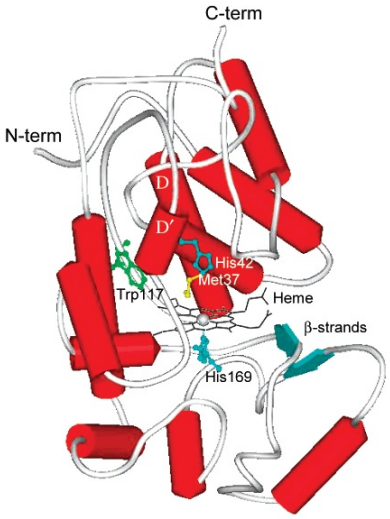

Figure 2.3 – SBP schematic from the crystallographic study.
Source: Kamal and Behere (2002).

The authors observed that SBP has an overall protein structure strikingly similar to HRP, with a degree of sequence similarity of 57%. Their common features include Fe(III) protoporphyrin IX (heme) as the prosthetic group, catalytic mechanism, conserved catalytic residues, four disulfide bonds, two Ca^{2+} binding sites located distal and proximal to the heme, eight glycans, and a single tryptophan (Trp117). SBP structure is also formed by other amino acids like methionine (Met37) and histidines (His42 and His169), and its molecular mass is approximately 37 kDa (KAMAL; BEHERE, 2002).

The advantages of SBP compared to other enzymes are (AL-ANSARI et al., 2011):

- SBP is cheaper than other enzymes used for the same application as laccases and HRP since it is a byproduct of the soybean processing industry;
- SBP covers a wide range of substrates;
- SBP can be used over a wide range of pH;
- SBP can operate at high temperatures (being active at 70ºC);
- SBP is less susceptible to irreversible inactivation by H_2O_2 compared to HRP;
- SBP is the most effective peroxidase, as judged by its specificity constant (k_{cat}/K_M).

It is worth mentioning that there is a large availability of soybean in Brazil since it is the largest soybean producer in the world (Table 2.2):

Table 2.2 – World Soybean Production (Harvest 2021/2022).

Country	Production (million tons)	Planted area (million hectares)	Productivity (kg/ha)
USA	121.528	34.929	3.480
Brazil	**123.829,5**	**40.921,9**	**3.026**
World	355.588	130.935	-

Source: EMBRAPA (2022).

2.3 CHLORINATED PHENOLIC POLLUTANTS

In this work, the enzymatic degradation of some pollutants is studied, including the chlorinated phenolic compounds 2,4,6-trichlorophenol (TCP) and triclosan (TCS), and also bisphenol A (BPA), which is not a chlorinated compound but is an important substrate for enzymatic degradation studies (WATANABE et al., 2011; JIANG; ZHENG, 2013). The degradation of these pollutants is also studied in a medium with a mixture of them, to evaluate a scenario closer to a real application where there is a possible competition in their degradation.

2.3.1 2,4,6-Trichlorophenol (TCP)

TCP has the molecular formula $C_6H_3Cl_3O$ and belongs to the group of organochlorines called chlorophenols. This compound is used in the manufacturing of antiseptics, pesticides in general (bactericides, fungicides, herbicides, germicides insecticides), and wood and glue preservatives (GOWDA et al., 1985; AI et al., 2021). TCP is a common chemical intermediate and can often appear as a pollutant in many industrial effluents as a byproduct of water chlorination and combustion processes. It is considered a priority pollutant of aquatic environments in many countries and has already been found in freshwater lakes (ZHANG et al., 2018).

It can also appear in the water supply as a result of hydrolysis of chlorinated benzene contaminants. Exposure to humans can thus occur by the ingestion of such waters, and the consumption of TCP has been linked to lymphomas, leukemia, and liver cancer (GOWDA et al., 1985). It has been considered a priority pollutant listed in the United States Environmental Protection Agency and in the Drinking Water Contaminant Candidate List, and also classified as a carcinogenic substance by International Agency for Research on Cancer (FERRARI et al., 1999; ZHANG et al., 2018; AI et al., 2021). Therefore, there is great interest in studying alternatives for the decomposition of this major pollutant.

TCP can exist in unionized and ionized forms in water according to the chemical equilibrium shown in Figure 2.4:

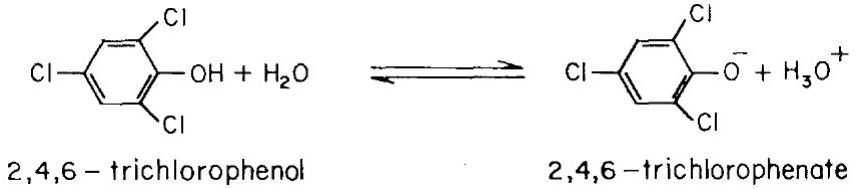

Figure 2.4 – Ionization of TCP in water.
Source: Gowda et al. (1985).

2.3.2 Triclosan (TCS)

TCS, or 5-chloro-2-(2,4-dichlorophenoxy)phenol, is a substance with molecular formula $C_{12}H_7Cl_3O_2$ and belongs to the group of polychlorinated phenoxyphenols. It is a fungicidal and bactericidal agent, with a slightly aromatic odor, used in the manufacture of personal care products such as soaps, toothpaste, deodorants, and medical skin creams (LI et al., 2016). This pollutant has already been found in many water matrices such as rivers, natural streams, maritime

environments, and drinking water tanks (BILAL et al., 2020). Consumption of large amounts of TCS can contribute to the development of bacterial resistance and cause health problems as it is a precursor of several highly harmful metabolites such as chlorinated dioxins and methyl triclosan (LI et al., 2016). For this reason, understanding the degradation of this substance is of great importance. Possible intermediate radicals of TCS are shown in Figure 2.5.

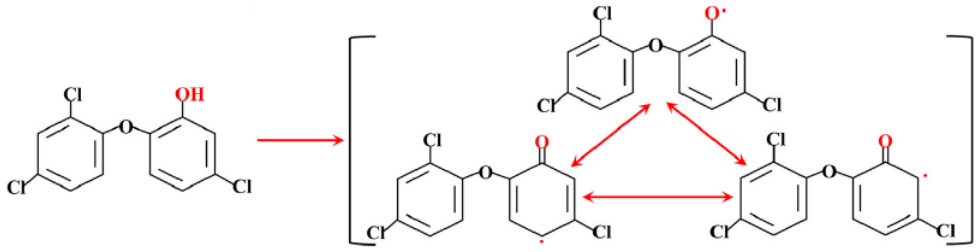

Figure 2.5 – Radical intermediates of TCS.
Source: Bilal et al. (2020).

2.3.3 Bisphenol A (BPA)

BPA, or 2,2-bis(hydroxyphenyl)propane, is a synthetic organic compound with molecular formula $C_{15}H_{16}O_2$. This substance is widely used as raw material for epoxy and polycarbonate resins in the manufacture of plastic food packaging, bottles, dental materials, and lacquers, and it is also used for coating concrete and steel tanks and pipes used in the water supply system, causing the deposition of BPA in drinking water (HUANG; WEBER JR, 2005). This is the reason why BPA is a common industrial pollutant that can be found in many water sources and wastewaters worldwide (HONGMEI; NICELL, 2011).

BPA is an anthropogenic compound suspected to be an endocrine disrupting compound (EDC) (ESCALONA et al., 2015). Exposure to BPA can cause testicular, prostate, and breast cancers, reduction in human sperm counts, feminization of organisms, alteration of immune functions, and decreased fertility in birds, fish, and mammals (YAMADA et al., 2010). Many countries proposed legislation to ban BPA in baby bottles and food packages (JIANG; ZHENG, 2013). Alternatives for efficient removal of this pollutant from the water are of great interest.

2.4 ENZYMATIC KINETICS

In this section, the fundamentals of enzymatic kinetics are described, which serve as a basis for the model development.

Enzyme kinetics is the study of the velocity, activity, and selectivity of the formation products, as well as the factors that influence it, such as pH, temperature, concentrations of reagents, enzymes, activators, inhibitors, and may also be the target of studies for control, optimization processes and the design of the most suitable equipment (reactors). The efficiency of the enzyme as a catalyst can be explained by its activity, determined by the reaction rate. The enzymatic activity corresponds to the amount of enzyme that catalyzes the product formation per unit of time (BORZANI et al., 2001).

2.4.1 Michaelis-Menten classic model

Enzymatic reactions are usually described by the classic model proposed by Michaelis-Menten, where a final product (P) is formed from the substrate (S), and the enzyme (E) is regenerated without changing its characteristics, via an enzyme-substrate complex (E·S), as represented on Equation 2.1 (FERSHT, 1999):

$$\mathrm{E} + \mathrm{S} \underset{k_{-1}}{\overset{k_1}{\rightleftharpoons}} \mathrm{E}\cdot\mathrm{S} \overset{k_2}{\rightarrow} \mathrm{E} + \mathrm{P} \tag{2.1}$$

The general expression for the reaction velocity (rate) is:

$$v = \frac{\mathrm{d}[\mathrm{P}]}{\mathrm{dt}} = k_2[\mathrm{E}\cdot\mathrm{S}] \tag{2.2}$$

It can be shown (FERSHT, 1999) that the reaction rate equation is given by:

$$v = \frac{v_{max}[\mathrm{E}_0][\mathrm{S}]}{K_M + [\mathrm{S}]} \tag{2.3}$$

where:

$$v_{max} = k_{cat}[\mathrm{E}_0] = k_2[\mathrm{E}_0] \tag{2.4}$$

$$K_M = \frac{k_2 + k_{-1}}{k_1} \tag{2.5}$$

Equation 2.3 is known by the Michaelis-Menten equation, and it shows that v is directly proportional to the total amount of enzyme, $[\mathrm{E}]_0$, but it follows saturation kinetics concerning the concentration of substrate towards a limiting maximum reaction rate, v_{max}, as shown on

Figure 2.6. The parameters k_{cat} and K_M are the catalytic constant and the apparent equilibrium constant of the reaction, respectively. K_M represents the substrate concentration necessary to achieve one-half of v_{max}. The k_{cat}/K_M ratio is called the "specificity constant" and is an important parameter for enzymatic reactions because it relates the catalytic efficiency of the enzyme to its affinity for the substrate (FERSHT, 1999).

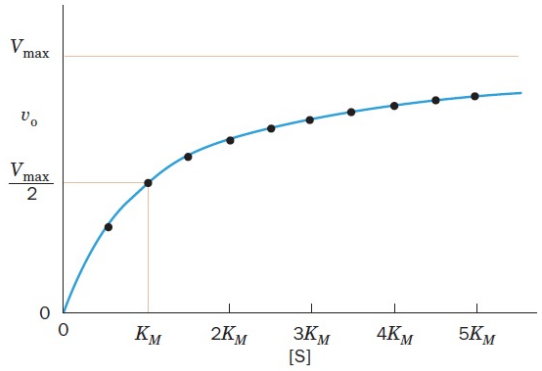

Figure 2.6 – Michaelis–Menten plot.
Source: Voet and Voet (2011).

There are several methods to determine the Michaelis-Menten parameters v_{max} and K_M, but the most used was formulated by Hans Lineweaver and Dean Burk, which considers the inverse of the Equation 2.3 and is given by:

$$\frac{1}{v} = \left(\frac{K_M}{v_{max}}\right)\frac{1}{[\mathrm{S}]} + \frac{1}{v_{max}} \tag{2.6}$$

This equation is linear in $1/v$ and $1/[\mathrm{S}]$, and can be plotted as shown in Figure 2.7, where the parameters can be obtained by the slope and intercept of this plot.

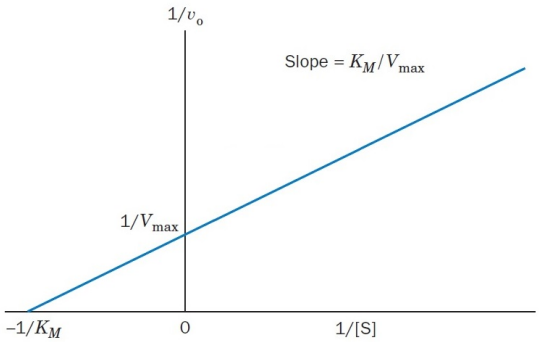

Figure 2.7 – Lineweaver-Burk plot for Michaelis-Menten model.
Source: Voet and Voet (2011).

2.4.2 Ping-Pong mechanism

The literature states that not all the enzymatic reactions follow the Michaelis-Menten classic model (NICELL; WRIGHT, 1997; NISSUM et al., 2001; AL-ANSARI et al., 2011; STEEVENSZ et al., 2014). Sometimes it happens because the reaction involves more than one substrate, and it can occur in a sequential mechanism, where all substrates react with the enzyme before the first product is formed, or in a Ping-Pong mechanism, where one or more products are generated before all substrates interact with the enzyme. However, peroxidases follow the Ping-Pong mechanism, taking into account the consumption of two substrates and the formation of two products, being called in this case Bi-Bi Ping Pong mechanism (FERSHT, 1999; VOET; VOET, 2011). Ping-Pong and sequential mechanisms for enzymatic reactions involving two substrates can be differentiated by steady-state reaction kinetics analysis using the procedures described by Cleland (1963b).

The general Bi-Bi Ping-Pong mechanism is represented below (FERSHT, 1999):

$$\mathrm{E} + \mathrm{A} \underset{k_{-1}}{\overset{k_1}{\rightleftharpoons}} \mathrm{E}\cdot\mathrm{A} \underset{k_{-2}}{\overset{k_2}{\rightleftharpoons}} \mathrm{E}\text{–}\mathrm{P} + \mathrm{Q} \tag{2.7}$$

$$\mathrm{E}\text{–}\mathrm{P} + \mathrm{B} \underset{k_{-3}}{\overset{k_3}{\rightleftharpoons}} \mathrm{E}\text{–}\mathrm{P}\cdot\mathrm{B} \overset{k_4}{\rightarrow} \mathrm{E} + \mathrm{P} \tag{2.8}$$

In these reactions, E-P is a modified form of the enzyme, E·A and E-P·B are enzyme-substrate complexes, A and B are the substrates and P and Q are the products. The velocity of the overall reaction, in this case, can be expressed by Equation 2.9 (VOET; VOET, 2011):

$$v = \frac{v_{max}[\mathrm{A}][\mathrm{B}]}{K_M^B[\mathrm{A}] + K_M^A[\mathrm{B}] + [\mathrm{A}][\mathrm{B}]} \tag{2.9}$$

where:

$$v_{max} = k_{cat}[\mathrm{E}_0] \tag{2.10}$$

In this case, k_{cat}, K_M^A, and K_M^B are general constants that relate to the constants of the single reactions, and these relations can be obtained depending on the model assumptions. These parameters have meanings similar to those for single-substrate reactions: v_{max} is the maximum velocity when both A and B are present at saturating concentrations, and K_M^A and K_M^B are the

respective concentrations of A and B necessary to achieve in the presence of a saturating concentration of the other. They can also be obtained by Lineweaver-Burk plots, similarly to that performed for the Michaelis-Menten equation, as shown on Figure 2.8. These plots are obtained by the inverse of Equation 2.9, given by:

$$\frac{1}{v} = \left(\frac{K_M^A}{v_{max}}\right)\frac{1}{[\mathrm{A}]} + \left(\frac{K_M^B}{v_{max}}\right)\frac{1}{[\mathrm{B}]} + \frac{1}{v_{max}} \tag{2.11}$$

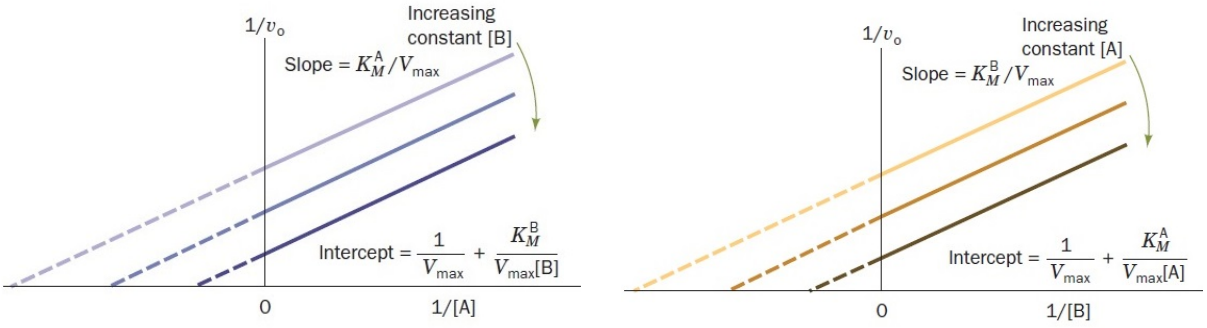

(a) Plots of 1/v x 1/A at constant B concentrations.

(b) Plots of 1/v x 1/B at constant A concentrations.

Figure 2.8 – Lineweaver-Burk plots for a Bi-Bi Ping-Pong mechanism.
Source: Voet and Voet (2011).

2.4.3 Peroxidase mechanism

The peroxidase reactions follow a bi-bi Ping-Pong mechanism, as illustrated on Figure 2.9 (STEEVENSZ et al., 2014; COSTA et al., 2020; CUNHA et al., 2021). It involves two-electron transfer to the first substrate (H_2O_2) that creates a first enzyme oxidized intermediate called 'compound I' (CpI), and two successive one-electron oxidation of the second substrate (S) to return the enzyme to its reduced state via a second enzyme intermediate called 'compound II' (CpII), as represented on Equations 2.12 to 2.14 (NICELL, 1994; AL-ANSARI et al., 2011). This mechanism is similar to that described in section 2.4.2, but with one more step of reaction with the second substrate and disregarding the formation of enzyme-substrate complexes (k_1, k_2, and k_3 are the apparent constants of the reactions).

$$\mathrm{E} + \mathrm{H_2O_2} \xrightarrow{k_1} \mathrm{CpI} + \mathrm{H_2O} \tag{2.12}$$

$$\mathrm{CpI} + \mathrm{S} \xrightarrow{k_2} \mathrm{CpII} + \mathrm{P} \tag{2.13}$$

$$\mathrm{CpII} + \mathrm{S} \xrightarrow{k_3} \mathrm{E} + \mathrm{H_2O} + \mathrm{P} \tag{2.14}$$

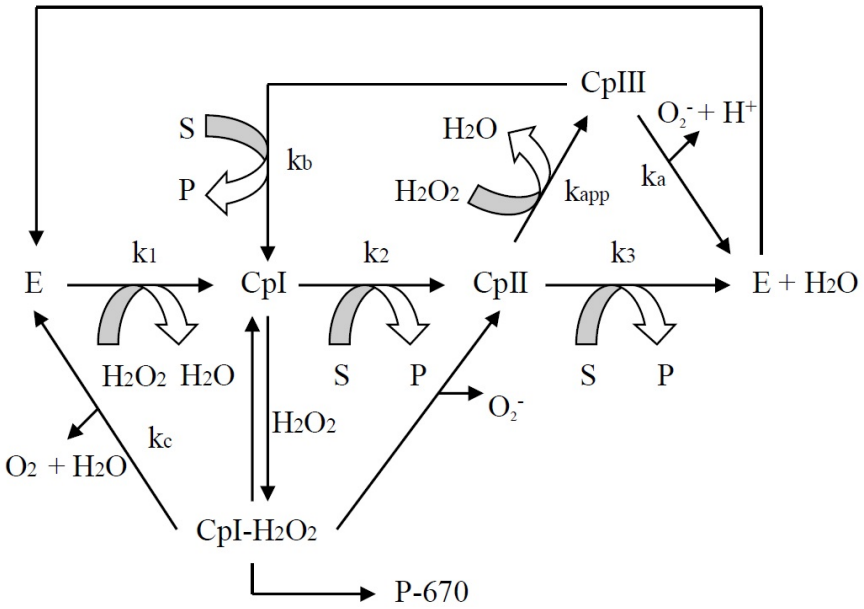

Figure 2.9 – Peroxidase mechanism and suicide pathways.
Source: Steevensz et al. (2014), Costa et al. (2020), Cunha et al. (2021).

The overall reaction can be expressed in Equation 2.15. Although this reaction indicates that two free radicals are generated for every molecule of peroxide consumed, the formation of phenolic compounds follows a 1:1 stoichiometry between peroxide and phenolic substrates, resulting from the formation of large polymers (NICELL et al., 1992).

$$H_2O_2 + 2\,S \xrightarrow{E} 2\,P + 2\,H_2O \tag{2.15}$$

However, peroxidase can be deactivated due to excess H_2O_2, generating a third enzyme oxidized intermediate called 'compound III' (CpIII) (Equation 2.16). Although CpIII is catalytically inactive, it can be decomposed back to the enzyme native form (Equation 2.17) or can also be reduced to CpI (Equation 2.18), which in turn can be oxidized back to the enzyme native form (Equation 2.19) (NICELL, 1994; AL-ANSARI et al., 2011).

$$CpII + H_2O_2 \xrightarrow{k_{app}} CpIII + H_2O \tag{2.16}$$

$$CpIII \xrightarrow{k_a} E + O_2^- + H^+ \tag{2.17}$$

$$CpIII + S \xrightarrow{k_b} CpI + P \tag{2.18}$$

$$CpI + H_2O_2 \xrightarrow{k_c} E + O_2 + H_2O \tag{2.19}$$

The kinetic constants k_{app}, k_a, k_b, and k_c are the apparent constants of the reactions, as well as the kinetic constants k_1, k_2, and k_3. That is, all forms of the enzyme can interact with the substrates forming enzyme-substrate complexes. Nicell (1994) states that there is no evidence of the formation of enzyme-substrate complexes for reactions with phenolic compounds, that is, only the interaction of H_2O_2 with the enzyme's oxidized intermediates can form enzyme-substrate complexes. Besides, only the existence of the CpI·H_2O_2 complex has been confirmed, and the interaction of CpI with H_2O_2 (Equation 2.19) can be replaced by Equation 2.20:

$$\mathrm{CpI} + \mathrm{H_2O_2} \underset{k_{-4}}{\overset{k_4}{\rightleftharpoons}} \mathrm{CpI \cdot H_2O_2} \xrightarrow{k_5} \mathrm{E} + \mathrm{O_2} + \mathrm{H_2O} \tag{2.20}$$

Nicell (1994) also reported that CpI·H_2O_2 complex can also generate an enzyme inactive form called verdohemoprotein (P-670). Besides, all the enzyme inactive forms are represented in this work by Equation 2.21, which also involves other factors such as free-radical inactivation and adsorption or entrapment on the end-product polymers. Once the reaction has gone to completion, the number of phenolic compounds formed per molecule of the enzyme in the solution is constant. Thus, the enzyme can be considered as a pseudo-substrate of the reaction, as represented below (NICELL, 1994):

$$\mathrm{E} + K_s\ \mathrm{S} \rightarrow \mathrm{E}_{inactive} + \mathrm{Products} \tag{2.21}$$

K_s is the number of S molecules removed per enzyme molecule after the reaction is complete, also known as the turnover number of an enzyme, and is calculated by:

$$K_s = \frac{[\mathrm{S}]_0 - [\mathrm{S}]_{final}}{[\mathrm{E}]_0} \tag{2.22}$$

Then the amount of inactivated enzyme can be calculated by:

$$[\mathrm{E}_{inactive}] = \frac{[\mathrm{S}]_0 - [\mathrm{S}]}{K_s} \tag{2.23}$$

2.5 MODELING, SIMULATION AND PARAMETER ESTIMATION

The process of building a model follows a sequence of steps that is the same used in the construction of a scientific theory. First, the nature of the process must be observed, how it behaves and how are the cause and effect relationships of the process. Then, it is possible to generate a set of hypotheses that can be assumed to represent this process. After these steps, it is possible to use the fundamental equations, such as the mass balances of the species involved in a chemical reaction. This procedure is called process modeling, that is, the process of building a model, which generates a set of mathematical equations to be solved (VIANNA JR., 2021).

The representation of the enzyme kinetic model, as well as other chemical reaction models, can be made by mathematical systems composed of systems of differential equations (ODEs) or systems of algebraic-differential equations (DAEs) that describe the process variables, such as concentrations. The response of these models allows obtaining predictions that corroborate for the simulation, design and optimization of the process. The systems of equations that represent the model can be revolved by several methods, and in this work the backward differentiation formula (BDF) is used. However, the description of this method is not part of the scope of the present work, and can be seen in more detail in Vianna Jr. (2021).

The parameter estimation procedure is a fundamental step for evaluating the adequacy of the model from experimental data. Parameters are variables that cannot be measured directly, and whose values must be estimated so that the model represents the experimental data as accurately as possible (SCHWAAB, 2005). Several methods can be used to determine the kinetic parameters of enzymatic reactions. One of these methods is the differential method, in which the parameters are obtained by equations containing the derivatives of one or more dependent variables relative to one or more independent variables. Another one is the integral method, based on determining the kinetic data through linear regression (SCHMALL, 2013). However, an experimental design must first be carried out to find the optimal experimental conditions where the new experiments should be performed, enabling the achievement of the objectives with a minimum of experimental effort (SCHWAAB; PINTO, 2007).

The parameter estimation procedure consists of adjusting the model parameters by the minimization of an objective function, which is a measure of the distance between the experimental data and the model predictions. The weighted least squares function, which measures the sum of the quadratic deviations of the model in relation to the experiment, is generally used. This function is generated from the maximum likelihood method. Once the objective function

has been defined, the next step is to minimize it by adjusting the parameters to obtain a model with the best possible prediction. The minimization methods traditionally used in parameter estimation are deterministic methods, in which, from an initial estimation of the parameters, the minimum of the objective function is sought (SCHWAAB; PINTO, 2007).

The advent of computers made possible the use of numerical methods for parameter estimation since this procedure involves the search for the minimum of a nonlinear function. In this work, the computational simulations are performed using MATLAB software version R2015a. This software has routines for the model calculation composed of systems of ODEs and DAEs, as well as constrained nonlinear optimization tools.

CHAPTER 3
LITERATURE REVIEW

3.1 SOYBEAN PEROXIDASE

The soybean seed hull is an abundant byproduct of the soybean industry from which peroxidase can be extracted; the seed coat of the mature soybean is about 4-8% in mass of the total seed (AL-ANSARI et al., 2011). There are several SBP extraction and purification processes in the literature, as published by Gillikin and Graham (1991), Gacche et al. (2003), Bassi et al. (2004), Ghaemmaghami et al. (2010), Silva et al. (2013) and Steevensz et al. (2013). Calza et al. (2016) developed a fast and efficient purification procedure, reaching a good relation between enzyme purity and total yield. This method was enhanced by Tolardo et al. (2019).

Steevensz et al. (2013) stated that the SBP activity can vary substantially among several cultivars. The activity can be characterized by different methods, but the most commonly used is the DMAB-MBTH method (NGO; LENHOFF, 1980). Other options are to measure activity with pyrogallol (GACCHE et al., 2003), by Worthington colorimetric assay at 25ºC using 4-aminoantipyrine (4-AAP) and H_2O_2 (FATIBELLO FILHO; VIEIRA, 2002) or by following the rate of conversion of guaiacol to tetraguaiacol. Furthermore, the products of the degradation of the substrates can be identified directly (LAURENTI et al., 2002, 2003), since the products usually show different toxicity than the reagents (SILVA et al., 2013).

3.1.1 Degradation mechanisms of chlorinated phenolic compounds

Torres and Ayala (2010) presented an example of TCP degradation in which the final metabolite is obtained by two one-electron oxidations catalyzed by peroxidase. Ferrari et al. (1999) presented a hypothetical scheme for the catalytic mechanism of TCP oxidative dechlorination by a peroxidase/H_2O_2 system, as shown in Figure 3.1. In this mechanism, TCP undergoes successive oxidations, and products were identified in the forms of 2,6-dichloro-1,4-benzoquinone and 2,6-dichlorohydroquinone.

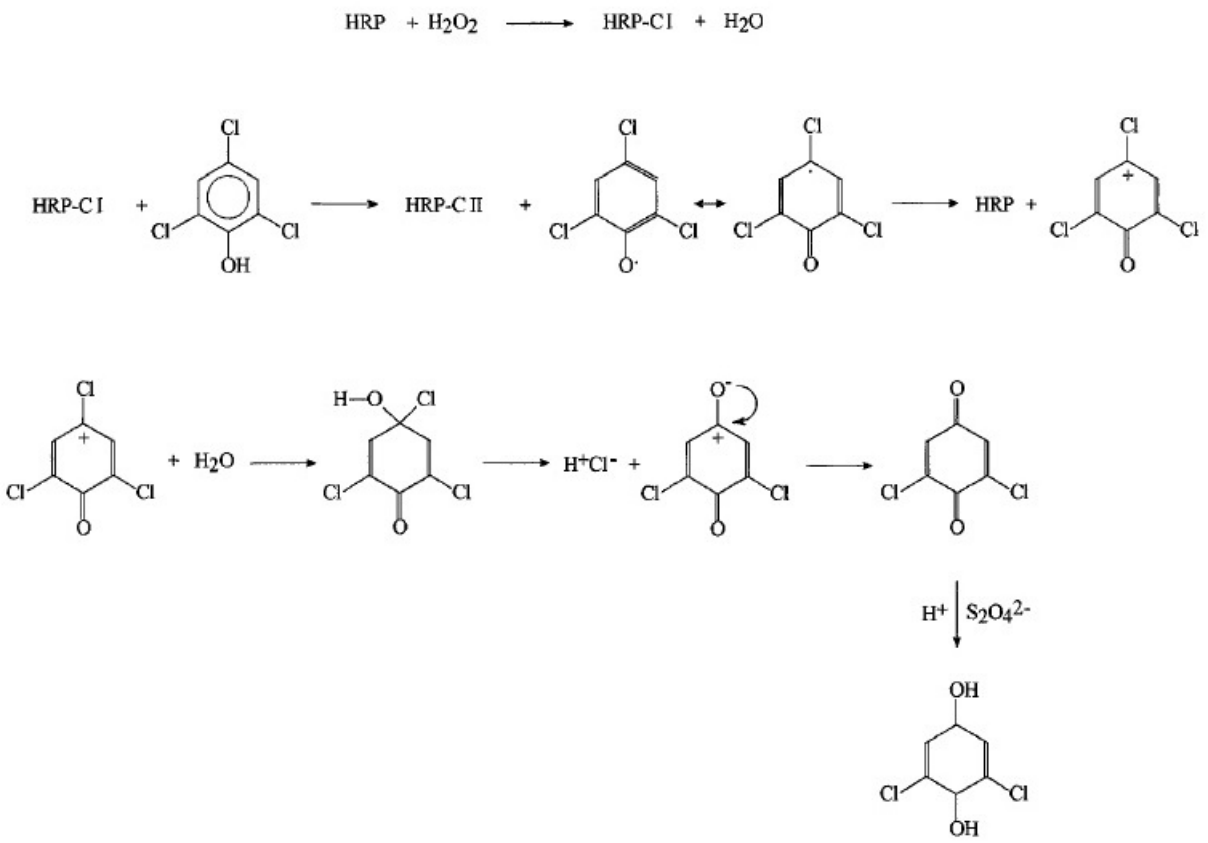

Figure 3.1 – Hypothetical mechanism of TCP dechlorination using HRP in the presence of hydrogen peroxide.
Source: Ferrari et al. (1999).

There are in the literature some mechanisms proposed with the identification of the products formed by the degradation of TCS with the laccase enzyme (DOU et al., 2018; BILAL et al., 2020), but no mechanisms with the TCS products obtained from the enzymatic degradation using peroxidases were found. Li et al. (2016) identified the formation of five different dimers and a trimer as major products of the reaction catalyzed by SBP. Additional research needs to be carried out for a better understanding of the degradation products of this pollutant.

Kobayashi (1998) performed the enzymatic oxidative polymerization reaction of BPA using SBP and HRP. The authors obtained by NMR and IR analyses that the polymer obtained is mainly composed of a mixture of phenylene and oxyphenylene. Huang and Weber Jr (2005) proposed the mechanism of BPA degradation with a total of 13 reaction intermediates and products, as shown in Figure 3.2, which were identified by LC/MS and GC/MS techniques. In this mechanism, all the intermediates and products detected can be interpreted as a result of either coupling or substitution reactions between BPA and other intermediates or products.

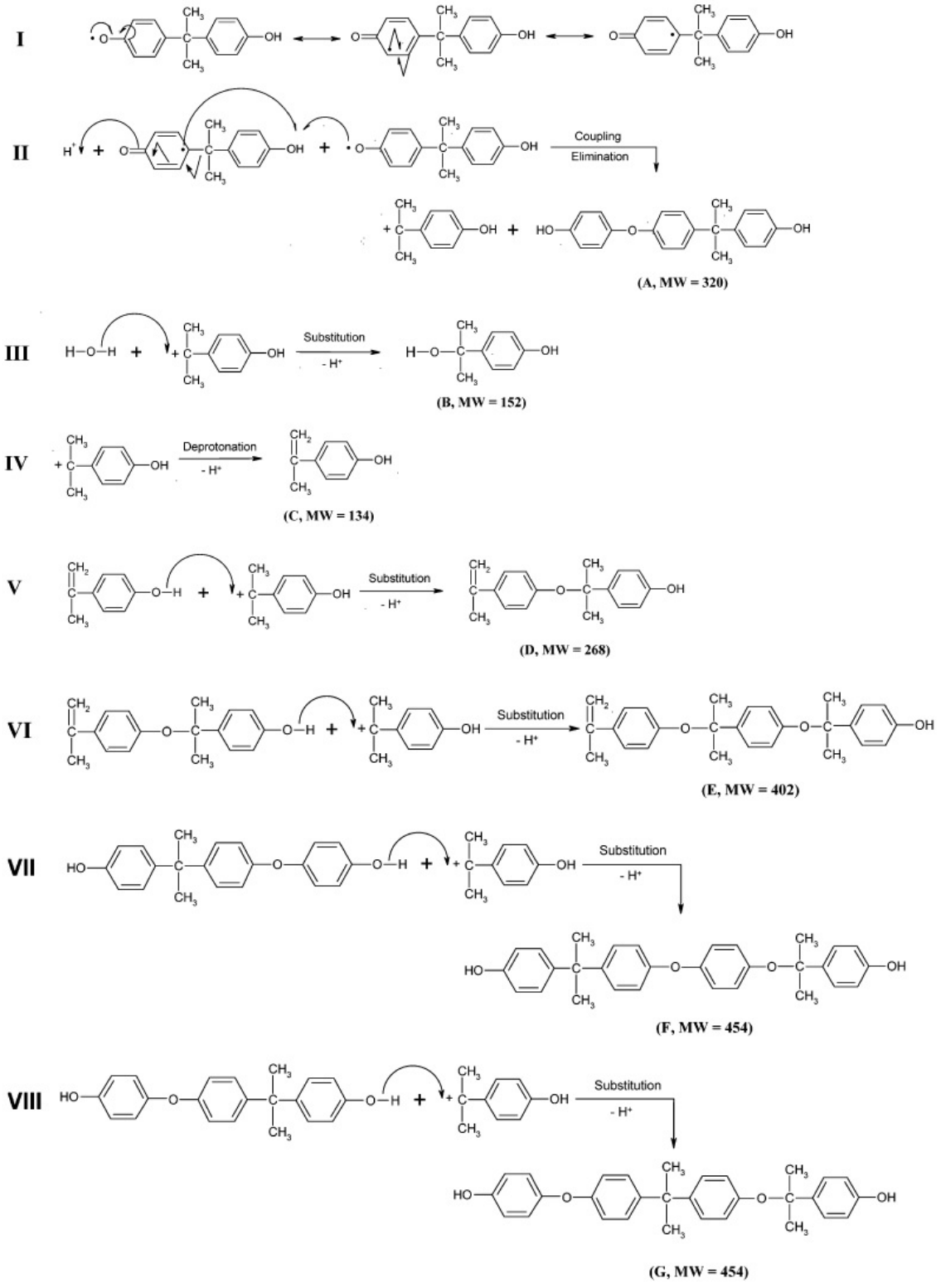

Figure 3.2 – Proposed mechanism of BPA degradation using HRP enzyme in the presence of hydrogen peroxide.

Source: Huang and Weber Jr (2005).

3.2 PROCESS APPLICATIONS

Ferrari et al. (1999) studied the oxidative dechlorination pathway catalyzed by HRP for TCP and showed that HRP has a relative catalytic efficiency higher than lignin peroxidases. They proposed a hypothetical mechanism of TCP dechlorination using HRP enzyme in the presence of hydrogen peroxide, as presented in the previous section. Laurenti et al. (2002) and Laurenti et al. (2003) studied the oxidative dechlorination of 2,6-dichlorophenol and 2,4-dichlorophenol, respectively, in the presence of hydrogen peroxide, using UV–visible spectroscopy and mass spectrometry finding consistent results.

Nissum et al. (2001) showed that SBP can also oxidize non-phenolic substrates, such as veratryl alcohol, like lignin peroxidase. The authors investigated the pH dependence, observing that the reaction is linearly dependent on H_2O_2 concentration at acid pH and hyperbolic dependant at basic pH. They obtained the second-order constants for the reduction of compound I and compound II, which were very similar. They also showed evidence of compound III formation, and no additional intermediates were observed. Shintaku et al. (2005) developed a microsecond-resolved absorption spectrometer to investigate the kinetic absorption spectra of HRP upon mixing with H_2O_2. The authors have not found evidence of a detectable intermediate before the formation of compound I, after realizing that the rate constant for the breakage of the oxygen's bond in H_2O_2 is very fast.

Bódalo et al. (2006) made a comparison between the HRP and SBP performance for the removal of phenol from wastewater. Regarding operational conditions, they concluded that both are suitable for phenol removal, but the process must be loosely controlled at around neutral pH and ambient temperature. Besides, they used polyethylene glycol (PEG) as a stabilization additive, showing that HRP acts faster than SBP but is more susceptible to inactivation and needs a higher amount of PEG addition. So the final choice must be based on economic considerations.

In the textile industries area, Marchis et al. (2011) reported the complete and fast decolorization of a Cu(II)-phthalocyanine-based reactive dye (Remazol Turquoise Blue G 133) using the SBP/H_2O_2 system. Kalsoom et al. (2013) showed the effectiveness of the SBP catalyzed reaction in the degradation of the diazo dye Trypan Blue in the aqueous phase. They realized that the SBP performance was found to be dependent upon the reaction time, dye concentration, enzyme concentration, H_2O_2 dose, and pH value. More recently, Altahir et al. (2020) have successfully demonstrated dye decoloration by SBP in the presence of H_2O_2, based on Acid Black 2 and Acid Orange 7 dyes that have wide industrial use.

In a review of SBP uses for industrial wastewater treatment (STEEVENSZ et al., 2014), some of the limitations and advancements in the field were highlighted. This review covers aspects such as cost, use of additives for increased enzyme economy, enzyme recycling, and studies already completed on industrial effluents. The authors concluded that there are many more studies on synthetic wastewater compared with a limited number of real effluents, and the feasibility to treat various industrial wastewaters has not yet been proven.

Calza et al. (2014) studied the synergistic effect of TiO_2 and commercial SBP in the degradation of TCP, obtaining an increase in the rate of removal. The degradation proceeds through the formation of less toxic intermediates than those produced by the system containing only TiO_2 because SBP is capable of activating the replacement of the chlorine atoms present on the benzene ring through the formation of a phenoxy radical. This finding was very motivating for future applications in the bioremediation field.

Calza et al. (2016) studied the removal of common orange dyes and the anticonvulsant drug carbamazepine from aqueous solutions by enzymatic and photocatalytic treatments, using SBP as a biocatalyst. They extended the studies on the TiO_2/SBP system previously done by Calza et al. (2014) in the degradation of TCP, confirming that the combination of the two catalysts leads to faster removal.

Many authors have performed BPA degradation studies using the enzyme HRP (HUANG; WEBER JR, 2005; HONG-MEI; NICELL, 2008; YAMADA et al., 2010; HONGMEI; NICELL, 2011; ESCALONA et al., 2015), SBP (CAZA et al., 1999; WATANABE et al., 2011; JIANG; ZHENG, 2013) and both (KOBAYASHI et al., 1998). Caza et al. (1999) carried out experiments to remove several different phenolic compounds from synthetic wastewater using SBP, including BPA. The authors observed that an increase in the H_2O_2 to BPA molar ratio beyond the optimum had no negative effect on the removal efficiency.

Jiang and Zheng (2013) carried out BPA degradation reactions using the SBP enzyme extracted and purified from soybean seed hulls. The authors observed a very positive effect on the removal of BPA from simulation wastewater at relatively higher concentration conditions. Watanabe et al. (2011) performed BPA removal from water using SBP enzyme and PEG as an additive. In this case, water-insoluble oligomers were generated, which were removed from the aqueous solutions by filtration.

Bilal et al. (2020) performed a literature review on TCS degradation using different oxidative enzymes, including laccases, and peroxidases including MnP, HRP, and SBP. Melo and

Dezotti (2013) used the enzyme HRP to catalyze the TCS removal. The authors observed that the antibacterial activity of TCS solution was effectively reduced after enzymatic treatment, being the enzyme HRP technically feasible for removing triclosan at environmentally relevant concentrations. Li et al. (2016) carried out TCS degradation experiments with SBP and HRP enzymes, observing a more efficient degradation performance using the SBP enzyme. According to the authors, SBP was able to oxidize 98% of TCS while HRP oxidized 36.5%, in 30 minutes of reaction, for the same enzyme concentration. The authors claim that this is the first report on the application of the SBP enzyme to remove TCS from water.

Zhang et al. (2018) evaluated the combined toxicity of TCP with 2,4-dichlorophenol and TCS. According to the authors, they are the most prevalent chlorinated phenolic pollutants in aquatic environments and some of the most carcinogenic chemicals in the world. TCP and 2,4-dichlorophenol have similar applications and both can be formed through TCS photolysis or chlorinated reaction. The authors tested the toxicity of these 3 pollutants on zebrafish (Danio rerio), where the exposure significantly affected fat metabolism in zebrafish embryos, leading to a series of malformations. These results provide a theoretical basis for evaluating the ecological risks of exposure to chlorinated phenolic pollutants in real-world aquatic environments.

Zheng and Colosi (2011) performed single and multiple-substrate degradation studies using the HRP enzyme. They evaluated a mixture containing six substrates, including EDCs such as estrone, estriol, 17α-ethynylestradiol, 17β-estradiol, BPA, and TCS, and reported pseudo-first-order rate constants by a model considering Michaelis–Menten approach. They observed that some kinetic constants of mixed degradation reactions tended to be greater than those of individual degradation, suggesting an improvement in the rate in the presence of other substrates. Sarro et al. (2018) showed the efficacy of ZnO-based and enzyme hybrid materials with SBP in the removal of contaminants in a mixture of six substrates (diclofenac, naproxen, iopamidol, imidacloprid, 2,4-dichlorophenol, and BPA) which mimics a real scenario.

One of the most recent studies of phenolic compounds removal using SBP has been published by Tolardo et al. (2019), who employed this enzyme in the treatment of aqueous solutions containing pentachlorophenol in the presence of H_2O_2. They performed the isolation and purification of SBP from soybean seed hulls successfully. Besides, they observed that the pentachlorophenol removal was not complete, maybe because of the interference of intermediates or reaction products. So the authors pointed out that further research is needed to determine to other pollutants this approach can be applied.

3.2.1 Available experimental data

A study on TCP degradation using the commercial SBP enzyme was carried out in a microreactor (COSTA, 2016; COSTA et al., 2020). The reactions were carried out in a Syrris 250 μL microreactor in the laboratory of the Department of Chemical Engineering, Polytechnic School, University of São Paulo, at pH 5.4 and a temperature of 25ºC. The authors used the commercial SBP provided by Bio-Research Products Inc., Iowa-USA. The data were obtained in two sets of experiments, increasing the number of points in the second one, considering the SBP concentrations of [SBP] = 5.2 x 10^{-9} M, [SBP] = 1.04 x 10^{-8} M, and 2.08 x 10^{-8} M. All measurements were performed in triplicate, being considered the average of the values. The initial concentrations of TCP and H_2O_2 were 0.25 mM and 0.6 mM, respectively. For the inhibition of the reaction process, 37% hydrochloric acid was used. At the end of the reaction process, a 0.1 mL sample was collected at the microreactor outlet, which was analyzed offline by high-performance liquid chromatography (Shimadzu LC-20AD Prominence).

To develop an appropriate model in the present work, experimental data reported by Costa (2016) and Costa et al. (2020) are used as a reference in the model development process, in addition to using the same experimental conditions as a basis for carrying out new experiments. These data reported by the authors are presented in Figure 3.3.

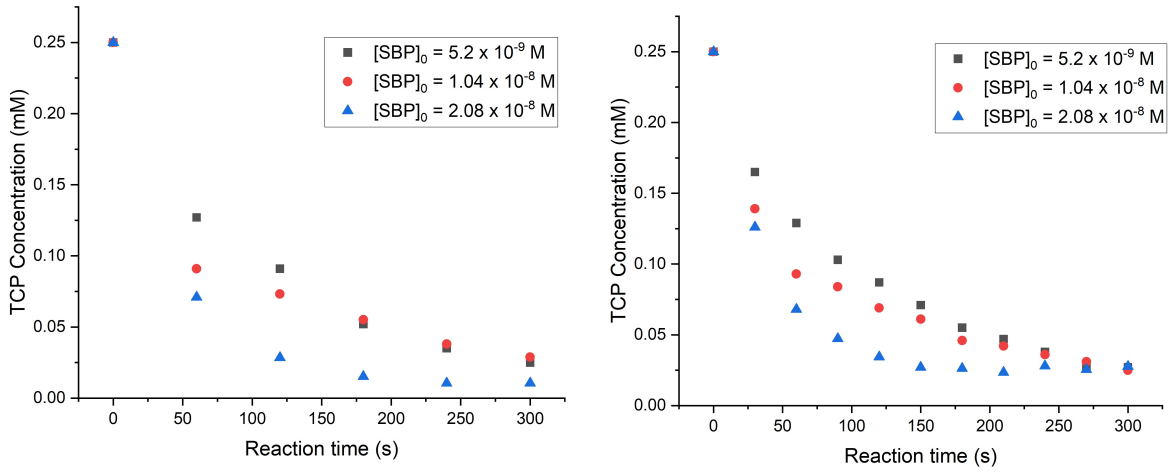

(a) First experimental data set (April/2015) (b) Second experimental data set (January/2016)

Figure 3.3 – Available data sets: TCP degradation over reaction time.
Source: Costa (2016), Costa et al. (2020).

The work of Costa et al. (2020) was published in partnership with the present research, where the kinetic data were analyzed through the modified bi-bi ping-pong model. This work was complemented by Cunha et al. (2021), focusing more deeply on the mathematical modeling. In this work, different scenarios of kinetic models were evaluated, considering the bi-bi ping-pong model, and the simulations were compared to experimental data, obtained in a microreactor. The importance of using the microreactor is discussed in the next section.

3.3 MICROREACTORS

The definition of kinetic parameters of the model can be carried out in a microreactor, which is suitable equipment for carrying out fast reactions, such as enzymatic reactions. A microreactor is a device that enables chemical reaction as an ordinary reactor but in the order of micrometers (LAURENTI; VIANNA JR, 2016). However, although microreactors have small volumes, larger production can be configured into long-term production without changing the size of the reactors, in a numbering-up strategy, since the microreactors operate continuously. Thus, a switch to industrial production is possible without changing reaction conditions. The main advantages of the use of microreactors are strict control of reaction conditions, safety in operation, improvement in mass and heat transfer, and energy efficiency (LAURENTI; VIANNA JR, 2016).

Yoshida et al. (2005) showed that microreactors allow better mass and heat transfer, based on their high surface-to-volume ratios. They carried out experiments with polymerization reactions and concluded that the efficient micromixing due to its short diffusion path increases the product selectivity of competitive parallel reactions and competitive consecutive reactions.

Tišma et al. (2009) studied the L-DOPA oxidation catalyzed by laccase in a microreactor. They developed a two-dimensional mathematical model composed of convection, diffusion, and enzymatic reaction terms, described by the Michaelis-Menten double substrate equation using kinetic parameters performed in batch experiments. Based on the developed model, the authors state that the design and optimization of additional processes are feasible.

Tusek et al. (2013) showed the efficiency of microreactor usage for phenolic compounds oxidation using laccase. The kinetic parameters of catechol oxidation were estimated using data collected from experiments carried out in a microreactor. The authors stated that the maximum reaction rate estimated in microreactor experiments was two times higher than one estimated using the initial reaction rate method.

Lloret et al. (2013) have proposed an innovative and efficient method for the preparation of laccase immobilized microreactors, conducted by the formation of an enzyme-polymeric membrane on the inner wall of microchannels using a cross-linking polymerization method. According to the authors, the obtained microreactors showed excellent performance and stability under a wide range of conditions.

Laurenti and Vianna Jr (2016) reviewed the literature on continuous flow and immobilized biomicroreactors for biocatalysis processes. The authors showed that the microdimensions, coupled with a high surface area/volume ratio, permit rapid heat exchange and mass transfer, resulting in higher reaction yields and rates than in conventional reactors. They also concluded that the lower energy consumption and easier separation of products permit these systems to have a lower environmental impact compared to macroscale reactors.

Costa et al. (2020) carried out a Computational Fluid Dynamics (CFD) analysis in a microreactor using ANSYS CFX software, as well as a study on TCP degradation using SBP. The authors confirmed the presence of secondary flows in the microchip curves of the microreactor, which results in diffusion mixing and consequently a better mixing in this piece of equipment.

Svetozarević et al. (2022) performed the biodegradation of anthraquinone dye in a microfluidic reactor using SBP and potato peroxidase. The authors confirmed via scanning electron microscope (SEM) analysis that the smaller reactor's diameter contributed to better mixing and an enhanced contact among reagents. These results corroborate the relevance and importance of using the microreactor for studies of fast kinetics such as enzymatic ones.

3.4 KINETIC MODELING AND PARAMETER ESTIMATION

One of the first works on parameter estimation in the context of enzyme kinetics models using computational techniques was published by Cleland (1963a). The authors presented different models of the reaction rate based on the Michaelis-Menten equation. Reich (1970) also proposed computational approaches for estimating parameters in kinetic models, and presented different statistical metrics for investigating the adequacy of models. Many other authors have carried out studies to estimate parameters of the Michaelis-Menten model (GARDINER; OTTAWAY, 1969; CORNISH-BOWDEN; EISENTHAL, 1974; CURRIE, 1982; SRINIVASAN; AIKEN, 1984; BROOKS; SUELTER, 1985).

Nicell (1994) developed steady-state, fully transient, and pseudo-steady-state models for the polymerization and precipitation of 4-chlorophenol catalyzed by HRP in the presence

of H_2O_2. The author implemented several simplifying assumptions, finding satisfactory results for the fully transient and pseudo-stationary models incorporating inactivation mechanisms. Besides, the computation time to solve the model was excessive for the fully transient model.

Nicell and Wright (1997) studied the effect of H_2O_2 concentration with an assay based on phenol as substrate and 4-AAP as a chromogen to measure peroxidase activity. The authors developed a steady-state kinetic model based on experimental data obtained by reactions with both SBP and HRP enzymes. The model indicated that SBP tends to form more compound III and is catalytically slower than HRP during the phenol oxidation reaction.

Buchanan and Nicell (1997) developed a pseudo-steady-state kinetic model for the process of phenol degradation using HRP enzyme in the presence of H_2O_2, improving significantly its predictive ability by incorporating enzyme inactivation mechanisms. The kinetic constants were obtained using a series of experimental data sets. The rate of enzyme inactivation due to end-product polymer was modeled as being proportional to the rate of polymer formation. They also confirmed the apparent rate of compound III decomposition as being first order concerning compound III concentration. These results together with those of Nicell (1994) and Nicell and Wright (1997) were very relevant for the present work.

Azizyan et al. (2012) developed studies on mathematical and computational modeling of bi-substrate enzymatic reactions with a ping-pong mechanism. They considered the solution of a system of differential equations obtained from the mass balance of the reaction species. The authors considered hypothetical values of kinetic constants to simulate the model. Azizyan et al. (2013) extended these studies by additionally considering competitive inhibition.

Durruty et al. (2011) performed batch experiments of multisubstrate degradation of a mixture solution containing pentachlorophenol, 2,3,5,6-tetrachlorophenol and TCP, using a mixed culture of *Pseudomonas aeruginosa* and *Acromobacter sp.* bacteria. They used the Monod kinetic model, which was able to predict the simultaneous degradation of chlorophenols in batch mode using results from single substrate experiments. The multisubstrate model considers the solution of a system of differential equations similar to the system for only one substrate, but considering a sum of all substrates present in the medium.

Zheng and Colosi (2011) and Sarro et al. (2018) performed multi-substrate degradation reaction of different mixtures containing six contaminants, but they reported only first-order kinetic pseudo-constants based on Michaelis–Menten approach.

Kong et al. (2017) performed the estimation of the kinetic parameters of the phenol ni-

tration process using the HRP enzyme based on the dual substrate ping-pong model to describe the reaction mechanism. They derived the global velocity equation for the two-substrate model and estimated the global constants by the Lineweaver-Burk graphical method (presented in this work in the section 2.4.2), which allows obtaining only the apparent equilibrium constants, instead of using the modified bi-bi ping pong model (peroxidase mechanism).

Until the closing of this thesis, no studies were found in the literature that perform the modeling, simulation and parameter estimation based on the modified bi-bi ping pong model by the method of solving differential or algebraic-differential equations for the degradation reactions of the TCP, TCS and BPA using SBP or HRP enzymes. Therefore, this is one of the main objectives of this work. A multi-substrate degradation model with this same approach is also proposed, being an important feature of the present work.

CHAPTER 4
METHODOLOGY

4.1 MODELING AND SIMULATION

4.1.1 Process modeling

The process modeling was obtained from the mass balance of all the species of the schematic reactions described in section 2.4.3. Several scenarios can be considered, depending on the hypotheses made for simplifying the bi-bi ping-pong model. The system of differential equations (ODE) generated by the model considering only the formation of CpI and CpII (reactions of Equations 2.12, 2.13, and 2.14) is presented on Equations 4.1a to 4.1f:

$$\frac{d[\mathrm{E}]}{dt} = -k_1[\mathrm{E}][\mathrm{H_2O_2}] + k_3[\mathrm{CpII}][\mathrm{S}] \tag{4.1a}$$

$$\frac{d[\mathrm{CpI}]}{dt} = k_1[\mathrm{E}][\mathrm{H_2O_2}] - k_2[\mathrm{CpI}][\mathrm{S}] \tag{4.1b}$$

$$\frac{d[\mathrm{CpII}]}{dt} = k_2[\mathrm{CpI}][\mathrm{S}] - k_3[\mathrm{CpII}][\mathrm{S}] \tag{4.1c}$$

$$\frac{d[\mathrm{H_2O_2}]}{dt} = -k_1[\mathrm{E}][\mathrm{H_2O_2}] \tag{4.1d}$$

$$\frac{d[\mathrm{S}]}{dt} = -k_2[\mathrm{CpI}][\mathrm{S}] - k_3[\mathrm{CpII}][\mathrm{S}] \tag{4.1e}$$

$$\frac{d[\mathrm{P}]}{dt} = k_2[\mathrm{CpI}][\mathrm{S}] + k_3[\mathrm{CpII}][\mathrm{S}] \tag{4.1f}$$

Steady-state can be assumed for all the enzymatic forms, as the equilibria in this case are reached quickly since the reactions are very fast:

$$\frac{d[\mathrm{E}]}{dt} = \frac{d[\mathrm{CpI}]}{dt} = \frac{d[\mathrm{CpII}]}{dt} = 0 \tag{4.2}$$

The total (initial) amount of enzyme, $[\mathrm{E}]_0$, is given by Equation 4.3, and as this value is known, [E] can be obtained.

$$[\mathrm{E}]_0 = [\mathrm{E}] + [\mathrm{CpI}] + [\mathrm{CpII}] \tag{4.3}$$

From Equations 4.1b, 4.1c, and 4.2, the concentrations of CpI and CpII can be obtained. In this way, a system of algebraic-differential equations (DAE) is obtained, consisting of:

$$[\mathrm{E}] = [\mathrm{E}]_0 - [\mathrm{CpI}] - [\mathrm{CpII}] \tag{4.4a}$$

$$[\mathrm{CpI}] = \frac{k_1[\mathrm{H_2O_2}][\mathrm{E}]}{k_2[\mathrm{S}]} \tag{4.4b}$$

$$[\mathrm{CpII}] = \frac{k_2[\mathrm{CpI}]}{k_3} \tag{4.4c}$$

$$\frac{d[\mathrm{H_2O_2}]}{dt} = -k_1[\mathrm{E}][\mathrm{H_2O_2}] \tag{4.4d}$$

$$\frac{d[\mathrm{S}]}{dt} = -k_2[\mathrm{CpI}][\mathrm{S}] - k_3[\mathrm{CpII}][\mathrm{S}] \tag{4.4e}$$

$$\frac{d[\mathrm{P}]}{dt} = k_2[\mathrm{CpI}][\mathrm{S}] + k_3[\mathrm{CpII}][\mathrm{S}] \tag{4.4f}$$

Analogously, the ODE system generated by the model considering also the formation of CpIII and also assuming the steady-state assumption for the concentrations of all enzyme forms can be obtained:

$$\frac{d[\mathrm{E}]}{dt} = -k_1[\mathrm{E}][\mathrm{H_2O_2}] + k_3[\mathrm{CpII}][\mathrm{S}] + k_a[\mathrm{CpIII}] + k_c[\mathrm{CpI}][\mathrm{H_2O_2}] \tag{4.5a}$$

$$\frac{d[\mathrm{CpI}]}{dt} = k_1[\mathrm{E}][\mathrm{H_2O_2}] - k_2[\mathrm{CpI}][\mathrm{S}] + k_b[\mathrm{CpIII}][\mathrm{S}] - k_c[\mathrm{CpI}][\mathrm{H_2O_2}] \tag{4.5b}$$

$$\frac{d[\text{CpII}]}{dt} = k_2[\text{CpI}][\text{S}] - k_3[\text{CpII}][\text{S}] - k_{app}[\text{CpII}][\text{H}_2\text{O}_2] \tag{4.5c}$$

$$\frac{d[\text{CpIII}]}{dt} = k_{app}[\text{CpII}][\text{H}_2\text{O}_2] - k_a[\text{CpIII}] - k_b[\text{CpIII}][\text{S}] \tag{4.5d}$$

$$\frac{d[\text{H}_2\text{O}_2]}{dt} = -k_1[\text{E}][\text{H}_2\text{O}_2] - k_{app}[\text{CpII}][\text{H}_2\text{O}_2] - k_c[\text{CpI}][\text{H}_2\text{O}_2] \tag{4.5e}$$

$$\frac{d[\text{S}]}{dt} = -k_2[\text{CpI}][\text{S}] - k_3[\text{CpII}][\text{TCP}] - k_b[\text{CpIII}][\text{S}] \tag{4.5f}$$

$$\frac{d[\text{P}]}{dt} = k_2[\text{CpI}][\text{S}] + k_3[\text{CpII}][\text{S}] + k_b[\text{CpIII}][\text{S}] \tag{4.5g}$$

The DAE system can also be obtained in this case, from the total (initial) amount of enzyme obtained analogously to Equation 4.3, and CpI, CpII and CpIII concentrations obtained by Equations 4.5b, 4.5c and 4.5d, respectively:

$$[\text{E}] = [\text{E}]_0 - [\text{CpI}] - [\text{CpII}] - [\text{CpIII}] \tag{4.6a}$$

$$[\text{CpI}] = \frac{k_1[\text{H}_2\text{O}_2][\text{E}] + k_b[\text{CpIII}][\text{S}]}{k_2[\text{S}] + k_c[\text{H}_2\text{O}_2]} \tag{4.6b}$$

$$[\text{CpII}] = \frac{k_2[\text{CpI}][\text{S}]}{k_3[\text{S}] + k_{app}[\text{H}_2\text{O}_2]} \tag{4.6c}$$

$$[\text{CpIII}] = \frac{k_{app}[\text{CpII}][\text{H}_2\text{O}_2]}{k_a + k_b[\text{S}]} \tag{4.6d}$$

$$\frac{d[\text{H}_2\text{O}_2]}{dt} = -k_1[\text{E}][\text{H}_2\text{O}_2] - k_{app}[\text{CpII}][\text{H}_2\text{O}_2] - k_c[\text{CpI}][\text{H}_2\text{O}_2] \tag{4.6e}$$

$$\frac{d[\text{S}]}{dt} = -k_2[\text{CpI}][\text{S}] - k_3[\text{CpII}][\text{S}] - k_b[\text{CpIII}][\text{S}] \tag{4.6f}$$

$$\frac{d[\text{P}]}{dt} = k_2[\text{CpI}][\text{S}] + k_3[\text{CpII}][\text{S}] + k_b[\text{CpIII}][\text{S}] \tag{4.6g}$$

Another possibility is considering also the formation of CpI·H_2O_2 (reaction of Equation 2.20 instead of Equation 2.19), and also assuming the steady-state assumption for the concentrations of all enzyme forms. In this case, the following ODE system can be obtained:

$$\frac{d[\mathrm{E}]}{dt} = -k_1[\mathrm{E}][\mathrm{H_2O_2}] + k_3[\mathrm{CpII}][\mathrm{S}] + k_a[\mathrm{CpIII}] + k_5[\mathrm{CpI}\cdot\mathrm{H_2O_2}] \tag{4.7a}$$

$$\frac{d[\mathrm{CpI}]}{dt} = k_1[\mathrm{E}][\mathrm{H_2O_2}] - k_2[\mathrm{CpI}][\mathrm{S}] + k_b[\mathrm{CpIII}][\mathrm{S}] - k_4[\mathrm{CpI}][\mathrm{H_2O_2}] + k_{-4}[\mathrm{CpI}\cdot\mathrm{H_2O_2}] \tag{4.7b}$$

$$\frac{d[\mathrm{CpII}]}{dt} = k_2[\mathrm{CpI}][\mathrm{S}] - k_3[\mathrm{CpII}][\mathrm{S}] - k_{app}[\mathrm{CpII}][\mathrm{H_2O_2}] \tag{4.7c}$$

$$\frac{d[\mathrm{CpIII}]}{dt} = k_{app}[\mathrm{CpII}][\mathrm{H_2O_2}] - k_a[\mathrm{CpIII}] - k_b[\mathrm{CpIII}][\mathrm{S}] \tag{4.7d}$$

$$\frac{d[\mathrm{CpI}\cdot\mathrm{H_2O_2}]}{dt} = k_4[\mathrm{CpI}][\mathrm{H_2O_2}] - (k_5 + k_{-4})[\mathrm{CpI}\cdot\mathrm{H_2O_2}] \tag{4.7e}$$

$$\frac{d[\mathrm{H_2O_2}]}{dt} = -k_1[\mathrm{E}][\mathrm{H_2O_2}] - k_{app}[\mathrm{CpII}][\mathrm{H_2O_2}] - k_4[\mathrm{CpI}][\mathrm{H_2O_2}] + k_{-4}[\mathrm{CpI}\cdot\mathrm{H_2O_2}] \tag{4.7f}$$

$$\frac{d[\mathrm{S}]}{dt} = -k_2[\mathrm{CpI}][\mathrm{S}] - k_3[\mathrm{CpII}][\mathrm{TCP}] - k_b[\mathrm{CpIII}][\mathrm{S}] \tag{4.7g}$$

$$\frac{d[\mathrm{P}]}{dt} = k_2[\mathrm{CpI}][\mathrm{S}] + k_3[\mathrm{CpII}][\mathrm{S}] + k_b[\mathrm{CpIII}][\mathrm{S}] \tag{4.7h}$$

The DAE system can also be obtained in this case, from the total (initial) amount of enzyme obtained analogously to Equation 4.3, and CpI, CpII, CpIII and CpI·H_2O_2 concentrations obtained by Equations 4.7b, 4.7c, 4.7d and 4.7e, respectively:

$$[\mathrm{E}] = [\mathrm{E}]_0 - [\mathrm{CpI}] - [\mathrm{CpII}] - [\mathrm{CpIII}] - [\mathrm{CpI}\cdot\mathrm{H_2O_2}] \tag{4.8a}$$

$$[\mathrm{CpI}] = \frac{k_1[\mathrm{H_2O_2}][\mathrm{E}] + k_b[\mathrm{CpIII}][\mathrm{S}] + k_{-4}[\mathrm{CpI}\cdot\mathrm{H_2O_2}]}{k_2[\mathrm{S}] + k_4[\mathrm{H_2O_2}]} \tag{4.8b}$$

$$[\mathrm{CpII}] = \frac{k_2[\mathrm{CpI}][\mathrm{S}]}{k_3[\mathrm{S}] + k_{app}[\mathrm{H_2O_2}]} \tag{4.8c}$$

$$[\text{CpIII}] = \frac{k_{app}[\text{CpII}][\text{H}_2\text{O}_2]}{k_a + k_b[\text{S}]} \tag{4.8d}$$

$$[\text{CpI} \cdot \text{H}_2\text{O}_2] = \frac{k_4[\text{CpI}][\text{H}_2\text{O}_2]}{k_{-4} + k_5} \tag{4.8e}$$

$$\frac{d[\text{H}_2\text{O}_2]}{dt} = -k_1[\text{E}][\text{H}_2\text{O}_2] - k_{app}[\text{CpII}][\text{H}_2\text{O}_2] - k_4[\text{CpI}][\text{H}_2\text{O}_2] + k_{-4}[\text{CpI} \cdot \text{H}_2\text{O}_2] \tag{4.8f}$$

$$\frac{d[\text{S}]}{dt} = -k_2[\text{CpI}][\text{S}] - k_3[\text{CpII}][\text{S}] - k_b[\text{CpIII}][\text{S}] \tag{4.8g}$$

$$\frac{d[\text{P}]}{dt} = k_2[\text{CpI}][\text{S}] + k_3[\text{CpII}][\text{S}] + k_b[\text{CpIII}][\text{S}] \tag{4.8h}$$

It is worth emphasizing that the enzyme inactive form, given by Equation 2.23, can be considered in the equations 4.4a, 4.6a, and 4.8a, if it is assumed its formation. For example, the equation for the total enzyme amount for the last case is given by equation 4.9:

$$[\text{E}] = [\text{E}]_0 - [\text{CpI}] - [\text{CpII}] - [\text{CpIII}] - [\text{CpI} \cdot \text{H}_2\text{O}_2] - [\text{E}_{inactive}] \tag{4.9}$$

4.1.2 Multi-substrate model

The following model is being proposed in this research considering the degradation of more than one substrate of the same solution, based on the fundamentals presented in section 2.4.3 and in the equations presented in the previous section. Due to the higher number of variables involved in this case, the simplest model will be assumed, considering only the CpI and CpII enzyme forms. Assuming that all substrates interact equally with the enzyme forms, the reactions of Equations 2.13 and 2.14, in this case, can be rewritten as:

$$\text{CpI} + \text{S}_i \xrightarrow{k_{2i}} \text{CpII} + \text{P}_i \tag{4.10}$$

$$\text{CpII} + \text{S}_i \xrightarrow{k_{3i}} \text{E} + \text{H}_2\text{O} + \text{P}_i \tag{4.11}$$

In these reactions, S_i and P_i refer to each substrate and its respective product, and k_{2i}, k_{3i} and k_{bi} are their relative kinetic constants. Then, it's possible to obtain the ODE system generated by the model:

$$\frac{d[\mathrm{E}]}{dt} = -k_1[\mathrm{E}][\mathrm{H_2O_2}] + \sum_{i=1}^{n} k_{3i}[\mathrm{S}_i][\mathrm{CpII}] \tag{4.12a}$$

$$\frac{d[\mathrm{CpI}]}{dt} = k_1[\mathrm{E}][\mathrm{H_2O_2}] - \sum_{i=1}^{n} k_{2i}[\mathrm{S}_i][\mathrm{CpI}] \tag{4.12b}$$

$$\frac{d[\mathrm{CpII}]}{dt} = \sum_{i=1}^{n} k_{2i}[\mathrm{S}_i][\mathrm{CpI}] - \sum_{i=1}^{n} k_{3i}[\mathrm{S}_i][\mathrm{CpII}] \tag{4.12c}$$

$$\frac{d[\mathrm{H_2O_2}]}{dt} = -k_1[\mathrm{E}][\mathrm{H_2O_2}] \tag{4.12d}$$

$$\frac{d[\mathrm{S}_i]}{dt} = -\sum_{i=1}^{n} k_{2i}[\mathrm{S}_i][\mathrm{CpI}] - \sum_{i=1}^{n} k_{3i}[\mathrm{S}_i][\mathrm{CpII}] \tag{4.12e}$$

$$\frac{d[\mathrm{P}_i]}{dt} = \sum_{i=1}^{n} k_{2i}[\mathrm{S}_i][\mathrm{CpI}] + \sum_{i=1}^{n} k_{3i}[\mathrm{S}_i][\mathrm{CpII}] \tag{4.12f}$$

The DAE system can also be obtained in this case, considering also the total (initial) amount of enzyme (Equation 4.3) and assuming the steady-state assumption for the concentrations of all enzyme forms:

$$[\mathrm{E}] = [\mathrm{E}]_0 - [\mathrm{CpI}] - [\mathrm{CpII}] \tag{4.13a}$$

$$[\mathrm{CpI}] = \frac{k_1[\mathrm{H_2O_2}][\mathrm{E}]}{\sum_{i=1}^{n} k_{2i}[\mathrm{S}_i]} \tag{4.13b}$$

$$[\mathrm{CpII}] = \frac{\sum_{i=1}^{n} k_{2i}[\mathrm{S}_i][\mathrm{CpI}]}{\sum_{i=1}^{n} k_{3i}[\mathrm{S}_i]} \tag{4.13c}$$

$$\frac{d[\mathrm{H_2O_2}]}{dt} = -k_1[\mathrm{E}][\mathrm{H_2O_2}] \tag{4.13d}$$

$$\frac{d[\mathrm{S}_i]}{dt} = -\sum_{i=1}^{n} k_{2i}[\mathrm{S}_i][\mathrm{CpI}] - \sum_{i=1}^{n} k_{3i}[\mathrm{S}_i][\mathrm{CpII}] \tag{4.13e}$$

$$\frac{d[\mathrm{P}_i]}{dt} = \sum_{i=1}^{n} k_{2i}[\mathrm{S}_i][\mathrm{CpI}] + \sum_{i=1}^{n} k_{3i}[\mathrm{S}_i][\mathrm{CpII}] \tag{4.13f}$$

4.1.3 Reaction constants used in model development

The kinetic constants taken from the literature listed in Table 4.1 are used as initial guesses for obtaining the kinetic constants in the model simulation and parameter estimation procedures. These reaction rate constants were reported by Nicell (1994) and Nicell and Wright (1997) who made a review based on different authors, and were obtained for the HRP enzyme with the substrates 4-chlorophenol (constants k_2 and k_3) and phenol (constant k_b) at 25ºC and pH 7 (the other kinetic constants are general obtained from the HRP enzyme and its modified forms with hydrogen peroxide as substrate). In this case, although the SBP and HRP enzymes are similar in structure and activity, the different behavior of these enzymes cannot be excluded in the absence of experimental evidence regarding these aspects.

Table 4.1 – Reaction constants used in the model development.

Constant	Value	Units	Source
k_1	2.0 x 10^7	$M^{-1}s^{-1}$	Yamazaki and Nakajima (1986)
k_2	1.13 x 10^7	$M^{-1}s^{-1}$	Job and Dunford (1976)
k_3	1.1 x 10^6	$M^{-1}s^{-1}$	Sakurada et al. (1990)
k_{app}	2.0 x 10^1	$M^{-1}s^{-1}$	Adediran and Lambeir (1989)
k_a	4.2 x 10^{-3}	s^{-1}	Nakajima and Yamazaki (1987)
k_b	9.5 x 10^{-1}	$M^{-1}s^{-1}$	Tamura and Yamazaki (1972)
k_c	1.0 x 10^3	$M^{-1}s^{-1}$	Nakajima and Yamazaki (1987)
k_4	5 x 10^2	$M^{-1}s^{-1}$	Arnao et al. (1990)
k_{-4}	$\simeq 0$	s^{-1}	Arnao et al. (1990)
k_5	1.76	s^{-1}	Arnao et al. (1990)

Source: Adapted from Nicell (1994) and Nicell and Wright (1997).

4.1.4 Model validation and parameter estimation procedures

Based on the model equations described before, the procedure for estimating kinetic constants can be performed, which consists of an optimization procedure with restrictions. The following restrictions for the parameters are considered (NICELL, 1994):

$$k_1 > k_2 > k_3 \gg k_{app}, k_a, k_b, k_c, k_4, k_5 \tag{4.14a}$$

$$k_4 \gg k_{-4} \tag{4.14b}$$

The parameter estimation procedure is implemented using the software MATLAB version R2015a and is illustrated in Figure 4.1:

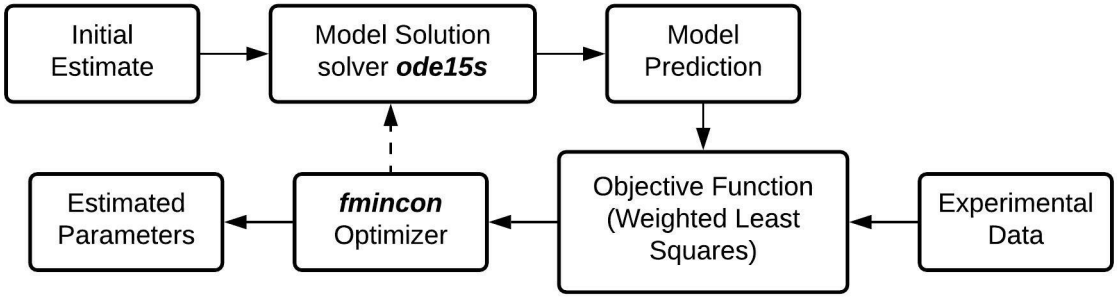

Figure 4.1 – Parameter estimation procedure.

In this procedure, there is a main routine that reads all experimental data and performs the optimization problem through the *fmincon* optimizer using the interior point method and tolerances of 10^{-10}. The model solution is then carried out by the backward differentiation formula (BDF) method, using *ode15s* solver implemented on MATLAB. Relative and absolute tolerances of 10^{-8} and 10^{-10}, respectively, are considered. Other method settings are considered as default. The values reported in Table 4.1 are used as initial estimates for obtaining the kinetic constants, and it is also performed a reparameterization of the kinetic constants with the natural logarithm of the values, to ensure that the system is using positive values, that is, with real physical meaning in this case that the kinetic constants are positive numbers.

The objective function (OF) is then minimized by means of the weighted least squares function, obtained from the maximum likelihood method (SCHWAAB; PINTO, 2007). This function takes into account the calculated values predicted by the model ($\widehat{u_i}$) and their respective experimental data set (u_i) for the number of points (n) and the number of experiments (m), as shown in Equation 4.15. This equation also considers the standard deviation of the experimental data (σ), calculated for each set of experiments according to Equation 4.16, where $\overline{u}_i$ is the average of the experimental data (CUNHA et al., 2021).

$$\mathrm{OF} = \min \sum_{j=1}^{m} \sum_{i=1}^{n} \frac{(\widehat{u}_{ij} - u_{ij})^2}{2\sigma_{ij}^2} \tag{4.15}$$

$$\sigma = \sqrt{\frac{\sum_{i=1}^{n} (u_i - \overline{u}_i)^2}{n}} \tag{4.16}$$

The model fit is then evaluated from the plots of model prediction and experimental data, and the calculated values of root-mean-square error (RMSE) and the adjusted coefficient of determination ($\mathrm{R}^2_{\mathrm{adjusted}}$), shown in Equations 4.17 and 4.18, respectively, where p is the number of parameters.

$$\mathrm{RMSE} = \left[\sum_{i=1}^{n} \frac{(\widehat{u}_i - u_i)^2}{n} \right]^{1/2} \tag{4.17}$$

$$\mathrm{R}^2_{\mathrm{adjusted}} = 1 - \frac{(1 - R^2)(n-1)}{n - (p+1)} \tag{4.18}$$

$$\mathrm{R}^2 = 1 - \frac{\sum_{i=1}^{n} (\widehat{u}_i - u_i)^2}{\sum_{i=1}^{n} (\widehat{u}_i - \overline{u}_i)^2} \tag{4.19}$$

The smaller the numerical value of RMSE and the higher the numerical value of the adjusted R^2, the better the model fit. Adjusted R^2 is used instead of R^2 because it is considered more appropriate for both evaluating model fit and comparing alternative models due to the inclusion of a penalty for additional parameters that do not contribute to model fit. In other words, adjusted R^2 penalizes the model adjustment for adding terms that are not useful, so it is very useful in evaluating and comparing regression models (PECK et al., 2012). However, as this criterion is not always reliable for non-linear models, it should always be used in conjunction with other criteria. The model fit is then evaluated by the value of OF obtained from Equation 4.15 in each case since a smaller value indicates a better minimization of the OF and consequently a better result in the optimization procedure.

The model simulation is first evaluated based on the process modeling considering six scenarios with different hypotheses to simplify the bi-bi ping-pong model, as shown below:

- **Model 1:** Formation of CpI and CpII (Equations 4.4a to 4.4f), to estimate parameters k_1, k_2, and k_3;
- **Model 2:** Formation of CpI, CpII, and CpIII (Equations 4.6a to 4.6g), to estimate parameters k_1, k_2, k_3, k_{app}, k_a, k_b, and k_c;
- **Model 3:** Formation of CpI, CpII, CpIII, and CpI·H_2O_2 (Equations 4.8a to 4.8h), to estimate parameters k_1, k_2, k_3, k_{app}, k_a, k_b, k_4, k_{-4}, and k_5;
- **Model 4:** Model 1 including enzyme inactivation (Equation 2.23), to estimate parameters k_1, k_2, and k_3;
- **Model 5:** Model 2 including enzyme inactivation (Equation 2.23), to estimate parameters k_1, k_2, k_3, k_{app}, k_a, k_b, and k_c;
- **Model 6:** Model 3 including enzyme inactivation (Equation 2.23), to estimate parameters k_1, k_2, k_3, k_{app}, k_a, k_b, k_4, k_{-4}, and k_5.

All these scenarios are considered to obtain preliminary results with the available experimental data presented in the next subsection, obtained for the reactions of substrate TCP with enzyme SBP. Further experiments are conducted to obtain the model also for the other substrates and conditions considered.

4.2 EXPERIMENTS

The experiments performed in this research can be divided into four parts. Firstly, the reactions of TCP degradation are conducted in a microreactor using a commercial sample of HRP enzyme to compare its performance with a commercial sample of SBP under the same conditions previously carried out by Costa (2016). Additionally, studies on the reaction conditions such as pH, temperature, and H_2O_2 concentration, and reactions of TCS degradation using HRP are also performed (reactions with BPA were conducted only in batch). This part is developed in the laboratory of the Department of Chemical Engineering, Polytechnic School, University of São Paulo.

The second part of the experiments consists of the process of extraction and purification of SBP from the soybean seed hulls, to produce this enzyme as efficiently as possible to be used

in further experiments. After this, further studies are performed using the produced enzyme for the degradation in batch of the substrates TCP, TCS and BPA both individually and as a mixture, to simulate a scenario closer to a real application. Finally, a toxicity test of the reaction products is also carried out. These experiments are performed in the laboratory of the Department of Chemistry, University of Turin.

4.2.1 Enzymatic reactions in the microreactor

The reactions are conducted in the microreactor shown in more detail in subsection 4.2.1.6. In all reactions in the microreactor, the experimental points are obtained in triplicate for a given residence time. When adjusting a flow rate on the equipment, there is a residence time ($t_{\text{residence}}$) that is equivalent to a point in the kinetics study. That is, considering the reaction volume in the microreactor of 250 μL, each residence time is calculated by:

$$t_{\text{residence}} = \frac{250\ \mu\text{L}}{\text{Flow}} \tag{4.20}$$

4.2.1.1 Study of TCP degradation

First, it is carried out a set of experiments in the microreator on TCP degradation in the same conditions as conducted previously by Costa (2016) (see section 3.2.1), but using the commercial enzyme HRP type VI-A provided by Sigma-Aldrich with purity claimed to be very close to 100%. By using two syringes, the dilution in the microreactor is 1:2, then all solutions shall be prepared at twice the concentration considered in the reaction: $[H_2O_2]$ = 0.6 mM, [TCP] = 0.5 mM and [HRP] = 1.04 x 10^{-8} M, 2.08 x 10^{-8} M, and 4.16 x 10^{-8} M. All the solutions are prepared in potassium phosphate buffer (0.2 M, pH 5.4). HCl 0.1 M solution is used as an inhibiting solution responsible for stopping the enzymatic reaction by the denaturation of the enzyme caused by the drop in pH. The solutions are prepared as the following:

- **Phosphate buffer:** It is diluted 27.8 g of KH_2PO_4 per liter of demineralized water, obtaining a solution of 0.2 M. NaOH is added to adjust the pH to 5.4. Data: KH_2PO_4 molar weight = 136.09 g/mol.

$$[KH_2PO_4\ \text{buffer}] = \frac{27.8\ \text{g}}{139.09\ \text{g/mol} \cdot 1\ \text{L}} = 0.2\ \text{M}$$

- **Hydrogen peroxide:** It is added 4 μL of H_2O_2 7.56 M in 50 mL of phosphate buffer solution, obtaining a 0.6 mM solution.

$$[H_2O_2] = \frac{0.004 \text{ mL} \cdot 7.56 \text{ M}}{50 \text{ mL}} = 0.6 \text{ mM}$$

- **TCP:** It is added 10 mg of solid TCP in 100 mL of phosphate buffer solution, obtaining a solution of 0.5 mM. Data: TCP molar weight = 197.45 g/mol.

$$[\text{TCP}] = \frac{0.01 \text{ g} / 0.1 \text{ L}}{197.45 \text{ g/mol}} = 0.5 \text{ mM}$$

- **HRP:** Firstly, it is prepared a concentrated solution using 3 mg of solid HRP and 10 mL of phosphate buffer solution. To calculate the real HRP concentration, it is necessary to do a UV-spectrophotometer analysis to obtain the UV-visible spectrum of the solution (see subsection 4.2.4). This solution is then diluted to obtain the desired concentrations.

4.2.1.2 TCP calibration curve

To obtain the TCP calibration curve, 1 mL samples containing 900 μL of HCl 0.1 M are used adding a varying volume of TCP solution 0.5 mM previously prepared, as shown in Table 4.2. These samples are analyzed in the HPLC system, and the areas obtained for each corresponding concentration are used to obtain the calibration curve.

Table 4.2 – Data to obtain the TCP calibration curve.

Sample	TCP volume (μL)	H_2O volume (μL)	HCl volume (μL)	TCP concentration (μL)
1	100	0	900	0.05
2	80	20	900	0.004
3	60	40	900	0.03
4	40	60	900	0.02
5	20	80	900	0.01
6	5	95	900	0.0025
7	0	100	900	0

4.2.1.3 TCP quantification

The samples of both the calibration curve and the reaction products are analyzed offline on ultra-fast liquid chromatography (Shimadzu LC-20AD Prominence). At the end of the reaction process, a 100 μL sample of the final solution is collected at the microreactor outlet and added to 900 μL of the reaction inhibitor (HCl) to stop the reaction and obtain reliable data. Thus, in all the cases the volume to be analyzed is the same.

The HPLC system operated at (COSTA, 2016):

- Column: Phenomenex Luna C18;
- Eluent: 60% acetonitrile + 40% demineralized water with 0.2% acetic acid;
- Flow: 0.6 mL/min;
- Temperature: 40 ºC;
- Estimated analysis time: 10 min;
- Detector, λ = 220 nm;
- Injection volume: 10 μL.

4.2.1.4 Study of pH, temperature, and H_2O_2 concentration influence

A set of experiments to analyze the influence of the operational conditions on the enzyme HRP activity is also carried out. To study the pH and temperature influence, TCP, H_2O_2, and HRP concentrations are fixed at 0.25 mM, 0.3 mM, and 1.04 x 10^{-8} M, respectively. The pH is varied from 4 to 7 at a fixed temperature of 25 °C, and the temperature is varied from 10 °C to 40 °C at a fixed pH of 7. Different phosphate buffer solutions to keep the solutions at the required pH are necessary, and the temperature can be varied simply by setting it on the microreactor. The H_2O_2 concentration influence is analyzed by considering the same TCP and HRP concentrations and varying the H_2O_2 concentrations from 0 to 0.6 mM.

4.2.1.5 Study of TCS degradation

Experiments of TCS degradation are also carried out regarding the same conditions considered for TCP degradation using HRP. The TCS solution is prepared by adding 14.5 mg of solid TCS in 100 mL of phosphate buffer solution, obtaining also a 0.5 mM solution (Data: TCS molar weight = 289.54 g/mol):

$$[\text{TCS}] = \frac{0.0145 \text{ g} / 0.1 \text{ L}}{289.54 \text{ g/mol}} = 0.5 \text{ mM}$$

Regarding the low solubility of TCS in water, it is necessary to add a small quantity of NaOH 0.01 M to increase its solubility (LI et al., 2016). The TCS calibration curve is carried out similarly as described for the TCP calibration curve. The TCS quantification is carried out in a similar way as described for TCP quantification, but considering the operational conditions as Li et al. (2016): methanol and water mixture (90%/10%) as eluent and flow rate of 0.8 mL/min.

4.2.1.6 Experimental unit

The reactions are carried out in a Syrris microreactor of the laboratory of the Department of Chemical Engineering, Polytechnic School, University of São Paulo. This equipment is suitable for fast reactions such as the enzymatic ones and has similar functions to the conventional chemical reactors but in micrometric dimensions (LAURENTI; VIANNA JR, 2016). It consists of subunits, where each module is responsible for a unitary operation, as Figure 4.2.

(a) Reagent storage system

(b) Flow control system

(c) Temperature control system

(d) Chip - Microreactor

(e) Microreactor base

Figure 4.2 – Microreactor components.
Source: SYRRIS (2022).

The vessels are for reagent storage but can also be used as pressure vessels, as shown in Figure 4.2(a). They can be pressurized with an inert gas injection to a pressure of 10 bar, and the outlet is maintained at a pressure of 1 bar. This allows good inlet flow and minimizes cavitation and gas bubble formation during pumping at high flow rates. A system with two pumps and micro syringes shown in Figure 4.2(b) is used for flow and pressure control. The system is controlled by a twisting front panel and the click of a control button. There is also a temperature control unit, as shown in Figure 4.2(c), where the microreactor (chip) shown in Figure 4.2(d) is coupled. The microreactor (chip) is made of glass, allowing the visualization of the reactive flow. The working temperature range is between -20 ºC to 250 ºC and the working pressure is up to 30 bar. The chip header, shown in Figure 4.2(e), allows alignment and connection of inputs and outputs through tubes and is fixed to the microreactor. All modules are Syrris branded and make up the Asia system for flow chemistry.

4.2.2 Soybean peroxidase extraction and purification

4.2.2.1 Soybean peroxidase extraction and catalytic evaluation

The SBP enzyme is obtained from the soybean seed hulls and its catalytic activity is evaluated. The extraction and purification are carried out by the following procedure (CALZA et al., 2016; TOLARDO et al., 2019):

- The soybean seeds are immersed in distilled water long enough for the hulls to be removed by hand. Then the hulls are dried and stored at -12 ºC until use;
- 100 grams of seed hulls are added to 600 mL of phosphate buffer (0.025 M, pH 7), stirred for 2 h at room temperature, separated from the solution by filtration with cotton gauze, and centrifuged for 20 min at 4000 RPM. Then the supernatant is separated and tested for peroxidase activity test with the H_2O_2/DMAB-MBTH system (see next subsection). This treatment is repeated with decreasing phosphate buffer volume until the resulting solution gives a negative response to the activity test;
- The SBP-containing solutions are concentrated by a tangential filter (cut-off 10000 Da). The proteins are then precipitated by the addition of ammonium sulfate until saturation (53 g/100 mL), and the mixture is left under stirring for one night at 4 ºC;
- The precipitate is centrifuged for 20 min at 4000 RPM and dissolved in 250 mL of phosphate buffer. The resulting solution is then dialyzed for 24h at 4 ºC in cellulose tubes against several aliquots of the same buffer;

- The dialyzed fraction is loaded onto a column containing ionic exchange resin (DEAE-Sepharose CL-6B), washed with 3 volumes of phosphate buffer, and eluted with a KCl gradient 0-0.5 M (500 mL) in the same buffer. The fractions are collected and analyzed by UV-visible spectroscopy. The selected fractions are pooled and concentrated by tangential filtration;
- The final SBP sample is then stored at -12 ºC until use.

4.2.2.2 Soybean peroxidase activity assay

The enzyme activity assay is carried out by the method developed by Ngo and Lenhoff (1980), which allows for studying the influence of H_2O_2 concentration on the SBP activity. This method is based on the oxidative coupling of 3-(dimethylamino)benzoic acid (DMAB) and 3-methyl-2-benzothiazolinone hydrazone (MBTH). In the presence of these reagents and H_2O_2, the peroxidase catalyzes the formation of a stable deep purple compound, which has a broad absorption band between 575 and 600 nm with a maximum of 590 nm. This compound has a molar absorptivity (ε) at 590 nm of 47600 $M^{-1}cm^{-1}$ (NGO; LENHOFF, 1980). The reaction is represented in Figure 4.3.

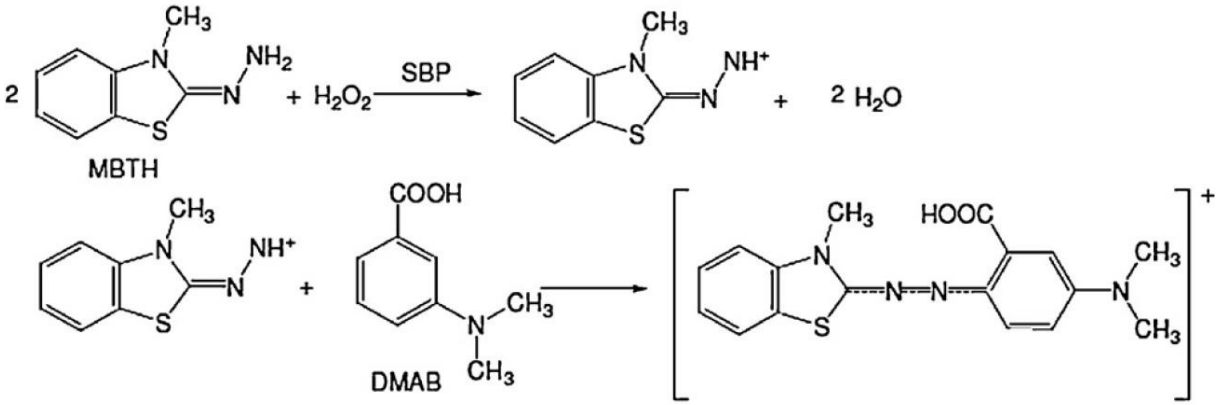

Figure 4.3 – The DMAB-MBTH reaction.
Source: Ngo and Lenhoff (1980).

The activity assay is carried out using spectrophotometric analysis at a wavelength fixed at 590 nm, following the development of color over time. The assay is realized as the following (TOLARDO et al., 2019):

- 10 μL of SBP containing supernatant is added to 3 mL of a solution containing DMAB 0.5 mM, MBTH 2 mM, H_2O_2 0.1 mM and acetate buffer (0.1 M, pH 5.4);

- The reaction is carried out in a cuvette and the enzymatic activity is measured by following the increase of absorbance at 590 nm of the reaction product for 3 minutes;
- The activity is graphically obtained from the slope of the initial linear section of the curve, which is expressed as ΔAbs/s or ΔAbs/min;
- From the slopes of the curves, the concentrations in moles of product per minute can be calculated from the Equation 4.21, where ε = 47600 $mol^{-1}cm^{-1}$ and b = 1:

$$Abs = C\ \varepsilon\ b \tag{4.21}$$

4.2.3 Enzymatic batch reactions

After obtaining the purified SBP, further experiments are performed in batches, to carry out the reactions in a scenario closer to a real application. In this case, the process represents a global kinetics, where mass transfer is also considered, unlike the microreactor, where the kinetics is intrinsic. It is evaluated the behavior of SBP in a medium with multiple organic substrates, composed of TCP, TCS, and BPA, and the degradation of these substrates in single-substrate solutions and in a multi-substrate solution is compared. It is also compared the behavior of the obtained SBP and the commercial HRP enzyme. All enzymatic batch reactions are conducted in a beaker with constant stirring using magnets, in a total reaction volume of 10 mL. Samples of 10 μL are collected and manually injected into the HPLC system to be analyzed throughout the reaction, so that the variation in the total reaction volume is not significant.

4.2.3.1 Preparation of solutions

For each substrate, it is prepared a mother solution in acetonitrile at a concentration of 1000 mg/L, to avoid problems with the solubility of the substrate in water. The final solutions may be prepared by diluting them in MilliQ water in a way that the acetonitrile concentration is less than 0.5%, which does not impact the enzyme (DOU et al., 2018). The reactions will be carried out considering fixed concentrations of 5 ppm and 0.1 mM for the substrates and H_2O_2, respectively, and enzyme concentrations of 4.39 x 10^{-9} M, 8.77 x 10^{-9} M, and 1.75 x 10^{-8} M. The solutions are prepared as the following:

- **Hydrogen peroxide:** It is added 13 μL of H_2O_2 9.7 M in 10 mL of MilliQ water, obtaining a solution of 0.0127 M. Then it is used 80 μL of this solution in 10 mL of reaction volume, obtaining a concentration of 0.1 mM in reaction.

- **SBP:** As the obtained SBP enzyme is a concentrated liquid, the procedure is only diluting it until obtaining the desired concentrations. To calculate the concentration, it is necessary to obtain the UV-visible spectrum of the solution (see subsection 4.2.4). This solution is then diluted to obtain the desired concentrations.
- **HRP:** As done for the reactions in the microreactor, it is prepared a concentrated solution using 3 mg of solid HRP and 10 mL of MilliQ water. The HRP concentration is calculated by the UV-visible spectrum of the solution (see subsection 4.2.4). This solution is then diluted to obtain the desired concentrations.
- **TCP:** It is added 25 mg of solid TCP in 25 mL of acetonitrile, obtaining a mother solution of 1000 mg/L (1000 ppm). Then is used 50 μL of mother solution per 10 mL of TCP solution, obtaining 5 ppm. Data: TCP molar weight = 197.45 g/mol.

$$[\text{TCP}] = \frac{5 \text{ ppm}}{197.45 \text{ g/mol}} = \frac{0.005 \text{ g/L}}{197.45 \text{ g/mol}} = 0.0253 \text{ mM}$$

- **TCS:** It is added 25 mg of solid TCS in 25 mL of acetonitrile, obtaining a mother solution of 1000 mg/L (1000 ppm). Then is used 50 μL of mother solution per 10 mL of TCS solution, obtaining 5 ppm. Data: TCS molar weight = 289.54 g/mol.

$$[\text{TCS}] = \frac{5 \text{ ppm}}{289.54 \text{ g/mol}} = \frac{0.005 \text{ g/L}}{289.54 \text{ g/mol}} = 0.0173 \text{ mM}$$

- **BPA:** It is added 25 mg of solid BPA in 25 mL of acetonitrile, obtaining a mother solution of 1000 mg/L (1000 ppm). Then is used 50 μL of mother solution per 10 mL of TCS solution, obtaining 5 ppm. Data: BPA molar weight = 228.29 g/mol.

$$[\text{BPA}] = \frac{5 \text{ ppm}}{228.29 \text{ g/mol}} = \frac{0.005 \text{ g/L}}{228.29 \text{ g/mol}} = 0.0219 \text{ mM}$$

4.2.3.2 Substrates quantification

Calibration curves are carried out for TCP, TCS, and BPA, by preparing solutions of different concentrations in MilliQ water, analyzing them in the HPLC system, and correlating the areas obtained with their corresponding concentrations. In this case, it is not necessary to dilute the samples in HCl, because it is not necessary to stop the reaction as it is used manual injection and the analyzes are carried out at the exact time of the reaction. The samples of the

calibration curve and the reactions are analyzed on ultra-fast liquid chromatography (Hitachi L-4000 UV Detector). The operational conditions for the HPLC system are set in such a way that it is possible to observe the curves of all three components well since they are also analyzed in a mixed solution. The HPLC system operated at:

- Column: LiChrospher 100 RP-18;
- Eluent: 70% acetonitrile + 30% phosphate buffer solution;
- Flow: 1 mL/min;
- Temperature: 40ºC;
- Estimated analysis time: 10 min;
- Detector, λ = 242 nm;
- Injection volume: 10 μL.

4.2.4 Spectrophotometer analysis of enzyme samples

Enzyme samples are analyzed in a double-beam Unicam UV 300 spectrophotometer, to obtain the UV/visible spectrum of the enzymes. The enzyme concentration can be calculated from the maximum absorbance of the Soret band at 403 nm (typical for Fe(III)-heme group in HRP and SBP). It is known that the HRP enzyme has a molar absorptivity (ε) at 403 nm of 102000 $M^{-1}cm^{-1}$ and SBP enzyme has a molar absorptivity at 403 nm of 94600 $M^{-1}cm^{-1}$ (KAMAL; BEHERE, 2002). Considering also a pathlength (L) of 1 cm, the enzyme concentration can be calculated as the following:

$$\varepsilon_{403nm} = \frac{\text{Abs}_{403nm}}{[\text{Enzyme}]\text{L}} \tag{4.22}$$

$$[\text{Enzyme}] = \frac{\text{Abs}_{403nm}}{\varepsilon_{403nm}\text{L}} \tag{4.23}$$

An evaluation of the degree of purity of the enzyme sample can be set from the RZ values (Reinheitszahl), which compare the absorption due to heme content with the protein structure. For peroxidases, the RZ is calculated by:

$$\text{RZ} = \frac{\text{Abs}_{403nm}}{\text{Abs}_{280nm}} \tag{4.24}$$

4.2.5 Toxicity test

A toxicity test of the mix solution with TCP, BPA, and TCS was also carried out, to confirm that the reaction products have lower toxicity than the reactants. Acute toxicity is evaluated by a bioluminescence inhibition assay using the marine bacterium *Vibrio fischeri* (JIMENEZ-HOLGADO et al., 2021). Changes in the natural emission of the luminescent bacteria were recorded in a Microtox Model 500 Toxicity Analyzer (Milan, Italy) after 3 different exposure times (5, 15 and 30 minutes) to the mix solution containing TCP, BPA and TCS, both before and after the degradation reaction with the SBP enzyme. It is noteworthy that in the toxicity tests the SBP enzyme immobilized in SiO_2 was used, so in this case the enzymatic reaction can be interrupted by simply removing the immobilized enzyme. Studies related to enzyme immobilization are not part of the scope of this work.

CHAPTER 5
EXPERIMENTAL RESULTS AND DISCUSSION

5.1 MICROREACTOR REACTIONS RESULTS

The first part of the experiments consisted of carrying out degradation reactions using the commercial enzyme HRP at the microreactor of the Department of Chemical Engineering, Polytechnic School, University of São Paulo. First, the reactions were carried out under the same conditions previously conducted by Costa (2016) using the commercial enzyme SBP. After, the influence of pH, temperature, and H_2O_2 concentration on the TCP degradation was studied. Finally, TCS degradation was also carried out. It should be noted that all the reaction times in the graphs presented in this section refer to the residence times in the microreactor.

5.1.1 Spectroscopic analysis of commercial HRP enzyme

First, the commercial enzyme HRP was analyzed at the spectrophotometer to calculate its concentration, and the UV/visible spectrum obtained is shown in Figure 5.1:

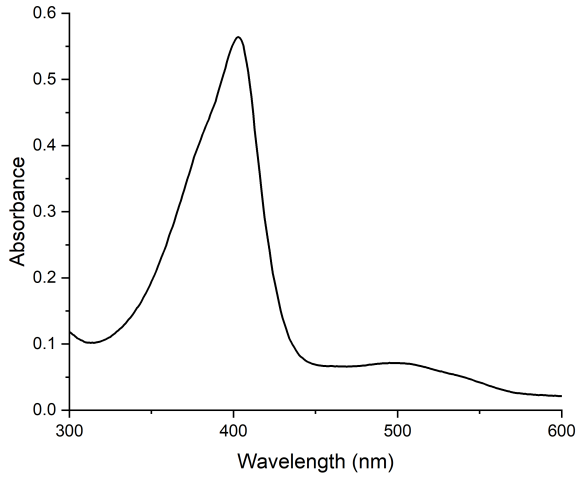

Figure 5.1 – UV/Visible spectrum of commercial HRP enzyme.

The maximum absorbance of the Soret band at 403 nm, in this case, was 0.564, and with this value the HRP concentration is calculated as described in subsection 4.2.4:

$$[\text{HRP}] = \frac{\text{Abs}_{403nm}}{\varepsilon_{403nm} L} = \frac{0.564}{102000\ \text{M}^{-1}\text{cm}^{-1}1\text{cm}} = 5.53\ \text{x}\ 10^{-6}\ \text{M} \tag{5.1}$$

Then, considering the concentration of [HRP] = 5.53 x 10^{-6} M of the HRP concentrated solution, it can be diluted to obtain the desired concentrations of 1.04 x 10^{-8} M, 2.08 x 10^{-8} M, and 4.16 x 10^{-8} M to carry out the degradation reactions.

5.1.2 2,4,6-Triclorophenol

5.1.2.1 Calibration curve of TCP

TCP was identified by HPLC analysis at a retention time of approximately 5.8 minutes. The TCP calibration curve was obtained as shown in Figure 5.2, with R^2 = 99.95%. It is used to quantify the TCP concentration on the degradation reactions with HRP.

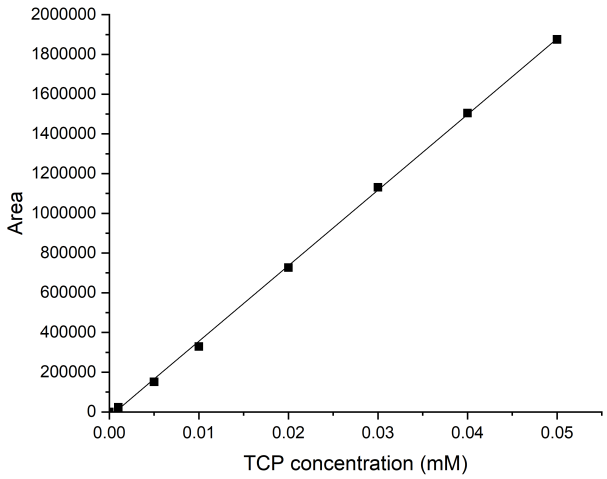

Figure 5.2 – TCP calibration curve.

5.1.2.2 TCP degradation

The curves of TCP degradation with HRP are shown in Figure 5.3. All the measurements were done in triplicate, with acceptable repeatability. These results can be compared to the TCP degradation with SBP obtained previously by Costa (2016), as shown in Figure 5.4.

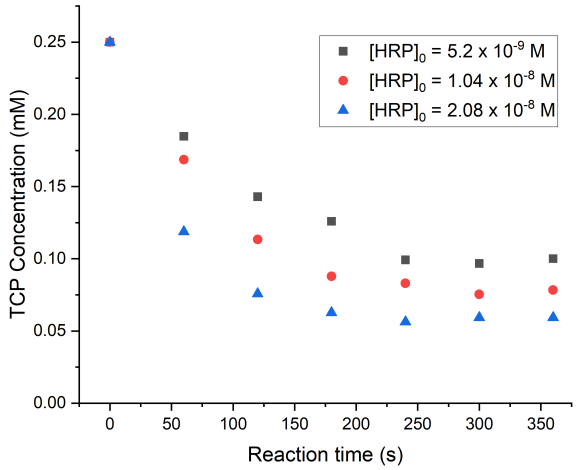

Figure 5.3 – TCP degradation with HRP.

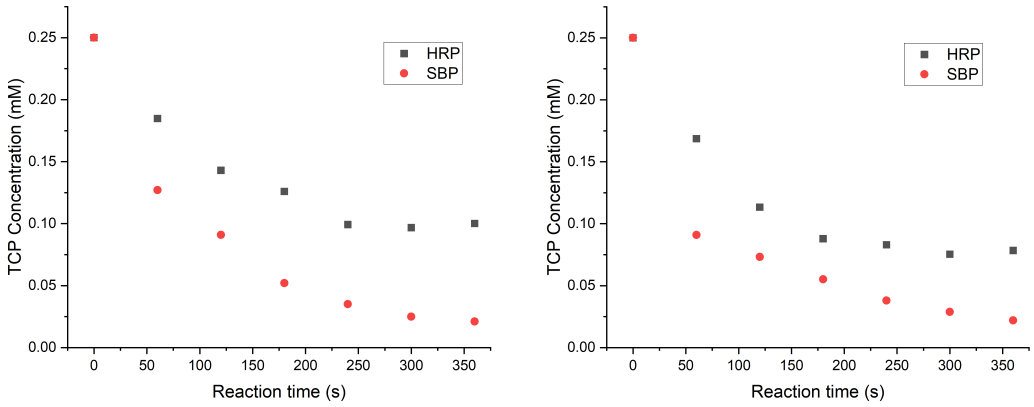

(a) E = 5.2 x 10^{-9} M.

(b) E = 1.04 x 10^{-8} M.

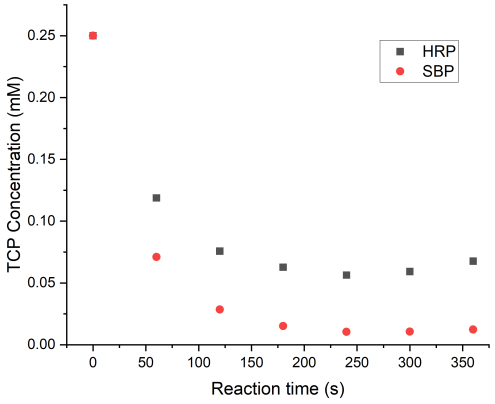

(c) E = 2.08 x 10^{-8} M.

Figure 5.4 – Comparison between TCP degradation with SBP and HRP enzymes.

For both the SBP and HRP enzymes, it was possible to verify the influence of the enzyme concentration in the reaction, with a higher degradation of TCP to a greater enzyme concentration. These data point out that the degradation was more efficient using the enzyme SBP. The maximum percentage of degradation achieved using SBP was approximately 96%, while for HRP it was approximately 78%. Different behavior of these enzymes was expected, but not necessarily at this level. However, it should be noted that doing this comparison directly is quite sensitive, as we are dealing with very small concentrations, with a series of approximations made in the concentration calculations, and mainly the experimental errors involved because they were performed on different occasions. Anyway, both results are also valid to confirm the good repeatability of the microreactor in carrying out the enzymatic reactions, which is also one important objective of this work.

5.1.2.3 Study of pH, temperature, and H_2O_2 concentration influence

It was carried out a study to analyze the influence of the operational conditions of the reactions, as shown in Figure 5.5. In all the cases, the TCP and HRP concentrations were fixed at 0.25 mM and 2.08 x 10^{-8} M, respectively. In Figures 5.5(a) and 5.5(b), the H_2O_2 concentration was fixed at 0.3 mM, and in Figure 5.5(c) the H_2O_2 concentration was varied from 0 to 0.6 mM. In Figures 5.5(a) and 5.5(c), the temperature was fixed at 25 ºC, and in Figures 5.5(b) and 5.5(c), the pH was fixed at 7.

In the case of pH, the data are in agreement with the literature (FERRARI et al., 1999), because it was expected a higher enzyme efficiency at pH between 5 and 6 and the opposite at pH out of this range, in which the efficiency gradually decreases. Substrate degradation varies with pH change because they depend on the changes in protonation of the amino acids responsible for the formation of compound I and substrate protonation state. As for the temperature, the enzyme efficiency decreased for temperatures above ambient conditions. This behavior is likely due to the contemporary presence of the opposite effects: enhancement of thermodynamic and structural modifications of the HRP active site (if the active site remains a little more open, as at higher temperatures, the formation of compound I is more difficult). Regarding the concentration of H_2O_2, a small change in the degradation rate was observed, with a slightly higher efficiency for 0.3 mM. Some TCP degradation was also observed in the absence of H_2O_2, which was not expected. This may have occurred due to traces of H_2O_2 present in the equipment.

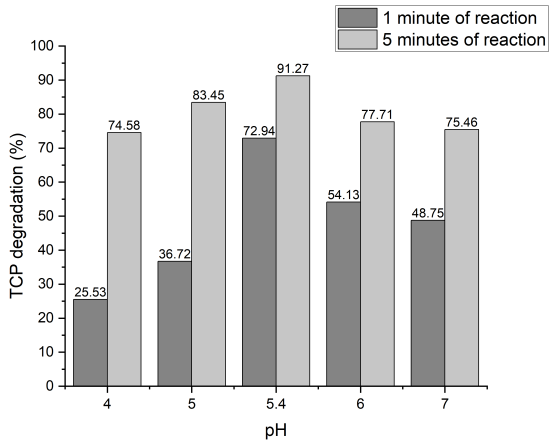

(a) pH influence.

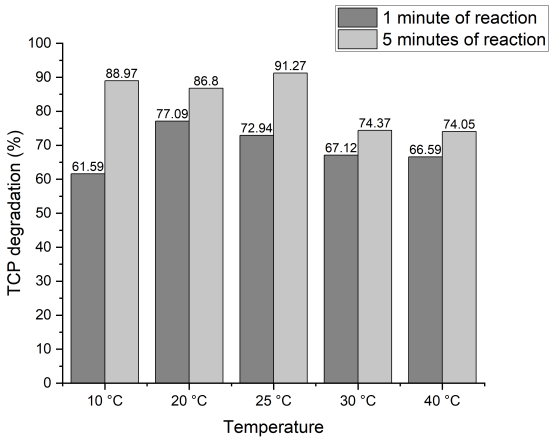

(b) Temperature influence.

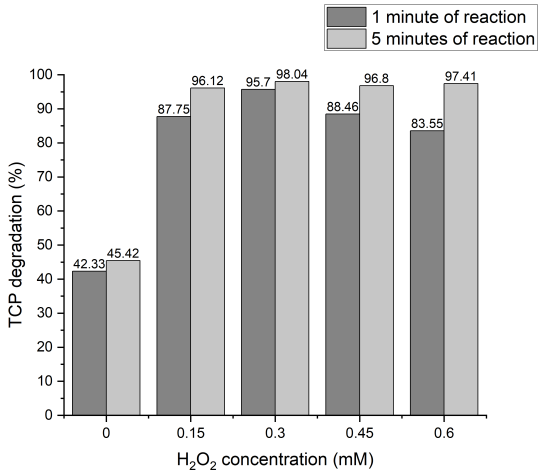

(c) H_2O_2 concentration influence.

Figure 5.5 – Study of pH, temperature, and H_2O_2 concentration influence.

5.1.3 Triclosan

5.1.3.1 Calibration curve of TCS

TCS was identified by HPLC analysis at a retention time of approximately 2.7 minutes. The TCS calibration curve was obtained as shown in Figure 5.2, with R^2 = 99.29%. It is used to quantify the TCS concentration on the degradation reactions with HRP.

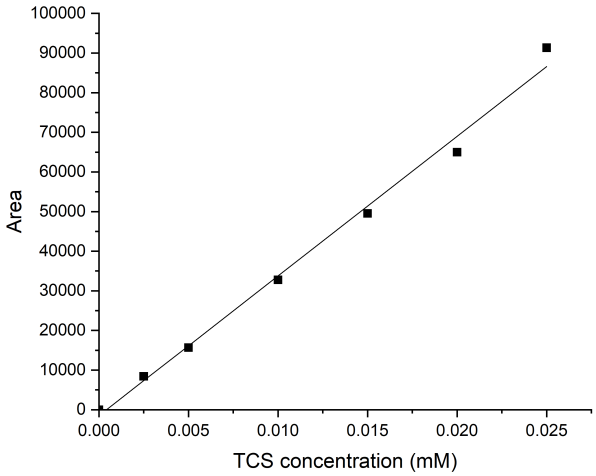

Figure 5.6 – TCS calibration curve.

5.1.3.2 TCS degradation

The curves of TCS degradation with 3 different concentrations of HRP are shown in Figure 5.7. All the measurements were done in triplicate, with acceptable repeatability.

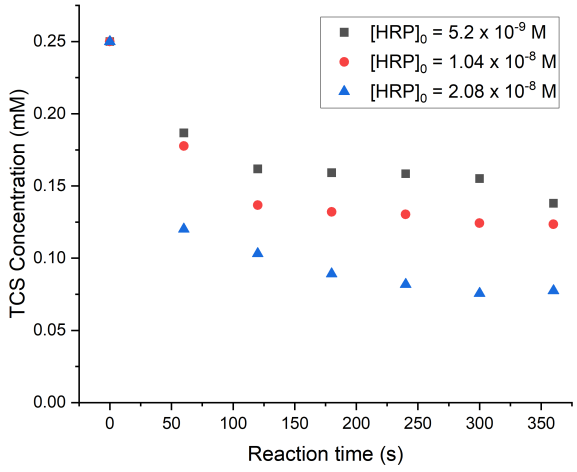

Figure 5.7 – TCS degradation with HRP.

It can be observed in this case a similar behavior as obtained before for TCP, with a higher degradation of TCS to a greater concentration of HRP. The maximum percentage of degradation achieved was approximately 70%, which can be considered a reasonable value. These results also corroborate the good repeatability of the microreactor, justifying its use for enzymatic reaction kinetic studies.

5.2 RESULTS OF THE EXTRACTED SOYBEAN PEROXIDASE

The enzyme SBP was obtained successfully by the soybean seed hulls after carrying out the procedure detailed in section 4.2.2.1. The activity test and spectroscopic analysis of the extracted enzyme are demonstrated in the next sections, confirming the presence of the SBP enzyme in the product obtained.

5.2.1 Activity test of the obtained SBP enzyme

The activity test is based on a colorimetric assay that uses the oxidative coupling of DMAB (3-(dimethylamino)benzoic acid) and MBTH (3-methyl-2-benzothiazolinone hydrazone), as described in section 4.2.2.2. The peroxidase, in the presence of this pair of reactants and H_2O_2, catalyzes the formation of a dark purple compound that absorbs between 575 and 600 nm with maximum absorption at 590 nm. The activity graphs obtained by the spectrophotometric analysis described in section 4.2.2.2 are shown in Figure 5.8.

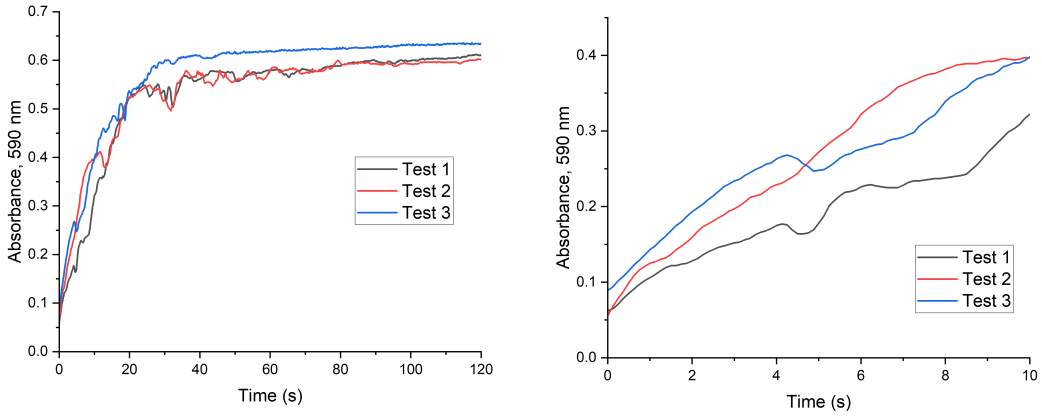

(a) 120-second reaction. (b) 10-second reaction.

Figure 5.8 – Activity test of the obtained SBP.

Using this assay, it is possible to construct a calibration curve, as Figure 5.9, which can be used to evaluate the amount of protein contained in the different extracts. Considering the average of the slopes, the activity of 35 μmol/min is obtained.

5.2.2 Spectroscopic analysis of obtained SBP enzyme

A small sample of the protein was diluted at 1:25 in MilliQ water to analyze its UV/visible spectrum, which is shown in Figure 5.10.

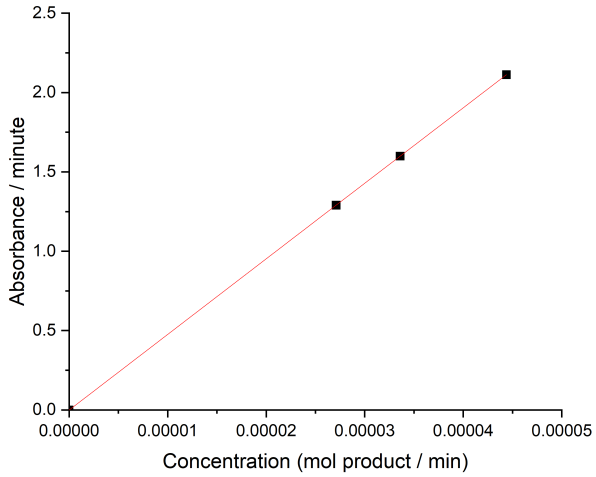

Figure 5.9 – Calibration curve of the activity test.

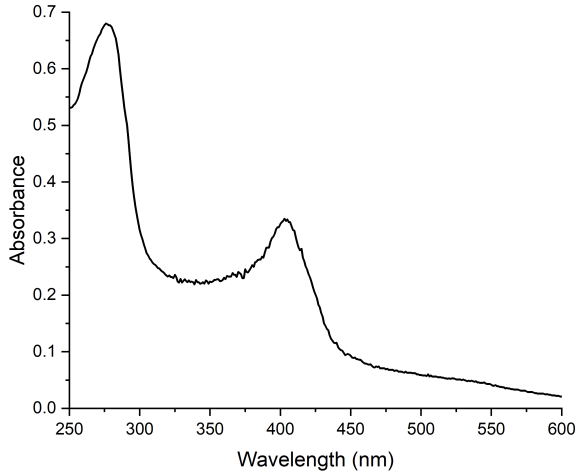

Figure 5.10 – UV/Visible spectrum of obtained SBP enzyme.

The maximum absorbance at 403 nm obtained was 0.335, and with this value the SBP concentration is calculated as described in subsection 4.2.4:

$$[\text{SBP}] = \frac{\text{Abs}_{403nm}}{\varepsilon_{403nm} L} = \frac{0.335}{94600\ \text{M}^{-1}\text{cm}^{-1}1\text{cm}} = 3.54\ \text{x}\ 10^{-6}\ \text{M} \tag{5.2}$$

Considering the dilution factor of 25, the concentration of the concentrated SBP solution is 8.85 x 10^{-5} M. This solution is then diluted in MilliQ water to obtain the desired concentrations. First, it is diluted at 1:10, then are taken 5 μL, 10 μL, or 20 μL per 10 mL of reaction volume to obtain the concentrations of 4.39 x 10^{-9} M, 8.77 x 10^{-9} M, and 1.75 x 10^{-8} M, respectively, which are considered in the degradation reactions.

From the UV/visible spectrum of Figure 5.10, it was also obtained an absorbance of 0.674 at 280 nm, then the RZ value can be calculated:

$$\mathrm{RZ} = \frac{\mathrm{Abs}_{403nm}}{\mathrm{Abs}_{280nm}} = \frac{0.335}{0.674} = 0.45 \tag{5.3}$$

This value suggests that the protein obtained is not particularly pure, probably because of an aging factor of the soybean hulls.

5.2.3 Spectroscopic analysis of commercial HRP enzyme

Commercial HRP enzyme is used for comparison with the obtained SBP enzyme and also to carry out degradation reactions. The concentrated solution (0.3 mg/mL) was diluted at 1:10 in MilliQ water, and the UV/visible spectrum obtained is shown in Figure 5.11:

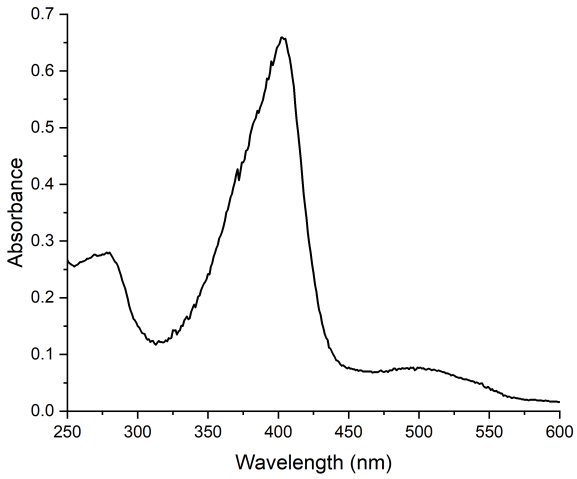

Figure 5.11 – UV/Visible spectrum of commercial HRP enzyme.

The maximum absorbance at 403 nm was 0.659, and with this value the HRP concentration is also calculated as described in subsection 4.2.4:

$$[\mathrm{HRP}] = \frac{\mathrm{Abs}_{403nm}}{\varepsilon_{403nm} L} = \frac{0.659}{102000\ \mathrm{M^{-1}cm^{-1}1cm}} = 6.46\ \mathrm{x}\ 10^{-6}\ \mathrm{M} \tag{5.4}$$

Considering the dilution factor of 10, the concentrated solution has a concentration of 6.46 x 10^{-6} M. This solution is diluted in MilliQ water to obtain the same initial concentration considered for SBP (8.85 x 10^{-5} M), then proceeding with dilutions in the same way to obtain the desired concentrations of 4.39 x 10^{-9} M, 8.77 x 10^{-9} M and 1.75 x 10^{-8} M.

From the UV/visible spectrum of Figure 5.11, it was also obtained an absorbance of 0.280 at 280 nm, resulting in an RZ of 2.35 (Equation 5.5). This value represents a high purity of the enzyme, which is expected for a commercial enzyme.

$$\mathrm{Rz} = \frac{\mathrm{Abs}(403)}{\mathrm{Abs}(280)} = \frac{0.659}{0.280} = 2.35 \tag{5.5}$$

5.3 BATCH REACTIONS

Batch reactions were carried out to study the enzymatic degradation reactions in a situation closer to a real application, in which a global reaction is carried out where the transport and mixing processes are considered. This study aims to carry out the following analyses:

- Batch reactions versus microreactor reactions;
- Single-substrate degradation versus multi-substrate degradation;
- Degradation with the obtained SBP versus commercial HRP.

In this study, degradation reactions of the pollutants TCP, TCS, and BPA were carried out using the enzymes SBP and HRP, as the following.

5.3.1 2,4,6-Triclorophenol

5.3.1.1 Calibration curves of TCP

First, TCP was identified by HPLC analysis with a retention time of approximately 2.77-2.79 minutes. In this case, two calibrations were performed for different concentration ranges: one for larger amounts (Figure 5.12(a)), to consider the same concentration conditions performed in the microreactor, and another for smaller amounts (Figure 5.12(b)), which are considered in the new reaction conditions considering the multi-substrate medium in a situation closer to a real application. These calibration curves were obtained with R^2 of 99.87% and 99.83%, respectively. Concentrations in ppm are considered for reasons of standardizing the amounts to be considered for the three different substrates (TCP, BPA, and TCS). It should be noted that the concentration of 0.25 mM, considered for the TCP in the microreactor, is equivalent to 50 ppm.

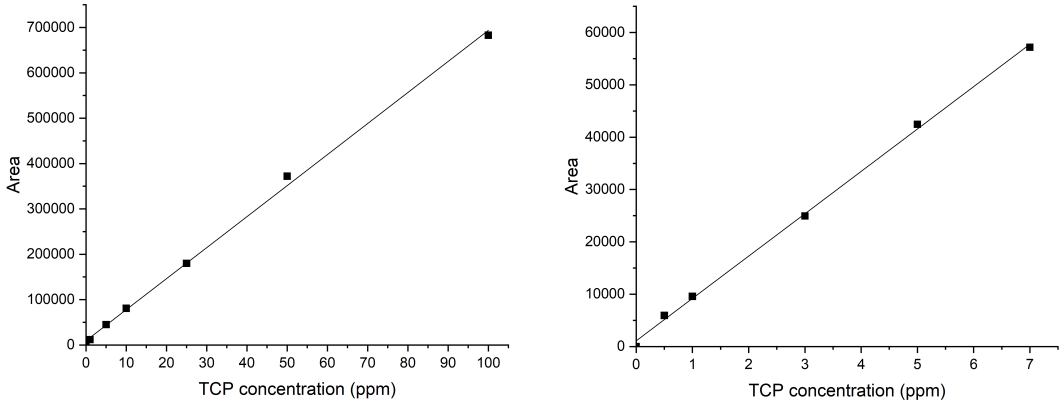

(a) Larger amounts. (b) Smaller amounts.

Figure 5.12 – TCP calibration curves.

5.3.1.2 TCP degradation

Figure 5.13 presents the results for TCP degradation considering the same conditions of the microreactor ([TCP] = 0.25 mM; [H_2O_2] = 0.3 mM; [SBP] = 5.2 x 10^{-9} M, 1.04 x 10^{-8} M and 2.08 x 10^{-8} M), and Figure 5.14 presents a comparison between TCP degradation in batch and in the microreactor, for the equivalent time between them. In this comparison, it can be seen that the reaction occurs faster in the microreactor, due to the controlled conditions of pH, temperature, and pressure considered in this case. However, it was not possible to achieve a 100% degradation in 5 minutes of reaction in the microreactor. For the batch reactions, this condition was reached at times of 120 (not shown in the graph), 40, and 20 minutes for the enzyme concentrations of 5.2 x 10^{-9} M, 1.04 x 10^{-8} M, and 2.08 x 10^{-8} M, respectively.

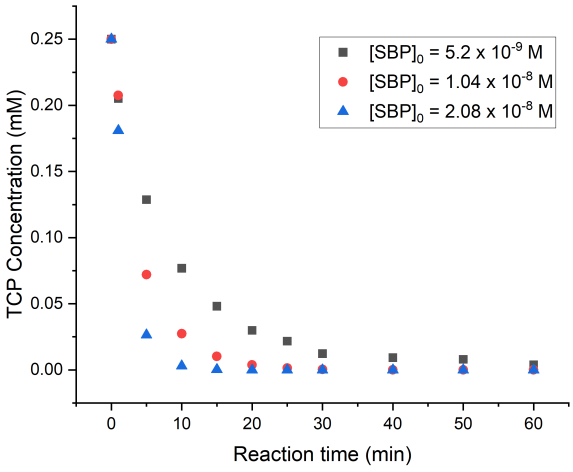

Figure 5.13 – TCP degradation results considering the same conditions of the microreactor.

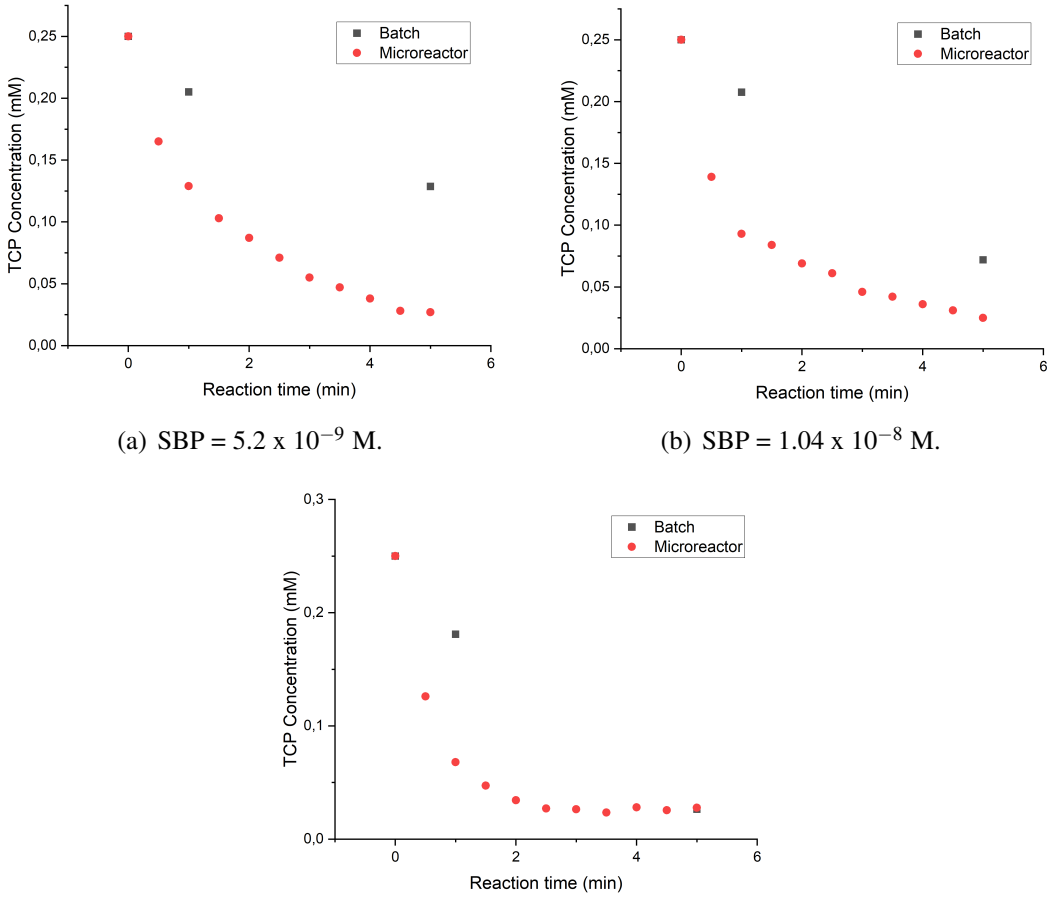

(a) SBP = 5.2 x 10^{-9} M.

(b) SBP = 1.04 x 10^{-8} M.

(c) SBP = 2.08 x 10^{-8} M.

Figure 5.14 – Comparison between TCP degradation in batch and in the microreactor.

Figures 5.15(a) and 5.15(b) presents the results for TCP degradation using SBP and HRP enzymes, respectively, considering the new conditions ([TCP] = 0.025 mM (5 ppm); [H_2O_2] = 0.1 mM; [E] = 4.39 x 10^{-9} M, 8.77 x 10^{-9} M and 1.75 x 10^{-8} M). Very similar behavior was observed for both enzymes. In both cases, the degradation was complete after 60, 20, and 10 minutes for the concentrations of 4.39 x 10^{-9} M, 8.77 x 10^{-9} M, and 1.75 x 10^{-8} M, respectively. It was also possible to observe the formation of two products, always at the same retention times of 1.25-1.28 and 1.83-1.84 minutes. Figures 5.16 and 5.17 illustrate these reaction products considering the areas obtained in the HPLC-UV analysis, since there is no calibration curve for these products. Although it is not possible to identify these reaction products through the HPLC-UV technique used, this result is consistent with the literature of Ferrari et al. (1999), where the authors identified by GC-MS techniques the supposed formation of two products from oxidative dechlorination of TCP in the presence of the enzyme HRP and H_2O_2, which would be 2,6-dichloro-1,4-benzoquinone and 2,6-dichlorohydroquinone (see section 2.3.1).

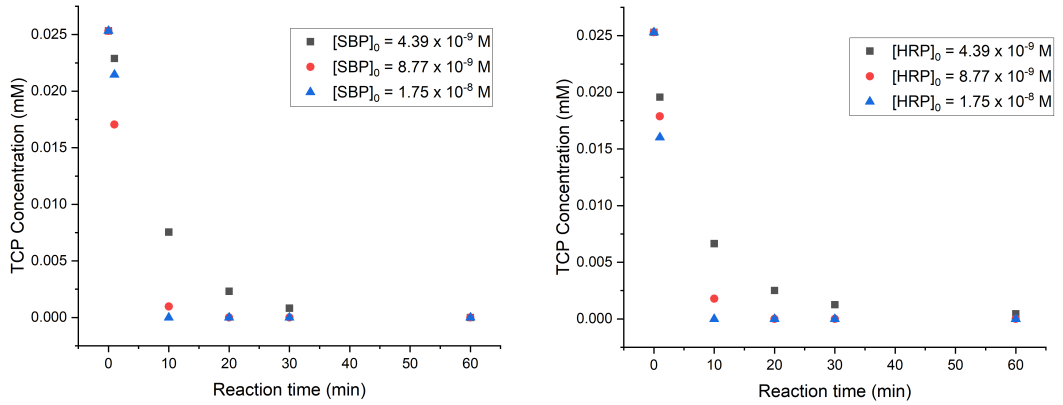

(a) SBP enzyme. (b) HRP enzyme.

Figure 5.15 – TCP degradation results considering new conditions.

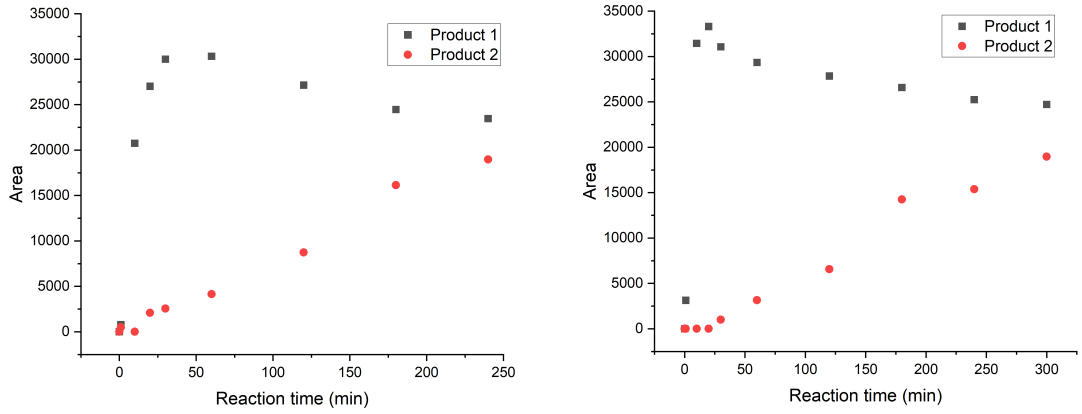

(a) SBP = 4.39 x 10^{-9} M. (b) SBP = 8.77 x 10^{-9} M.

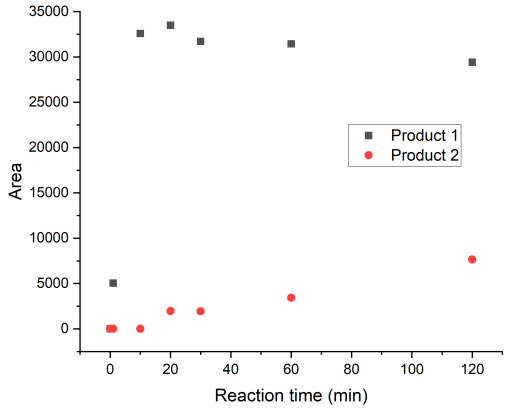

(c) SBP = 1.75 x 10^{-8} M.

Figure 5.16 – TCP degradation products with SBP.

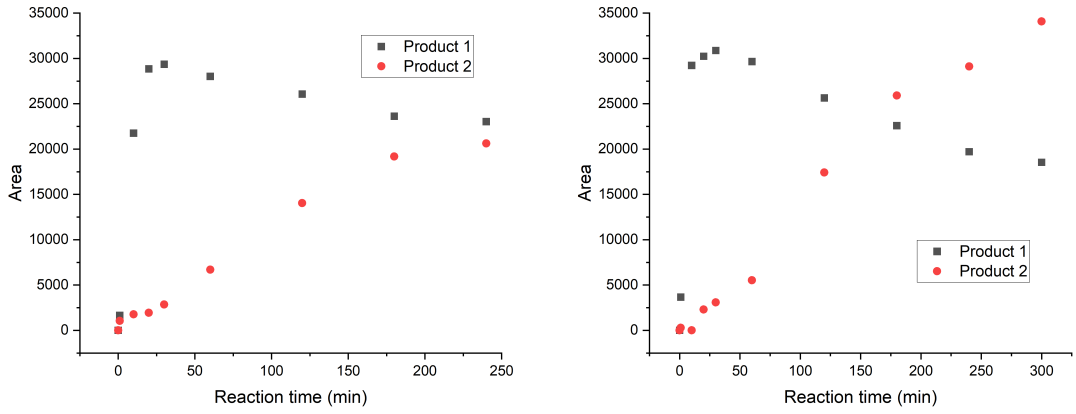

(a) HRP = 4.39 x 10^{-9} M.

(b) HRP = 8.77 x 10^{-9} M.

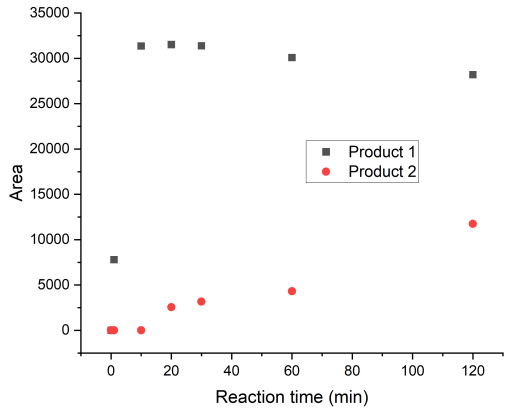

(c) HRP = 1.75 x 10^{-8} M.

Figure 5.17 – TCP degradation products with HRP.

5.3.2 Bisphenol A

5.3.2.1 Calibration curve of BPA

BPA was identified by HPLC analysis with a retention time of approximately 1.58-1.60 minutes, and its calibration curve is shown in Figure 5.18, with R^2 = 99.5%.

5.3.2.2 BPA degradation

BPA degradation results with SBP are shown in Figure 5.19. The expected behavior of greater degradation with increasing enzyme concentration was also observed. The degradation was complete after 180, 60, and 20 minutes for the concentrations of 4.39 x 10^{-9} M, 8.77 x 10^{-9} M, and 1.75 x 10^{-8} M, respectively.

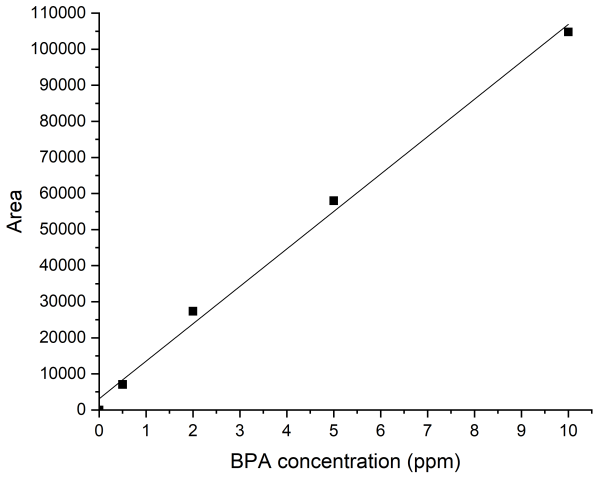

Figure 5.18 – BPA calibration curve.

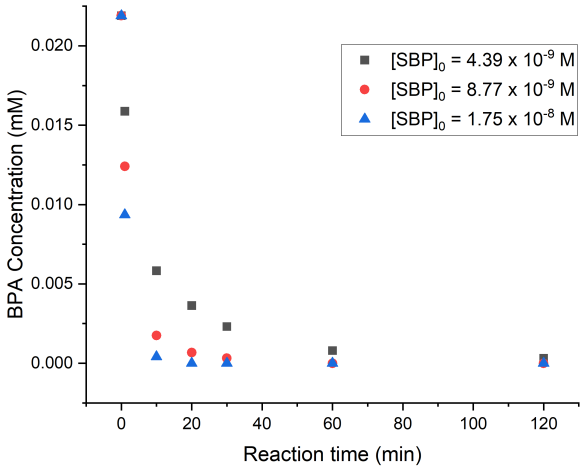

Figure 5.19 – BPA degradation results with SBP.

For BPA, it was not possible to observe the reaction products consistently, probably because the wavelength chosen for HPLC-UV analysis was not the most suitable for these specific compounds, or even because they were also degraded in the reaction. Only two peaks were observed at retention times of 2.01 and 2.66 in the first minute of the reaction.

5.3.3 Triclosan

5.3.3.1 Calibration curve of TCS

TCS was identified by HPLC analysis with a retention time of approximately 4.42-4.44 minutes, and its calibration curve is shown in Figure 5.20, with R2 = 99.84%.

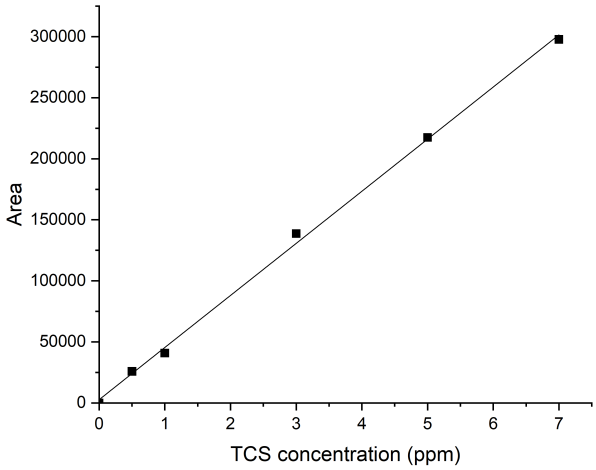

Figure 5.20 – TCS calibration curve.

5.3.3.2 TCS degradation

TCS degradation results with SBP are shown in Figure 5.21. In this case, the degradation was complete only with the highest concentration of enzyme (1.75 x 10^{-8} M) after 240 minutes of reaction. This longer degradation time probably occurred because TCS has a more complex molecule, resulting in a less intense interaction with the enzyme. Regarding the reaction products, it was possible to observe a major product at a retention time of 1.21-1.25 minutes, and several momentary products at retention times ranging from 0.58 seconds to 3.97 minutes. These results are illustrated in Figure 5.22, considering the areas obtained in the HPLC analysis, since there is no calibration curve for these products. According to the literature (DOU et al., 2018; BILAL et al., 2020), TCS is a very unstable substance that can appear in the form of different dimers and trimers, so this result is consistent with the expected.

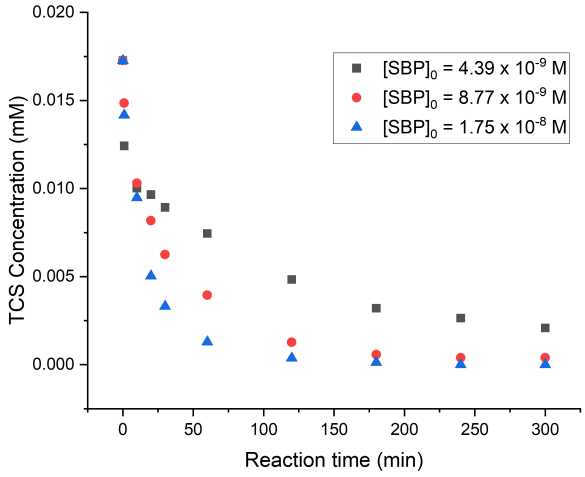

Figure 5.21 – TCS degradation results.

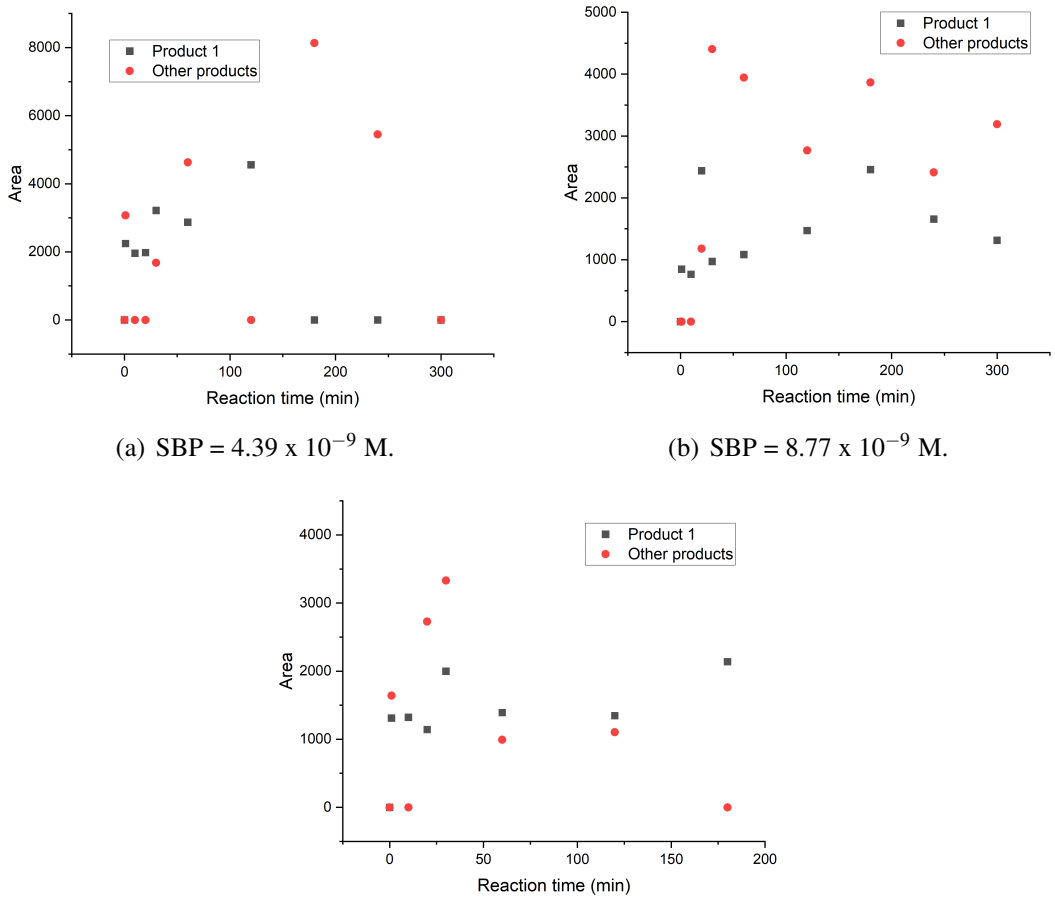

(a) SBP = 4.39 x 10^{-9} M.

(b) SBP = 8.77 x 10^{-9} M.

(c) SBP = 1.75 x 10^{-8} M.

Figure 5.22 – TCS degradation products.

5.3.4 Single-substrate degradation comparison

Figure 5.23 presents a comparison between the degradation behavior of BPA, TCP and TCS contaminants, presented in the Figures 5.15, 5.19 and 5.21, for comparison purposes with the multi-substrate degradation that will be presented in the next section.

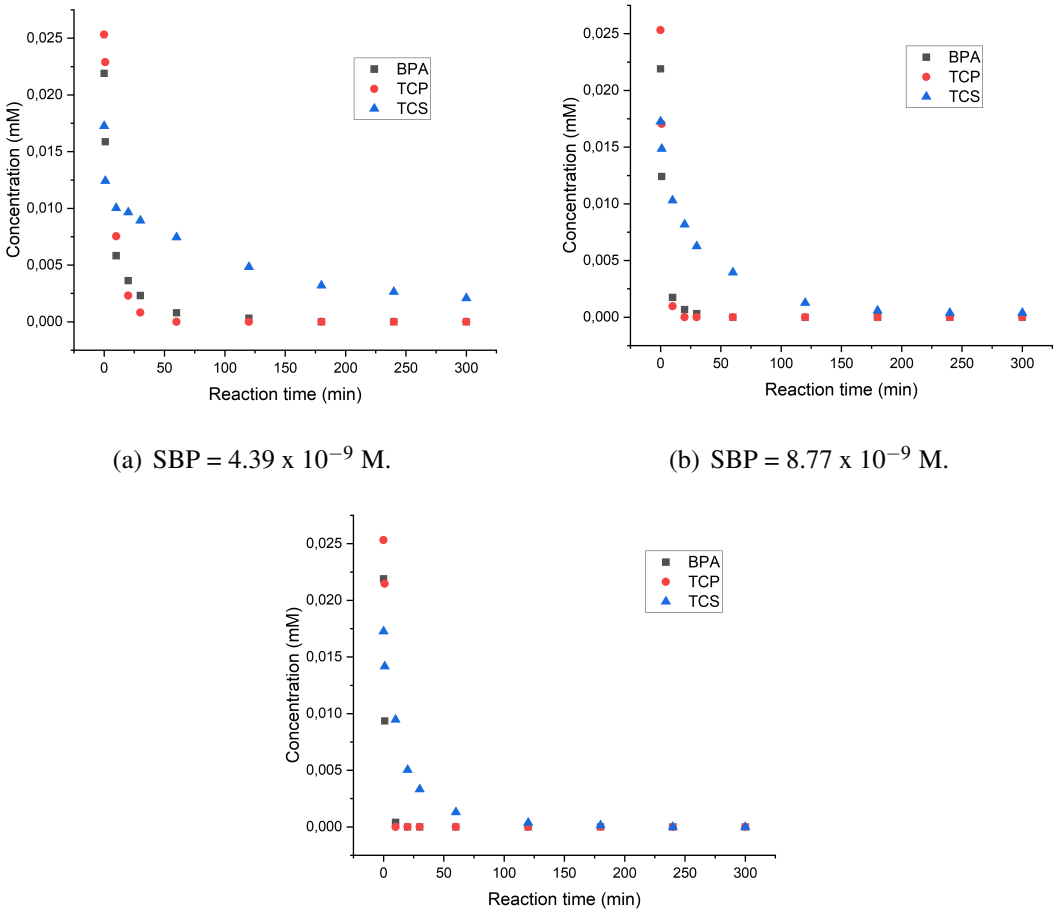

(a) SBP = 4.39 x 10^{-9} M.

(b) SBP = 8.77 x 10^{-9} M.

(c) SBP = 1.75 x 10^{-8} M.

Figure 5.23 – Single-substrate degradation results with SBP.

5.3.5 Multi-substrate degradation

It was possible to perform the degradation in a multi-substrate medium containing TCP, BPA, and TCS, both with the SBP enzyme and with the HRP enzyme, as observed in the Figures 5.24 and 5.25, respectively. This is a way of emulating industrial effluents, which generally have several components as potential pollutants (ZHENG; COLOSI, 2011; SARRO et al., 2018). In these reactions, for enzyme concentrations of 4.39 x 10^{-9} M and 8.77 x 10^{-9} M, a reaction medium with a total substrate concentration of 5 ppm was considered, while for enzyme concentration of 1.75 x 10^{-8} M, a total substrate concentration of 15 ppm was considered, with equal amounts of substrates in both cases.

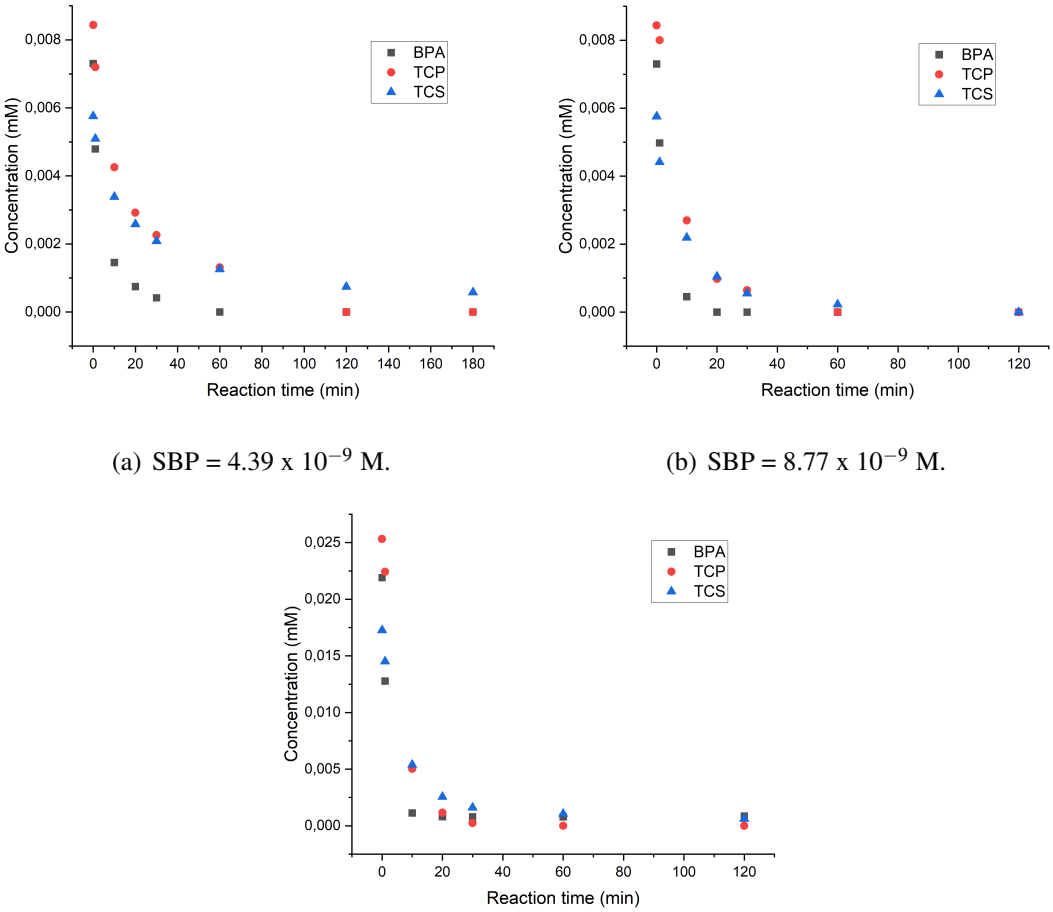

(a) SBP = 4.39 x 10^{-9} M.

(b) SBP = 8.77 x 10^{-9} M.

(c) SBP = 1.75 x 10^{-8} M.

Figure 5.24 – Multi-substrate degradation results with SBP.

Comparing the results of the multi-substrate degradation with SBP enzyme (Figure 5.24) with the results of the single-substrate degradation with SBP enzyme (Figure 5.23), it can be observed that the degradation of BPA was more effective in the mix solution, the opposite occurring for TCP. This behavior can be explained by the fact that the TCP molecule is more complex than BPA, due to the presence of three Cl atoms in its structure. In addition, the degradation of TCS was the most difficult in both cases, maybe due to the greater complexity of this molecule. Furthermore, this behavior highlights possible competitions between substrates and different behaviors between mixtures and simple solutions.

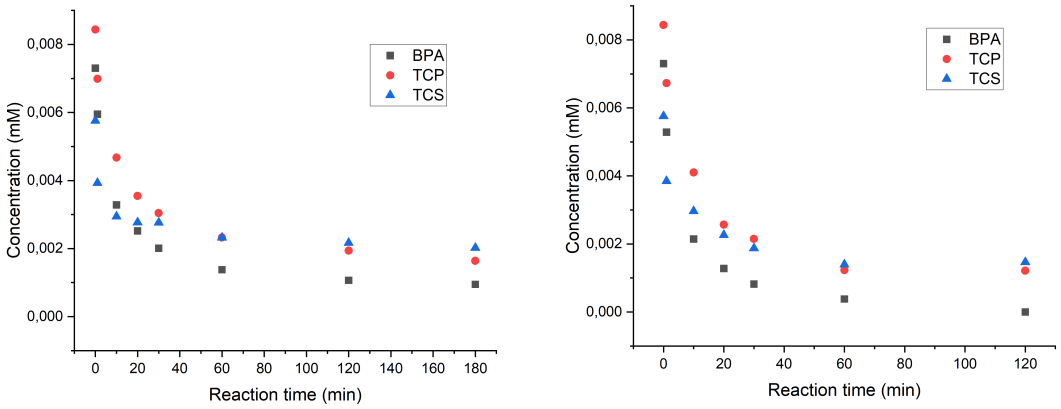

(a) HRP = 4.39 x 10^{-9} M.

(b) HRP = 8.77 x 10^{-9} M.

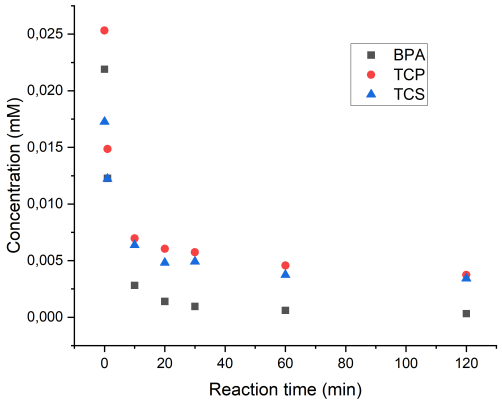

(c) HRP = 1.75 x 10^{-8} M.

Figure 5.25 – Multi-substrate degradation results with HRP.

In general, a faster degradation was observed with the SBP enzyme. For the enzyme concentration of 4.39 x 10^{-9} M, Figures 5.24(a) and 5.25(a), SBP completely degraded BPA in 60 minutes, TCP in 120 minutes, and not completely degraded TCS in 180 minutes, whereas HRP did not completely degrade any of the substrates in 180 minutes. For the enzyme concentration of 8.77 x 10^{-9} M, Figures 5.24(b) and 5.25(b), in turn, SBP completely degraded BPA in 20 minutes, TCP in 60 minutes, and TCS in 120 minutes, whereas HRP completely degraded BPA in 120 minutes, and did not completely degrade TCP and TCS in 120 minutes. Finally, for the enzyme concentration of 1.75 x 10^{-8} M, Figures 5.24(c) and 5.25(c), SBP completely degraded only TCP, while HRP degraded completely only BPA, being observed in both cases the degradation up to 240 minutes. In these cases where the degradation was not complete, there was probably an interaction between the intermediate compounds or the formation of products that acted as inhibitors in the reaction process.

Figure 5.26 presents a comparative summary between the single-substrate degradation and the degradation in multi-substrate medium, being evidenced that a substrate may behave differently depending on the situation.

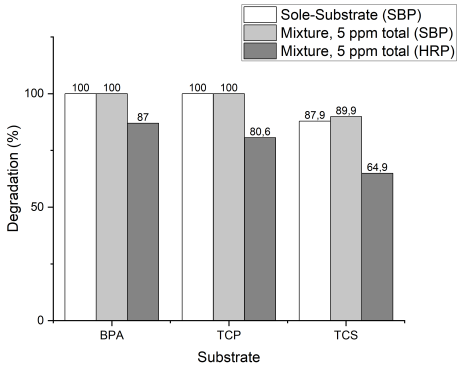

(a) % Degradation; E = 4.39 x 10^{-9} M.

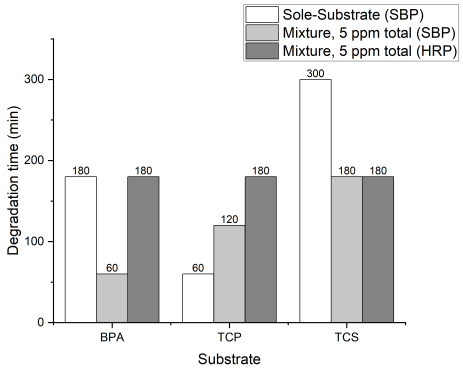

(b) Degradation time; E = 4.39 x 10^{-9} M.

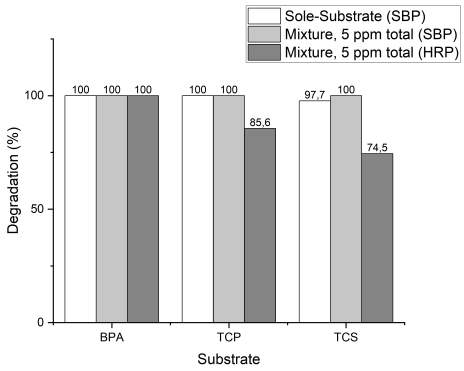

(c) % Degradation; E = 8.77 x 10^{-9} M.

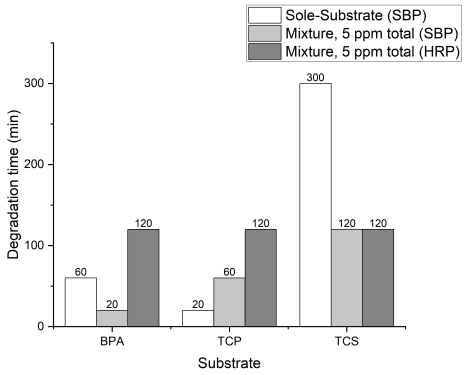

(d) Degradation time; E = 8.77 x 10^{-9} M.

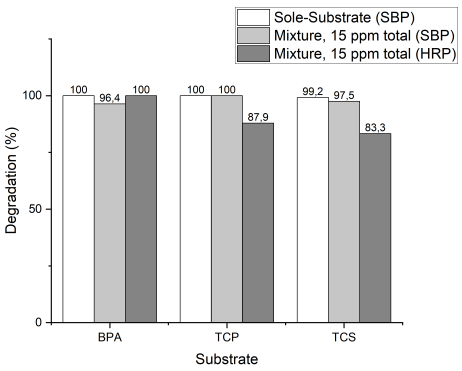

(e) % Degradation; E = 1.75 x 10^{-8} M.

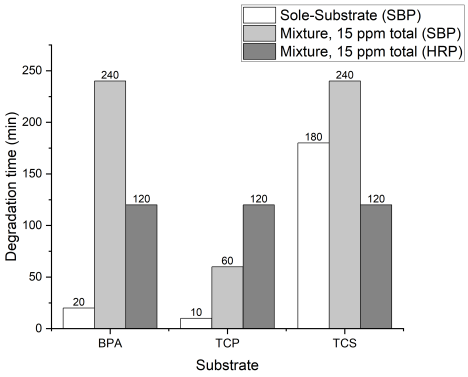

(f) Degradation time; E = 1.75 x 10^{-8} M.

Figure 5.26 – General multi-substrate degradation results.

In the case of BPA, it was observed that the degradation was complete for single-substrate degradation and in mixture using SBP for enzyme concentrations of 4.39 x 10^{-9} M and 8.77 x 10^{-9} M. However, the BPA degradation was faster in the mixture for these SBP concentrations, and for the SBP concentration of 1.75 x 10^{-8} M the behavior was the opposite, with complete and much faster degradation in the case of single-substrate degradation. TCP, in turn, showed complete degradation both for single-substrate degradation and for degradation in mixture with SBP for all enzyme concentrations. In this case, the degradation was faster in the case of single-substrate degradation, in contrast to BPA for lower enzyme concentrations. TCS, on the other hand, degraded better in the mixture for SBP concentrations of 4.39 x 10^{-9} M and 8.77 x 10^{-9} M, and presented a better single-substrate degradation at a SBP concentration of 1.75 x 10^{-8} M. However, TCS degradation was not complete in any case. These behaviors happen due to a possible competition between the pollutants.

It is worth mentioning that the pH of the reactions were measured at the beginning and at the end of the reactions, in all cases, and values close to 6 were always found, which is the pH of the MilliQ water used in the preparation of the solutions. That is, there was no influence of pH on the reactions and the hypothesis of decreased enzyme activity due to pH is discarded.

5.4 TOXICITY TEST

The results of the toxicity test are shown in Figure 5.27. As can be seen in the figure, the effect of toxicity was measured at different reaction times. The luminescence was read at 3 different exposure times (5, 15 and 30 minutes) of the solution to the bacteria. It can be observed that, before the reaction, the toxicity effect was close to 100%, but it decreased throughout the reaction until reaching considerably lower values after the complete degradation of TCP, BPA and TCS. Although further experiments are needed to better define the role of each substance in the observed residual toxicity, these data indicate that the increased viability of the bacteria correlates with the removal of the three pollutants.

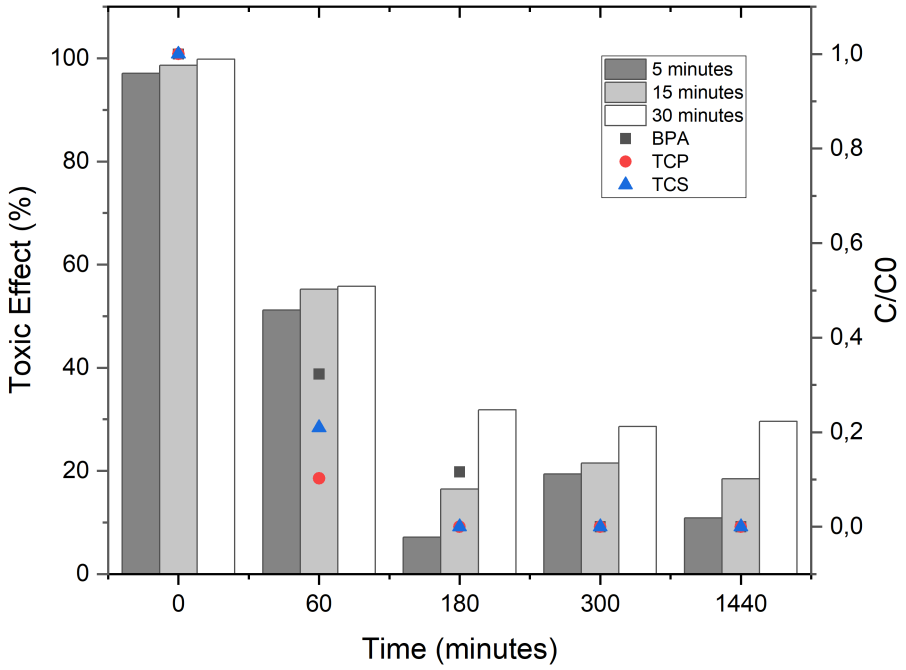

Figure 5.27 – Toxicity test results.

CHAPTER 6
MODELING AND SIMULATION RESULTS AND DISCUSSION

6.1 REACTIONS ON MICROREACTOR

6.1.1 TCP degradation with SBP

As reported in Chapter 3, a study was first carried out to develop the modified bi-bi ping-pong model using the experimental data of Costa (2016). Six different possibilities were carried out in the model simulation, considering different assumptions to simplify the model. It is noteworthy that several other possibilities were tested before obtaining this approach, such as the Michaelis-Menten model, considering only TCP as a substrate, and also other models considering different combinations of intermediate reaction complexes, reverse reactions, and others. In some approaches, a very large set of parameters should be considered, which did not allow obtaining a single set of adjusted parameters in the estimation procedure. In this case, the strategy was to start with the simplest model and gradually add assumptions.

The parameter estimation procedure was carried out in MATLAB as described in Chapter 3. It was considered in the model solution both the ODE and DAE systems, but the solution with the second one was less sensitive to the initial estimates, so in this case only those results are considered. Table 6.1 presents the estimated parameters and Figures 6.1 to 6.6 present the model prediction and experimental data. These results have already been published in the paper by Cunha et al. (2021). All the experiments were performed in triplicate, with average errors of ± 0.00033 mM, ± 0.00024 mM, and ± 0.00027 mM for the enzyme concentrations of [SBP] = 5.2 x 10^{-9} M, [SBP] = 1.04 x 10^{-8} M, and 2.08 x 10^{-8} M, respectively. However, these values were so small that it was not possible to display error bars at the experimental points. These experimental results show the good reproducibility and repeatability of the experiments in the microreactor, which is adequate equipment for studies of the kinetics of fast reactions such as enzymatic ones (CUNHA et al., 2021).

Table 6.1 – Estimated parameters and model fit evaluation of TCP degradation reactions using the SBP enzyme in the microreactor.

Parameter	Model 1 (CpI and CpII)	Model 2 (CpI, CpII, and CpIII)	Model 3 (CpI, CpII, CpIII, and CpI·H_2O_2)	Model 4 (CpI, CpII, and SBP inactivation)	Model 5 (CpI, CpII, CpIII, and SBP inactivation)	Model 6 (CpI, CpII, CpIII, CpI·H_2O_2, and SBP inactivation)	Unit
k_1	2.0 x 10^{7}	2.0 x 10^{7}	2.0 x 10^{7}	2.0 x 10^{7}	2.0 x 10^{7}	2.0 x 10^{7}	$M^{-1}s^{-1}$
k_2	3.4 x 10^{6}	2.52 x 10^{6}	3.36 x 10^{6}	6.38 x 10^{6}	6.79 x 10^{6}	8.19 x 10^{6}	$M^{-1}s^{-1}$
k_3	8.8 x 10^{5}	9.72 x 10^{5}	8.85 x 10^{5}	2.47 x 10^{6}	2.75 x 10^{6}	3.01 x 10^{6}	$M^{-1}s^{-1}$
k_{app}	-	7.92 x 10^{-1}	8.99 x 10^{-2}	-	6.6 x 10^{0}	1.26 x 10^{-1}	$M^{-1}s^{-1}$
k_a	-	4.28 x 10^{-2}	6.48 x 10^{-2}	-	1.09 x 10^{-2}	9.56 x 10^{-3}	s^{-1}
k_b	-	4.23 x 10^{-1}	3.74 x 10^{-1}	-	9.3 x 10^{-1}	1.93 x 10^{0}	$M^{-1}s^{-1}$
k_c	-	1.96 x 10^{2}	-	-	8.99 x 10^{2}	-	$M^{-1}s^{-1}$
k_4	-	-	3.41 x 10^{1}	-	-	2.82 x 10^{2}	$M^{-1}s^{-1}$
k_{-4}	-	-	7.26 x 10^{-7}	-	-	1.22 x 10^{-5}	$M^{-1}s^{-1}$
k_5	-	-	1.41 x 10^{0}	-	-	8.71 x 10^{-1}	s^{-1}
OF	1.9405 x 10^{-1}	1.9422 x 10^{-1}	1.9413 x 10^{-1}	5.6834 x 10^{-2}	5.6276 x 10^{-2}	5.5741 x 10^{-2}	-
RMSE	2.7666 x 10^{-9}	2.7691 x 10^{-9}	2.7677 x 10^{-9}	8.1945 x 10^{-10}	8.1177 x 10^{-10}	8.0479 x 10^{-10}	-
$R^2_{adjusted,1}$	90.48%	86.24%	82.33%	94.88%	92.71%	90.65%	-
$R^2_{adjusted,2}$	83.89%	76.69%	70.05%	98.01%	97.13%	96.39%	-
$R^2_{adjusted,3}$	89.56%	84.91%	80.60%	96.75%	95.34%	94.09%	-

Source: Results have already been published by Cunha et al. (2021).

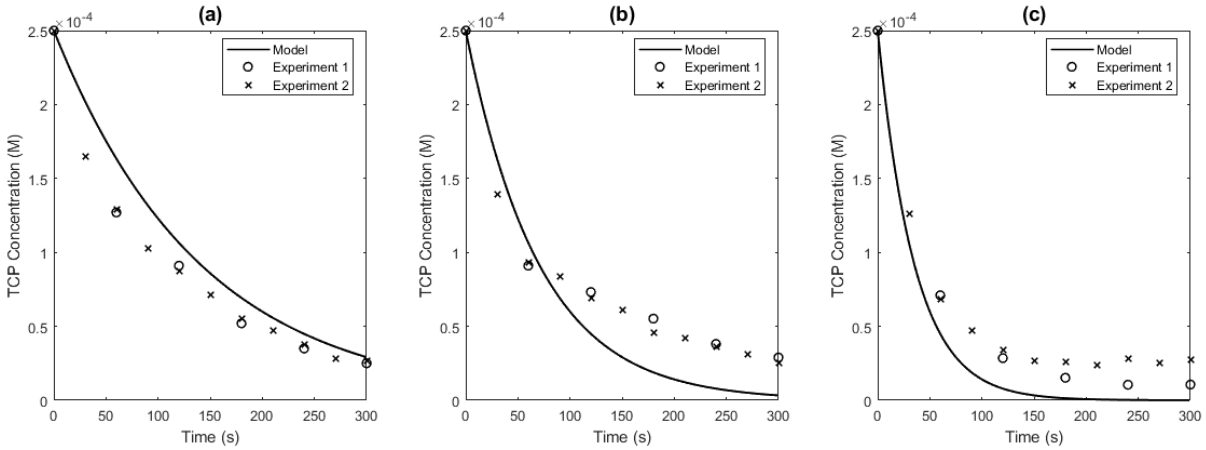

Figure 6.1 – Model prediction for TCP degradation with SBP in the microreactor (Model 1). SBP concentrations of: (a) 5.2 x 10^{-9} M; (b) 1.04 x 10^{-8} M; (c) 2.08 x 10^{-8} M.

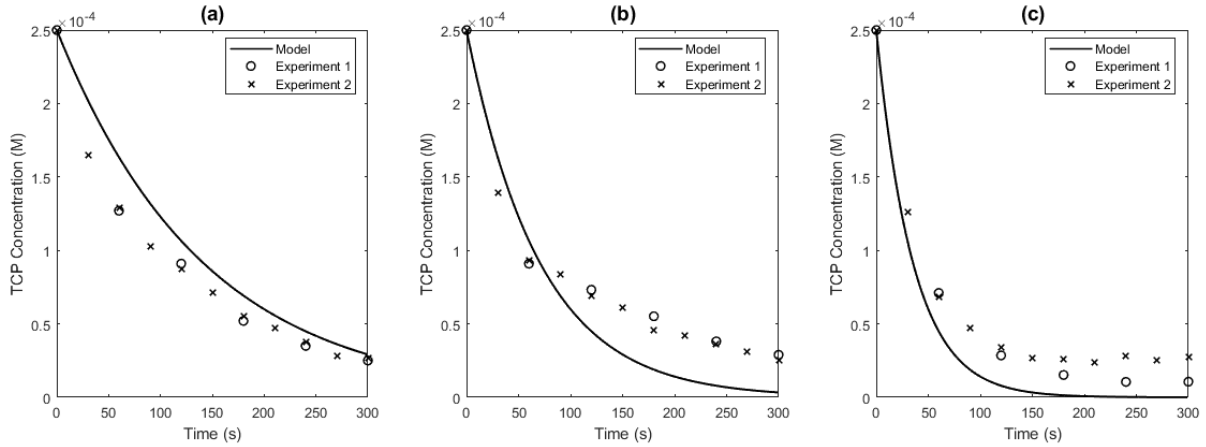

Figure 6.2 – Model prediction for TCP degradation with SBP in the microreactor (Model 2). SBP concentrations of: (a) 5.2 x 10^{-9} M; (b) 1.04 x 10^{-8} M; (c) 2.08 x 10^{-8} M.

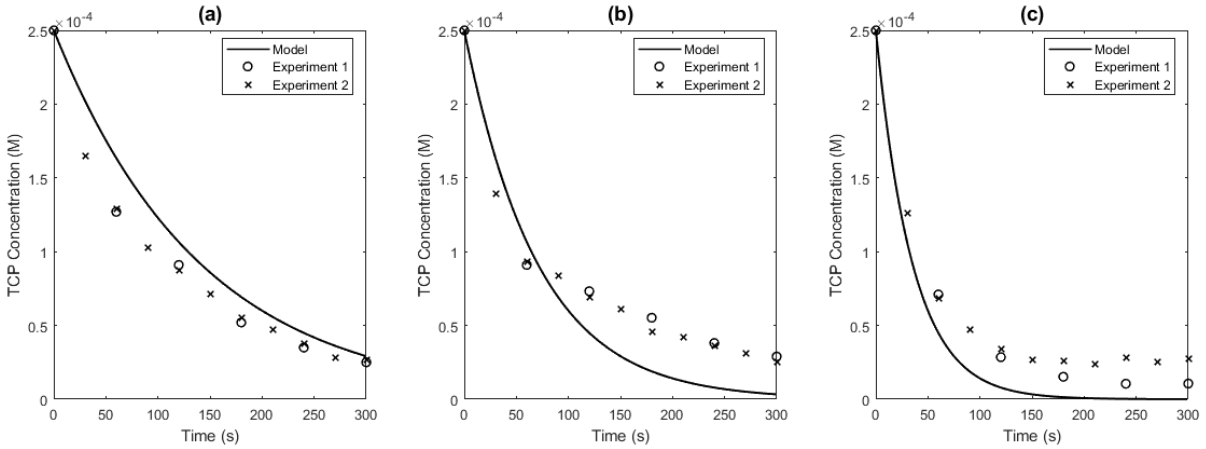

Figure 6.3 – Model prediction for TCP degradation with SBP in the microreactor (Model 3). SBP concentrations of: (a) 5.2 x 10^{-9} M; (b) 1.04 x 10^{-8} M; (c) 2.08 x 10^{-8} M.

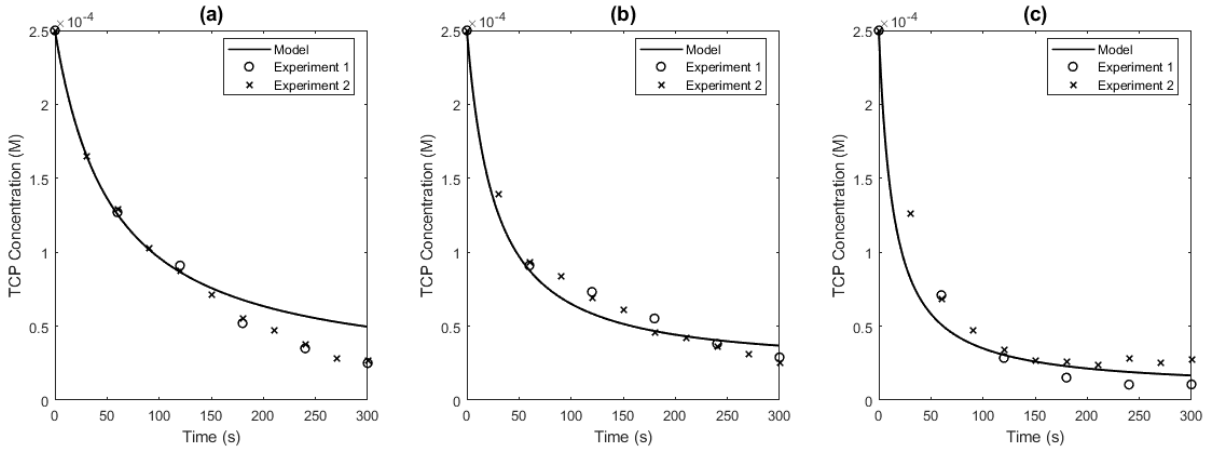

Figure 6.4 – Model prediction for TCP degradation with SBP in the microreactor (Model 4). SBP concentrations of: (a) 5.2 x 10^{-9} M; (b) 1.04 x 10^{-8} M; (c) 2.08 x 10^{-8} M.

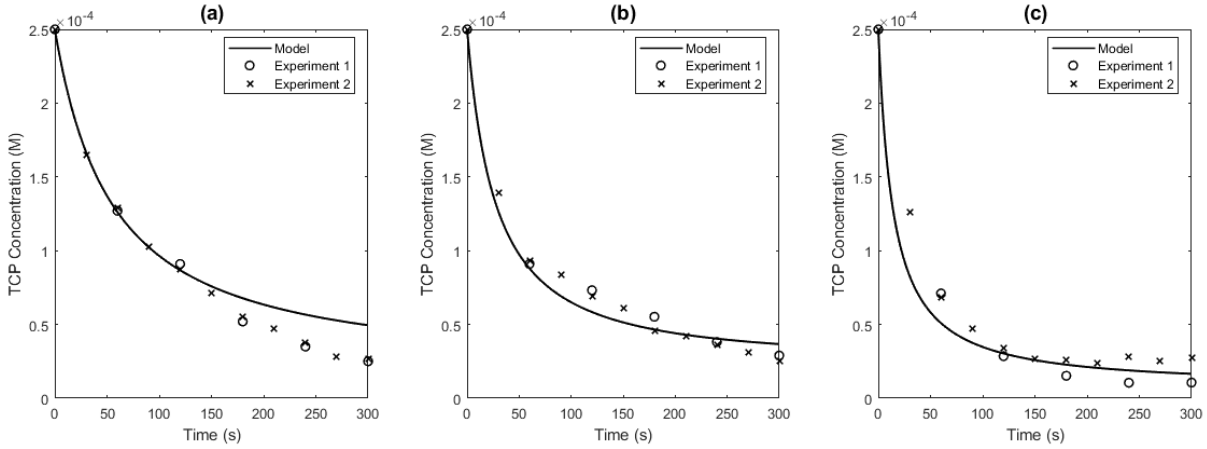

Figure 6.5 – Model prediction for TCP degradation with SBP in the microreactor (Model 5). SBP concentrations of: (a) 5.2 x 10^{-9} M; (b) 1.04 x 10^{-8} M; (c) 2.08 x 10^{-8} M.

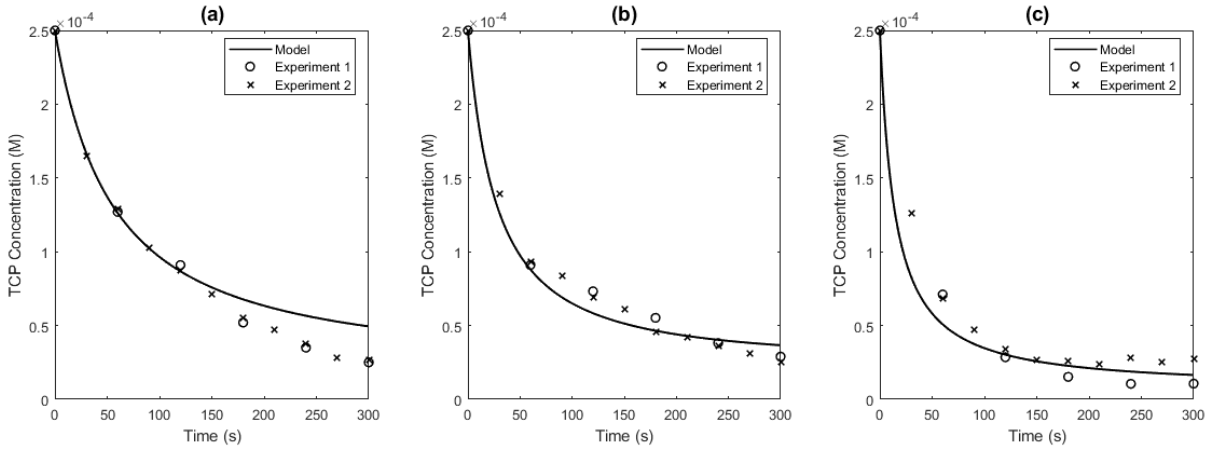

Figure 6.6 – Model prediction for TCP degradation with SBP in the microreactor (Model 6). SBP concentrations of: (a) 5.2 x 10^{-9} M; (b) 1.04 x 10^{-8} M; (c) 2.08 x 10^{-8} M.

In Figures 6.1 to 6.6, in general, a coherent fit of the experimental data for the bi-bi ping pong model is observed. Models 1, 2 and 3 presented almost equal adjustments, as well as Models 4, 5 and 6, for the three sets of experiments with different enzyme concentrations. However, the results of these two groups of models were considerably different, which can be explained by the addition of the enzyme inactivation in Models 4, 5 and 6. These models visually present curves closer to the experimental points, except for experiments with an enzyme concentration of 5.2 x 10^{-9} M at longer reaction times. Nonetheless, the curves of all models respect the expected behavior of a higher TCP degradation at higher enzyme concentrations.

The numerical results are presented in Table 6.1, where the three values of adjusted R^2 refer to the experiments at the different enzyme concentrations. In general, it can be observed that Models 4, 5, and 6, which consider the enzyme inactivation, presented a considerably better fit than the Models 1, 2, and 3, which do not consider the enzyme inactivation, because they presented higher values of adjusted R^2 and lower values of OF and RMSE. So, it can be inferred that considering the enzyme inactivation resulted in a relevant gain for the model fit.

Comparing the fit for the three sets of experiments by the different values of adjusted R^2, a better fit can be observed for the lowest enzyme concentration in Models 1, 2 and 3, in which enzyme inactivation was not considered, while a better fit was obtained for the higher enzyme concentrations in models Models 4, 5 and 6, in which enzyme inactivation is considered. This could be explained because, in the first set of experiments, a smaller amount of initial enzyme would result in a smaller quantity of inactivated enzyme, so this consideration would not be so relevant in this specific case.

Analyzing the effect of considering the formation of the enzyme forms CpIII (Models 2 and 4) and CpI·H_2O_2 (Models 3 and 6), the results indicate that the consideration of more complex model results in lower values of adjusted R^2, which would mean, at first, a worsening of the model's fit. However, it can also be seen that the values of OF and RMSE reflect an improvement in the model fit. It is known that adjusted R^2 includes a correction for the additional parameters added to the model, but perhaps this penalty was greater than it should have been so that the number of experimental points would not be enough to compensate. That is why this criterion is not always reliable for evaluating nonlinear model adjustments (PECK et al., 2012). So, if only the OF and RMSE criteria are considered, in the models without considering enzyme inactivation, the adjustment worsens from Model 1 to Model 2 and improves from Model 2 to Model 3, while in models considering enzyme inactivation the adjustment improves sequen-

tially from Model 4 to Model 6. In general, the models with enzyme inactivation resulted in an improvement in the model and the OF and RMSE criteria were more reliable than adjusted R^2 in this case, so the global analysis can infer that Model 6 presented more consistent results among the considered hypotheses. This result corroborates the considerations made regarding the formation of compound CpIII and CpI·H_2O_2 complex. However, taking into account that few data were used and that there are experimental errors involved, it cannot be concluded with complete certainty that these assumptions were completely adequate, and it is necessary to verify further by performing new experiments.

Simulations of the concentration profile of all reaction components were performed. Figures 6.7 and 6.8 present the simulations of the substrates and product concentrations for Models 1, 2, and 3 and Models 4, 5, and 6, respectively. The simulations of the enzyme forms and the enzyme-substrate complexes can be seen in Figures 6.9 to 6.14. Although the enzyme can be regenerated to its initial state, all the models indicate that its concentration always decreases throughout the reaction, since it can generate its oxidized forms or be inactivated. In Models 1, 2, and 3, all other forms of the enzyme grow slightly until they reach a condition of equilibrium, depending on the model's considerations. In Models 4, 5, and 6, all enzyme forms decrease throughout the reaction until reaching a condition of equilibrium, except the inactive form, which substantially increases. The models also indicate that the most significant enzyme form in the reaction is CpII, followed by CpI, CpIII, and CpI·H_2O_2, respectively, when applicable.

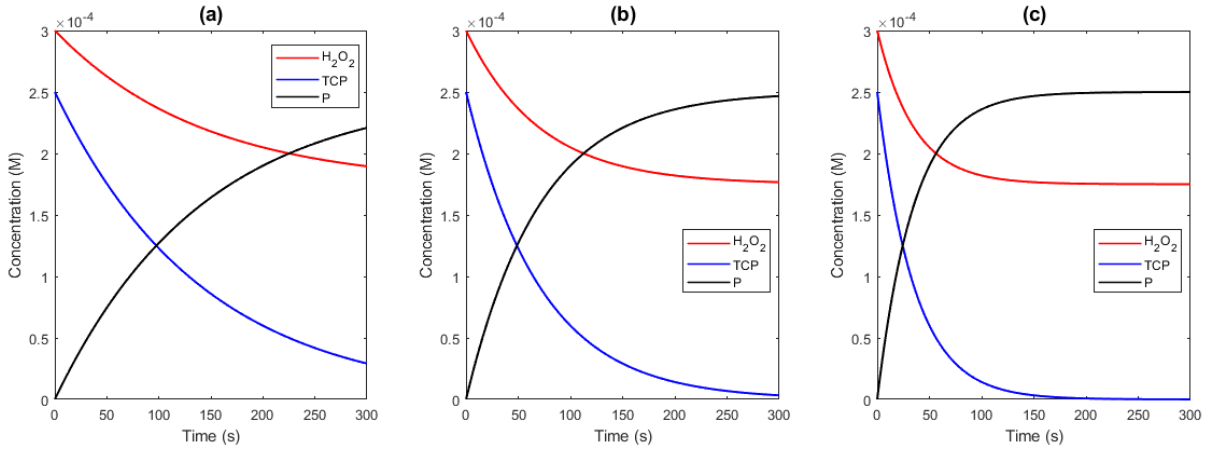

Figure 6.7 – Simulation of substrates and product concentrations for TCP degradation with SBP in the microreactor (Models 1, 2, and 3).

SBP concentrations of: (a) 5.2 x 10^{-9} M; (b) 1.04 x 10^{-8} M; (c) 2.08 x 10^{-8} M.

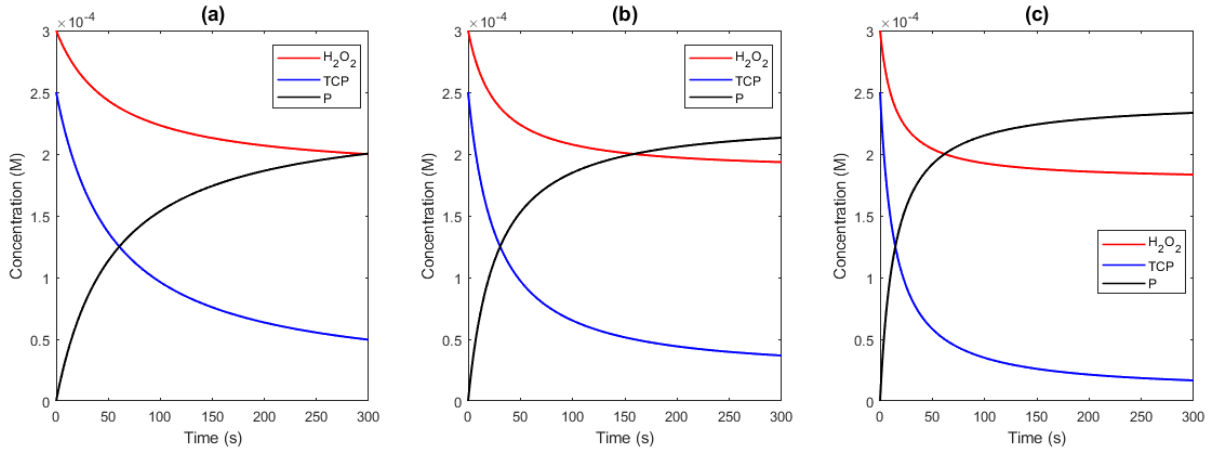

Figure 6.8 – Simulation of substrates and product concentrations for TCP degradation with SBP in the microreactor (Models 4, 5, and 6).

SBP concentrations of: (a) 5.2 x 10^{-9} M; (b) 1.04 x 10^{-8} M; (c) 2.08 x 10^{-8} M.

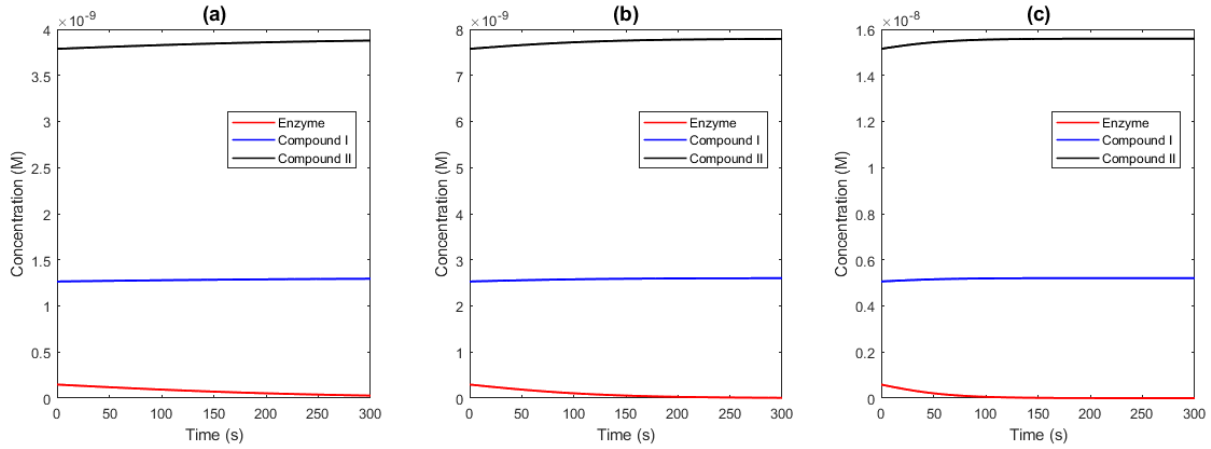

Figure 6.9 – Simulation of SBP form concentrations for TCP degradation in the microreactor (Model 1).

SBP concentrations of: (a) 5.2 x 10^{-9} M; (b) 1.04 x 10^{-8} M; (c) 2.08 x 10^{-8} M.

Besides, it is worth mentioning that these results are based exclusively on the model considered and the set of experimental data obtained. Experimental identification of the intermediate forms of the enzyme should be made to clearly state the mechanism of the reaction, and this is not part of the scope of the present work.

It is also interesting to highlight the difference in the model solution using ODE or DAE systems. Figures 6.15 and 6.16 present examples of simulations of the enzyme forms by solving the model with the ODE system, where it is possible to verify an instability in the solution. This shows that the model solution using DAE systems is more suitable.

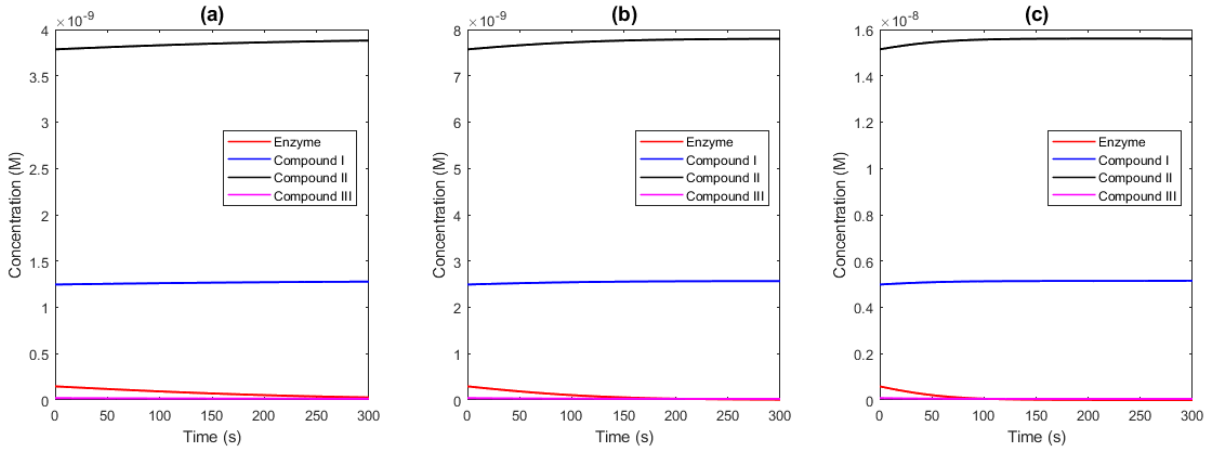

Figure 6.10 – Simulation of SBP form concentrations for TCP degradation in the microreactor (Model 2).
SBP concentrations of: (a) 5.2 x 10^{-9} M; (b) 1.04 x 10^{-8} M; (c) 2.08 x 10^{-8} M.

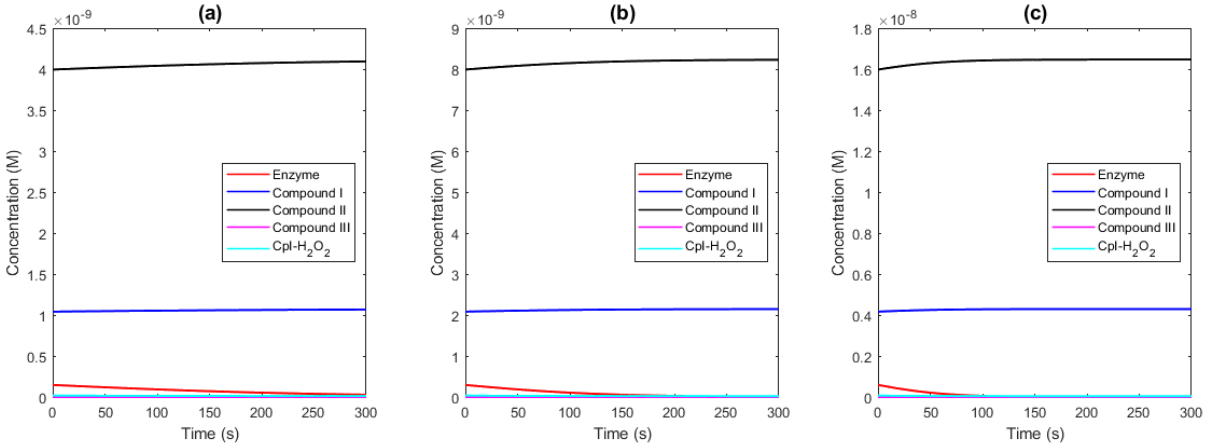

Figure 6.11 – Simulation of SBP form concentrations for TCP degradation in the microreactor (Model 3).
SBP concentrations of: (a) 5.2 x 10^{-9} M; (b) 1.04 x 10^{-8} M; (c) 2.08 x 10^{-8} M.

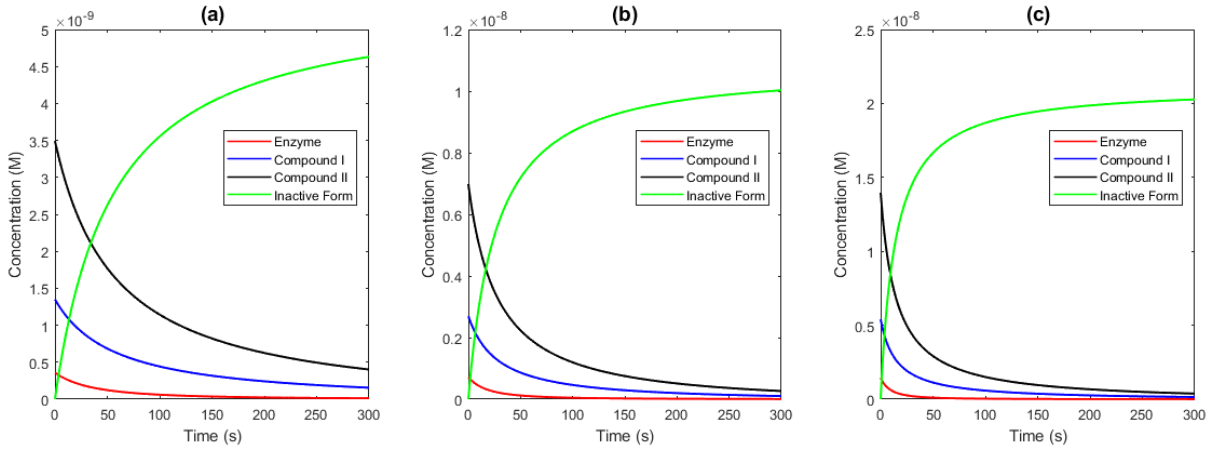

Figure 6.12 – Simulation of SBP form concentrations for TCP degradation in the microreactor (Model 4).
SBP concentrations of: (a) 5.2 x 10^{-9} M; (b) 1.04 x 10^{-8} M; (c) 2.08 x 10^{-8} M.

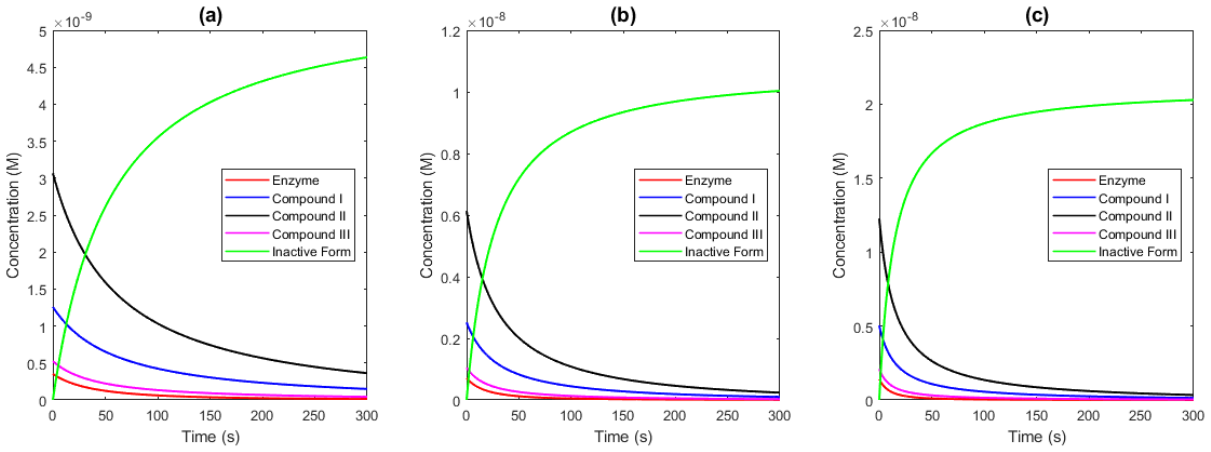

Figure 6.13 – Simulation of SBP form concentrations for TCP degradation in the microreactor (Model 5).
SBP concentrations of: (a) 5.2 x 10^{-9} M; (b) 1.04 x 10^{-8} M; (c) 2.08 x 10^{-8} M.

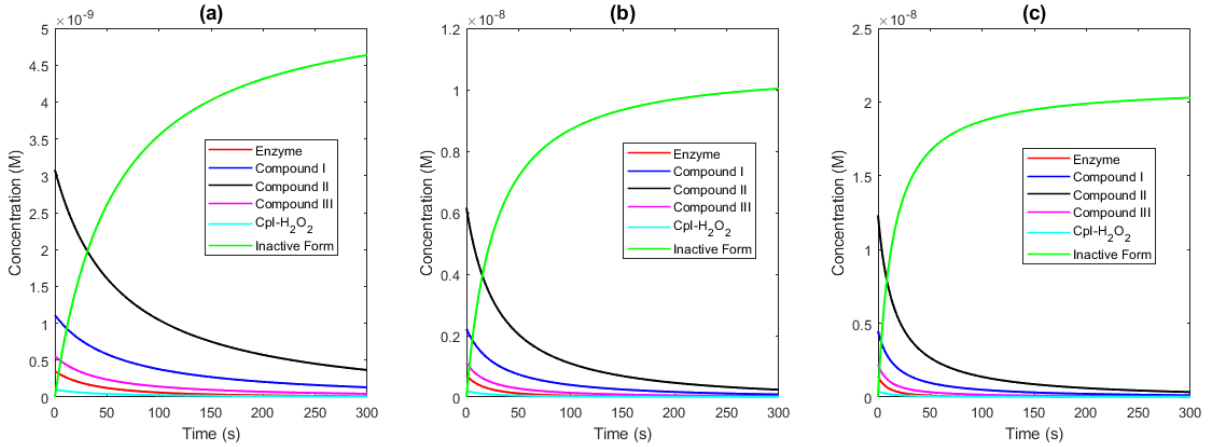

Figure 6.14 – Simulation of SBP form concentrations for TCP degradation in the microreactor (Model 6).
SBP concentrations of: (a) 5.2 x 10^{-9} M; (b) 1.04 x 10^{-8} M; (c) 2.08 x 10^{-8} M.

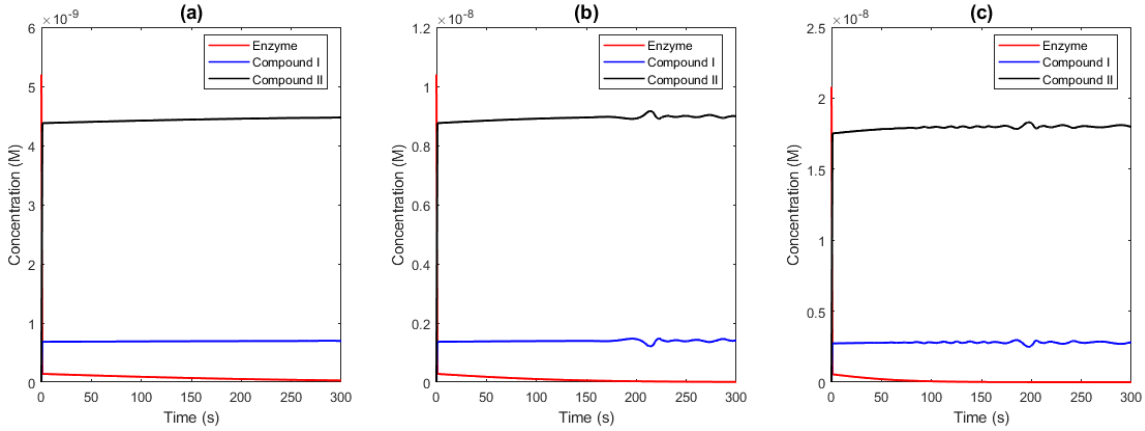

Figure 6.15 – Simulation of SBP form concentrations for TCP degradation in the microreactor using ODE's solver (Model 1).
SBP concentrations of: (a) 5.2 x 10^{-9} M; (b) 1.04 x 10^{-8} M; (c) 2.08 x 10^{-8} M.

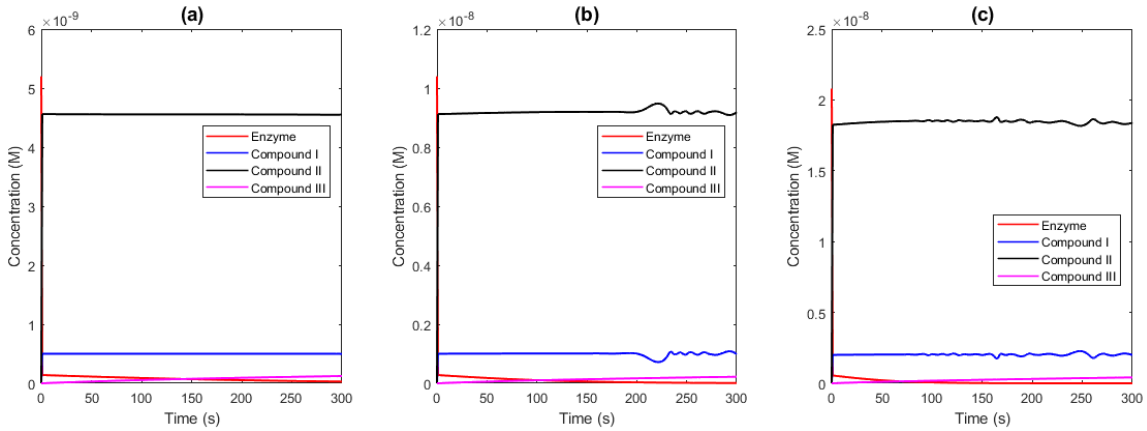

Figure 6.16 – Simulation of SBP form concentrations for TCP degradation in the microreactor using ODE's solver (Model 2).
SBP concentrations of: (a) 5.2 x 10^{-9} M; (b) 1.04 x 10^{-8} M; (c) 2.08 x 10^{-8} M.

6.1.2 TCP and TCS degradation with HRP

Table 6.2 presents the results of the parameter estimation procedures carried out for the TCP and TCS degradation reactions in the microreactor. In this case, it was considered the complete model that takes into account all the enzyme forms (species CpI, CpII, CpIII, CpI·H_2O_2, and enzyme inactivation). The table presents the data of the TCP degradation with the SBP enzyme, already presented in Table 6.1, and adding the results of the degradation of TCP and TCS with the HRP enzyme.

Table 6.2 – Estimated parameters and model fit evaluation of TCP and TCS degradation reactions in the microreactor.

Parameter	SBP and TCP	HRP and TCP	HRP and TCS	Unit
k_1	2.0 x 10^{7}	2.0 x 10^{7}	2.0 x 10^{7}	$M^{-1}s^{-1}$
k_2	8.19 x 10^{6}	1.55 x 10^{7}	3.37 x 10^{6}	$M^{-1}s^{-1}$
k_3	3.01 x 10^{6}	1.18 x 10^{7}	6.77 x 10^{5}	$M^{-1}s^{-1}$
k_{app}	1.26 x 10^{-1}	9.51 x 10^{1}	3.96 x 10^{-1}	$M^{-1}s^{-1}$
k_a	9.56 x 10^{-3}	1.82 x 10^{-3}	4.30 x 10^{-2}	s^{-1}
k_b	1.93 x 10^{0}	1.01 x 10^{-1}	8.88 x 10^{-1}	$M^{-1}s^{-1}$
k_4	2.82 x 10^{2}	4.63 x 10^{2}	4.62 x 10^{1}	$M^{-1}s^{-1}$
k_{-4}	1.22 x 10^{-5}	1.29 x 10^{-5}	4.36 x 10^{-6}	$M^{-1}s^{-1}$
k_5	8.71 x 10^{-1}	2.80 x 10^{-1}	3.71 x 10^{-1}	s^{-1}
OF	5.5741 x 10^{-2}	3.2637 x 10^{-2}	9.19 x 10^{-3}	-
RMSE	8.0479 x 10^{-10}	5.8280 x 10^{-10}	1.6418 x 10^{-10}	-
$R^2_{adjusted,1}$	90.65%	84.95%	86.63%	-
$R^2_{adjusted,2}$	96.39%	89.68%	95.92%	-
$R^2_{adjusted,3}$	94.09%	96.36%	98.94%	-

Figures 6.17 and 6.18 present the model prediction and experimental data for the TCP and TCS degradation with the HRP enzyme, respectively. All measurements of the experimental data were performed in triplicate and considered the same enzyme concentrations as previously carried out by Costa et al. (2020) with SBP enzyme. A consistent fit of the experimental data for the considered model can be observed in both cases. These results also corroborate the good repeatability and reproducibility of the experiments conducted on the microreactor.

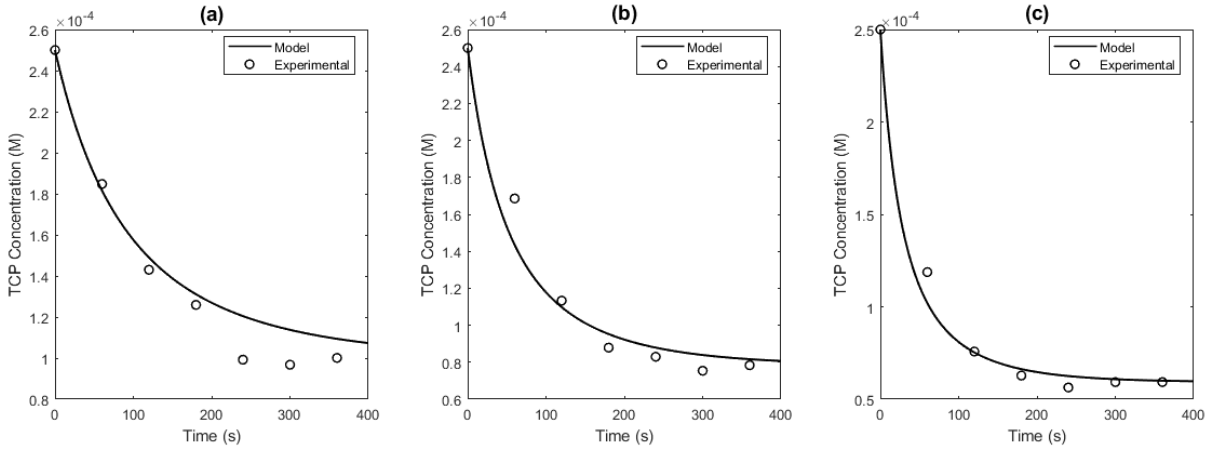

Figure 6.17 – Model prediction for TCP degradation with HRP in the microreactor.
HRP concentrations of: (a) 5.2 x 10^{-9} M; (b) 1.04 x 10^{-8} M; (c) 2.08 x 10^{-8} M.

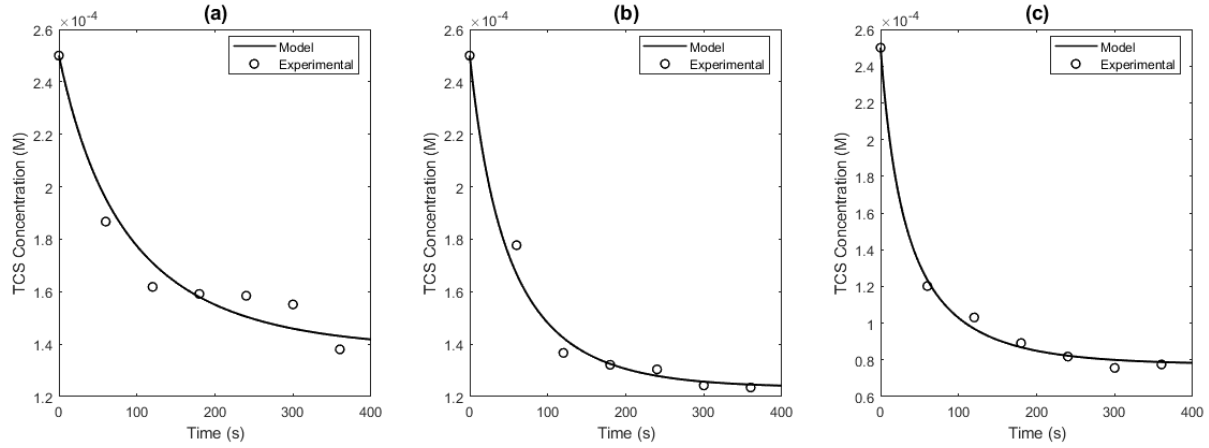

Figure 6.18 – Model prediction for TCS degradation with HRP in the microreactor.
HRP concentrations of: (a) 5.2 x 10^{-9} M; (b) 1.04 x 10^{-8} M; (c) 2.08 x 10^{-8} M.

Simulations of the concentration profile of all reaction components were also carried out. Figures 6.19 and 6.20 present the simulations of the substrates and product concentrations for the TCP and TCS degradation, respectively, and Figures 6.21 and 6.22 present the simulations of all the enzyme forms for the TCP and TCS degradation, respectively.

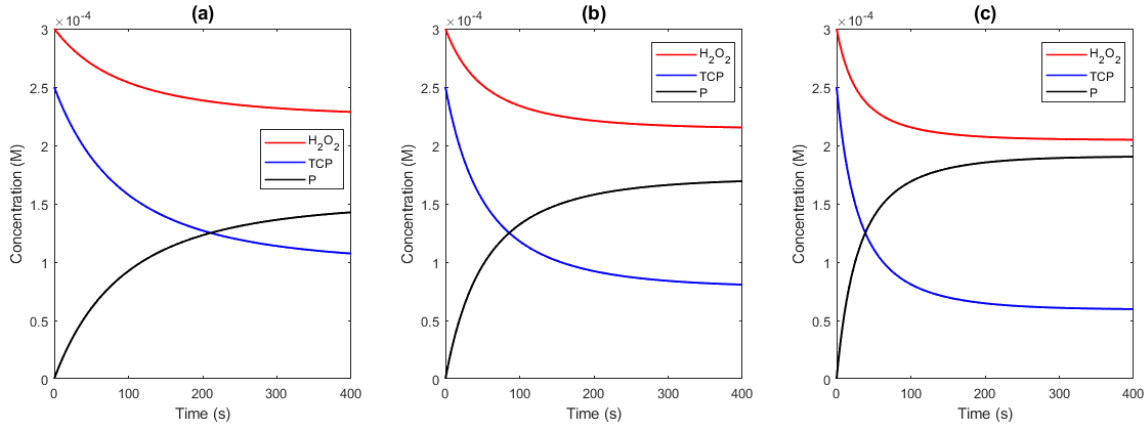

Figure 6.19 – Simulation of substrates and product concentrations for TCP degradation with HRP in the microreactor.
HRP concentrations of: (a) 5.2 x 10^{-9} M; (b) 1.04 x 10^{-8} M; (c) 2.08 x 10^{-8} M.

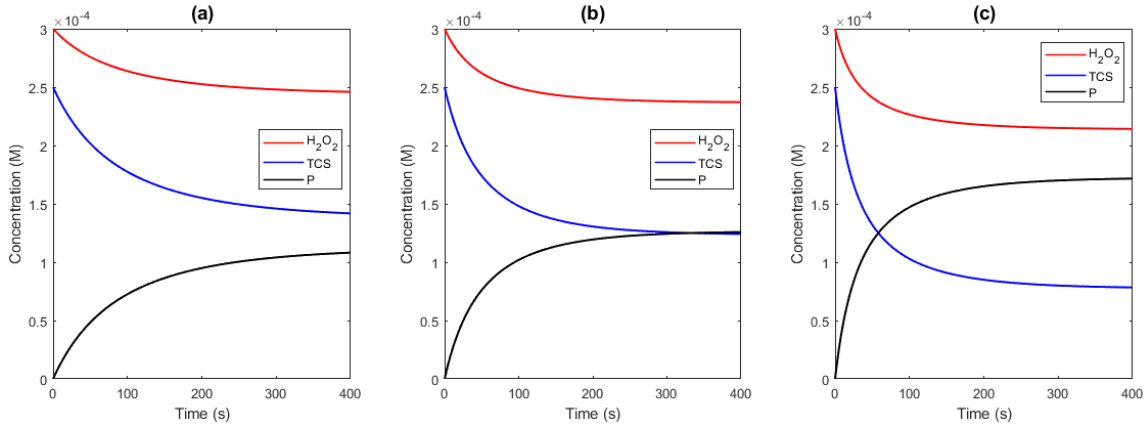

Figure 6.20 – Simulation of substrates and product concentrations for TCS degradation with HRP enzyme in the microreactor.
HRP concentrations of: (a) 5.2 x 10^{-9} M; (b) 1.04 x 10^{-8} M; (c) 2.08 x 10^{-8} M.

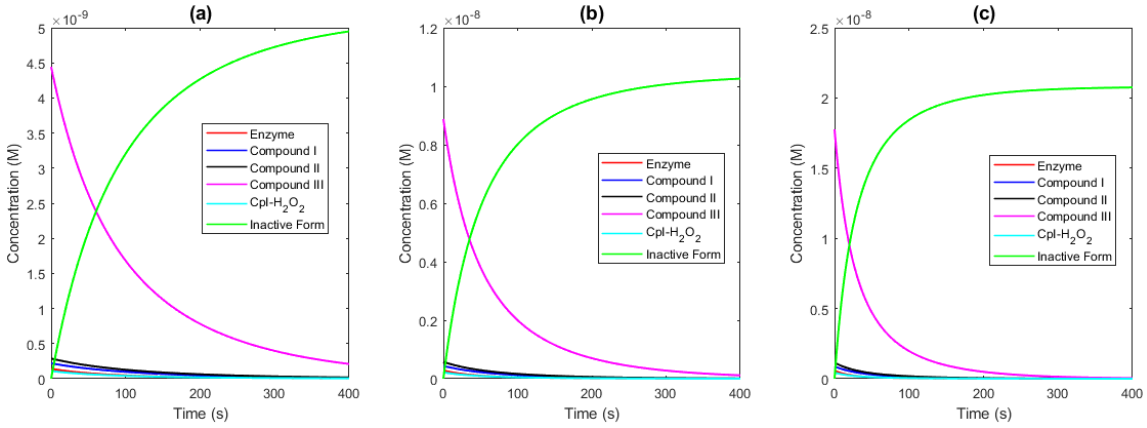

Figure 6.21 – Simulation of HRP form concentrations for TCP degradation in the microreactor.
HRP concentrations of: (a) 5.2 x 10^{-9} M; (b) 1.04 x 10^{-8} M; (c) 2.08 x 10^{-8} M.

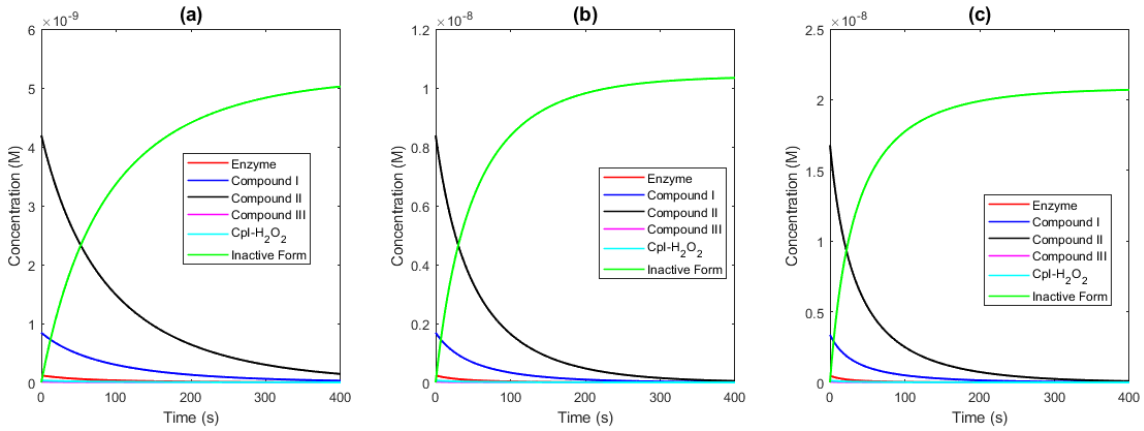

Figure 6.22 – Simulation of HRP form concentrations for TCS degradation in the microreactor.
HRP concentrations of: (a) 5.2 x 10^{-9} M; (b) 1.04 x 10^{-8} M; (c) 2.08 x 10^{-8} M.

These results are in agreement with those obtained for the degradation of TCP with the enzyme SBP. A different behavior was found for the concentrations of the enzyme forms, with a higher concentration of CpIII for the degradation of TCP and CpII for the degradation of TCS. So, it can be seen that the concentration profile of the enzyme forms can vary substantially depending on the enzyme and substrate considered. However, no evidence was found to explain this difference.

6.2 BATCH REACTIONS

6.2.1 Single-substrate degradation

Single-substrate degradation reactions were carried out in batches, to compare the behavior of SBP enzyme in the degradation of the substrates TCP, BPA, and TCS, and also a comparison of degradation with SBP and HRP enzymes. Table 6.3 presents the estimated parameters and model fit evaluation for the single-substrate degradation, and Figures 6.23 to 6.26 illustrate the model prediction and experimental data for these cases. The simplest model (Model 1) was considered with the formation of only CpI and CpII, to enable the comparison with the multi-substrate model, in which there is an increase in the number of parameters due to the greater number of substrates, as presented in the multi-substrate model development in Chapter 4. These results show that the single-substrate model represented well the single-substrate degradation data, presenting an adjusted R^2 always greater than 90%, except for the first set of TCS degradation experiments, which presented an adjusted R^2 of 64.65%.

Table 6.3 – Estimated parameters and model fit evaluation for single-substrate degradation.

Parameter	TCP (with SBP)	TCP (with HRP)	BPA (with SBP)	TCS (with SBP)	Unit
k_1	2.0 x 10^7	2.0 x 10^7	2.0 x 10^7	2.0 x 10^7	$M^{-1}s^{-1}$
k_2	2.98 x 10^6	3.43 x 10^6	3.81 x 10^6	1.60 x 10^6	$M^{-1}s^{-1}$
k_3	2.26 x 10^5	2.76 x 10^5	4.21 x 10^5	3.20 x 10^4	$M^{-1}s^{-1}$
OF	3.2512 x 10^{-2}	9.0529 x 10^{-3}	3.8340 x 10^{-2}	1.6043 x 10^{-1}	-
RMSE	8.31 x 10^{-12}	2.06 x 10^{-12}	4.37 x 10^{-12}	9.03 x 10^{-12}	-
$R^2_{adjusted,1}$	99.81%	98.22%	93.25%	64.65%	-
$R^2_{adjusted,2}$	96.86%	99.51%	97.96%	96.01%	-
$R^2_{adjusted,3}$	94.98%	99.67%	99.85%	97.61%	-

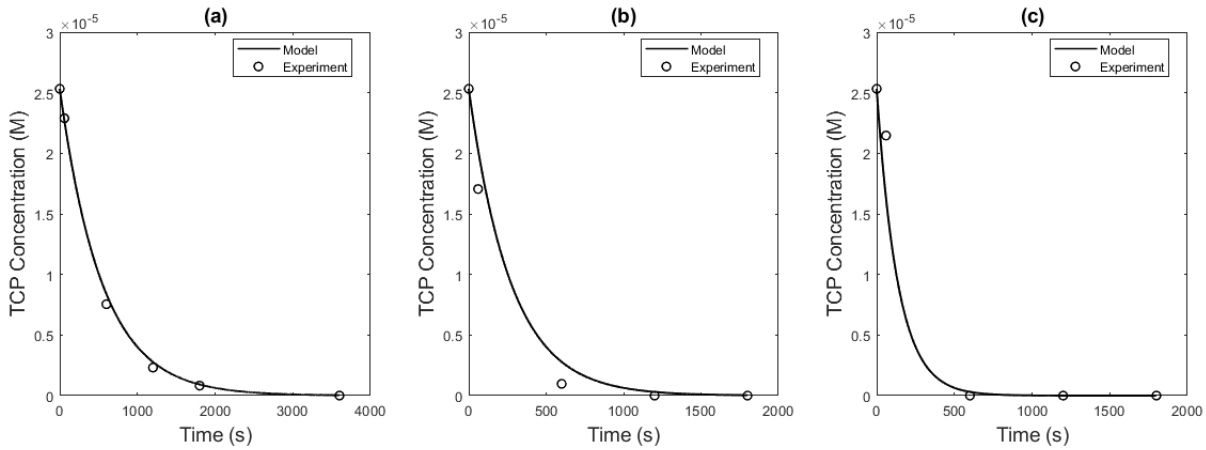

Figure 6.23 – Model prediction of TCP single-substrate degradation with SBP in batch.

SBP concentrations of: (a) 4.39 x 10^{-9} M; (b) 8.77 x 10^{-9} M; (c) 1.75 x 10^{-8} M.

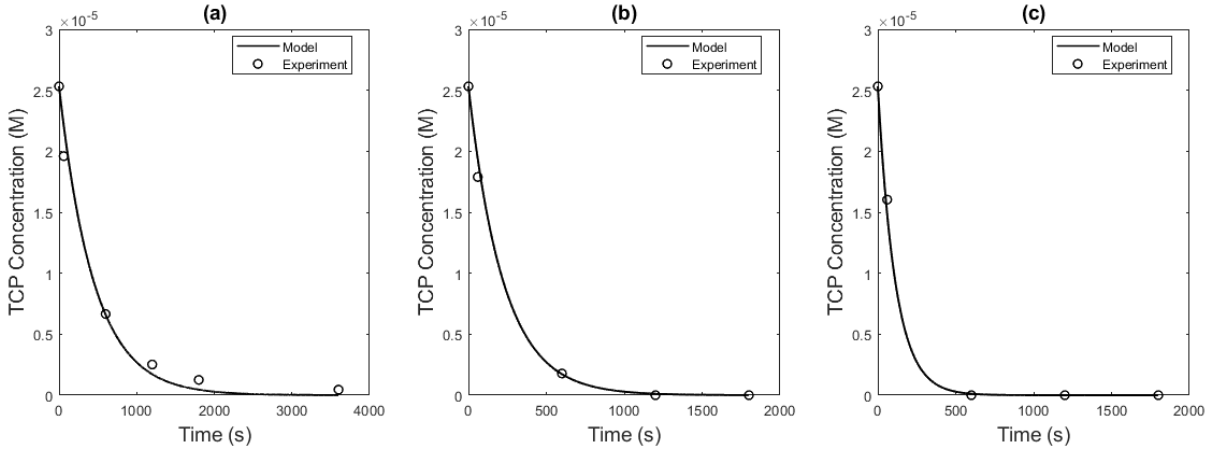

Figure 6.24 – Model prediction of TCP single-substrate degradation with HRP in batch.

HRP concentrations of: (a) 4.39 x 10^{-9} M; (b) 8.77 x 10^{-9} M; (c) 1.75 x 10^{-8} M.

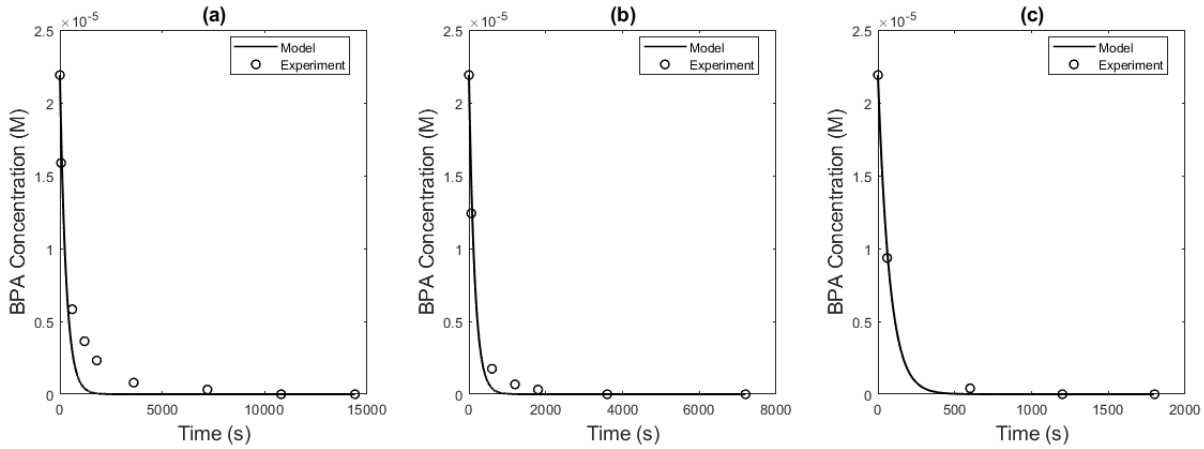

Figure 6.25 – Model prediction of BPA single-substrate degradation with SBP in batch.

SBP concentrations of: (a) 4.39 x 10^{-9} M; (b) 8.77 x 10^{-9} M; (c) 1.75 x 10^{-8} M.

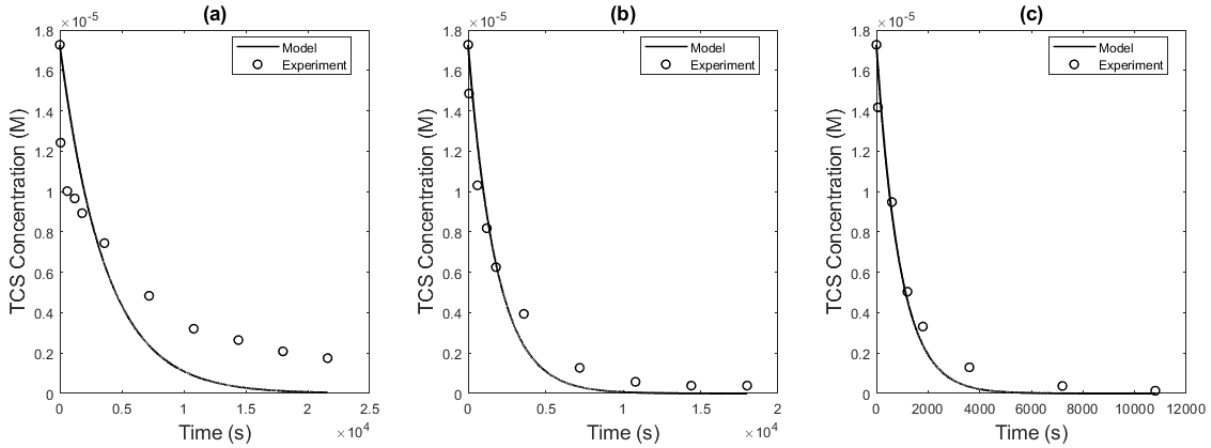

Figure 6.26 – Model prediction of TCS single-substrate degradation with SBP in batch.

SBP concentrations of: (a) 4.39 x 10^{-9} M; (b) 8.77 x 10^{-9} M; (c) 1.75 x 10^{-8} M.

6.2.2 Multi-substrate degradation

Multi-substrate degradation reactions were also carried out, to compare the behavior of SBP and HRP enzymes in the degradation of the substrates TCP, BPA, and TCS individually and in a mixture. First, the estimated parameters of the single-substrate degradation data were used to simulate the model with the data obtained for the multi-substrate degradation. Table 6.4 and Figures 6.27 to 6.30 present the results of these simulations.

Table 6.4 – Simulation considering single-substrate degradation model and multi-substrate degradation data.

Parameter	TCP (with SBP)	TCP (with HRP)	BPA (with SBP)	TCS (with SBP)	Unit
k_1	2.0 x 10^7	2.0 x 10^7	2.0 x 10^7	2.0 x 10^7	$M^{-1}s^{-1}$
k_2	2.98 x 10^6	3.43 x 10^6	3.81 x 10^6	1.60 x 10^6	$M^{-1}s^{-1}$
k_3	2.26 x 10^5	2.76 x 10^5	4.21 x 10^5	3.20 x 10^4	$M^{-1}s^{-1}$
RMSE	9.08 x 10^{-12}	2.70 x 10^{-11}	1.77 x 10^{-12}	5.04 x 10^{-12}	-
$R^2_{adjusted,1}$	80.56%	17.37%	95.24%	65.80%	-
$R^2_{adjusted,2}$	91.86%	44.47%	99.78%	55.48%	-
$R^2_{adjusted,3}$	91.69%	61.14%	96.70%	92.60%	-

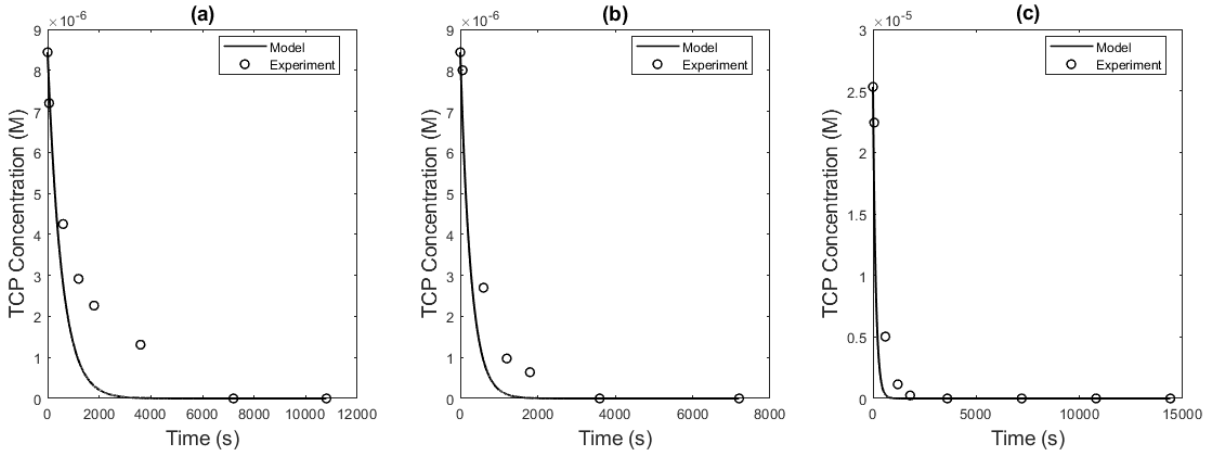

Figure 6.27 – Model simulation of TCP single-substrate degradation and TCP multi-substrate degradation data (in a reaction medium with BPA and TCS) with SBP in batch.

SBP concentrations of: (a) 4.39 x 10^{-9} M; (b) 8.77 x 10^{-9} M; (c) 1.75 x 10^{-8} M.

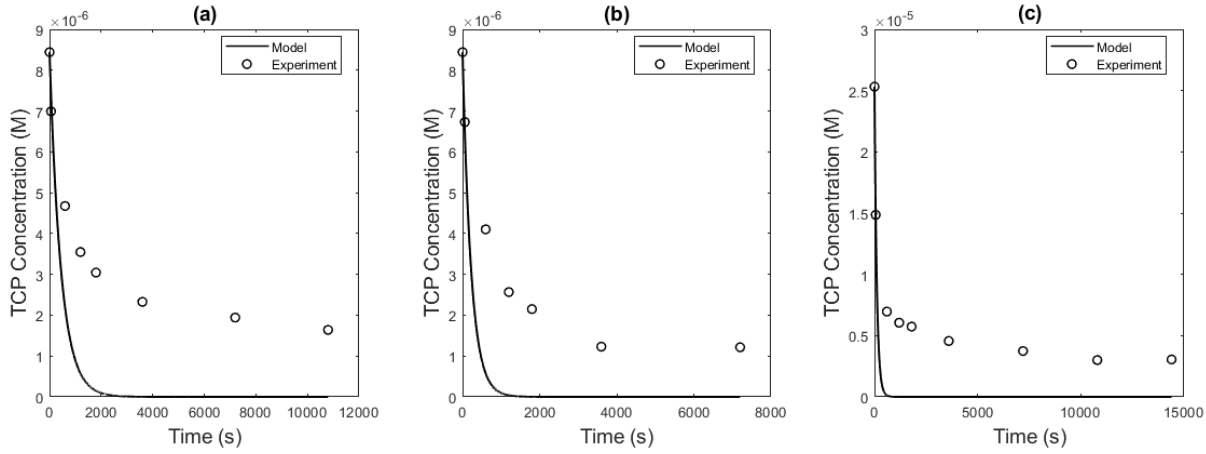

Figure 6.28 – Model simulation of TCP single-substrate degradation and TCP multi-substrate degradation data (in a reaction medium with BPA and TCS) with HRP in batch.

HRP concentrations of: (a) 4.39 x 10^{-9} M; (b) 8.77 x 10^{-9} M; (c) 1.75 x 10^{-8} M.

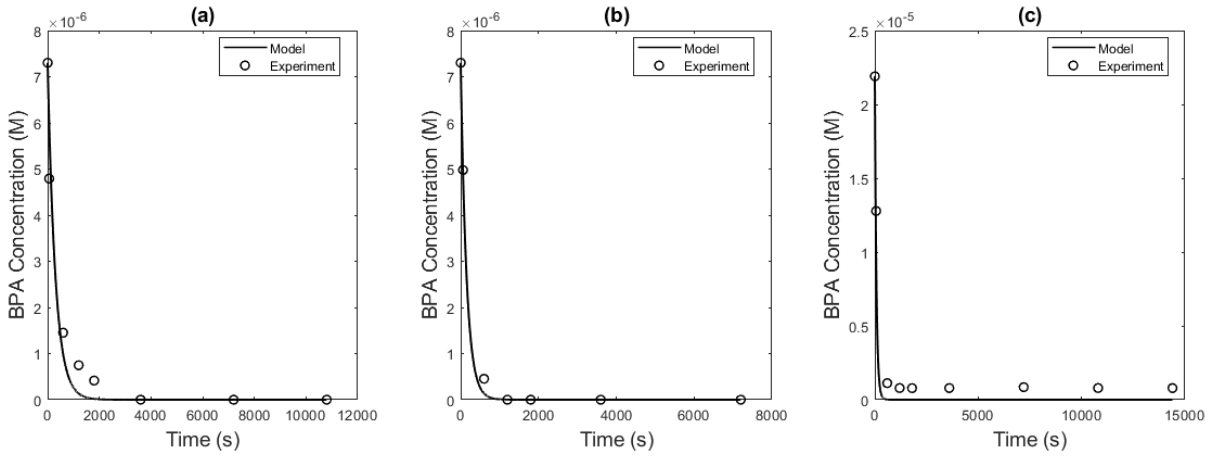

Figure 6.29 – Model simulation of BPA single-substrate degradation and BPA multi-substrate degradation data (in a reaction medium with TCP and TCS) with SBP in batch.

SBP concentrations of: (a) 4.39 x 10^{-9} M; (b) 8.77 x 10^{-9} M; (c) 1.75 x 10^{-8} M.

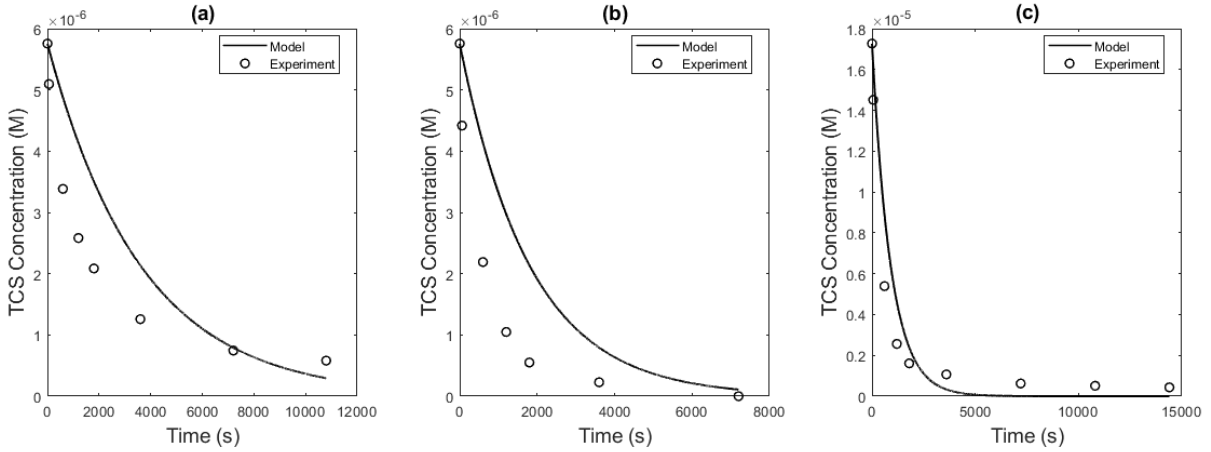

Figure 6.30 – Model simulation of TCS single-substrate degradation and TCS multi-substrate degradation data (in a reaction medium with BPA and TCP) with SBP in batch.

SBP concentrations of: (a) 4.39 x 10^{-9} M; (b) 8.77 x 10^{-9} M; (c) 1.75 x 10^{-8} M.

It can be observed that the single-substrate model cannot represent well the multi-substrate degradation data, mainly in the case of TCP with HRP and TCS with SBP. This simulation can be used as a basis for comparison with the parameter estimation results using the multi-substrate model, which are presented in Table 6.5 and Figures 6.31 to 6.36.

Table 6.5 – Estimated parameters and model fit evaluation for multi-substrate degradation in a reaction medium with TCP (A), BPA (B), and TCS (C).

Parameter	Degradation with SBP	Degradation with HRP	Unit
k_1	2.0 x 10^7	2.0 x 10^7	$M^{-1}s^{-1}$
k_{2A}	1.12 x 10^6	2.10 x 10^6	$M^{-1}s^{-1}$
k_{3A}	9.80 x 10^4	2.82 x 10^4	$M^{-1}s^{-1}$
k_{2B}	1.21 x 10^6	5.36 x 10^5	$M^{-1}s^{-1}$
k_{3B}	5.36 x 10^5	3.41 x 10^5	$M^{-1}s^{-1}$
k_{2C}	1.63 x 10^6	2.22 x 10^6	$M^{-1}s^{-1}$
k_{3C}	1.16 x 10^4	1.85 x 10^3	$M^{-1}s^{-1}$
OF	7.3492 x 10^{-2}	3.7562 x 10^{-1}	-
RMSE	2.64 x 10^{-12}	1.70 x 10^{-11}	-
$R^2_{adjusted,1}$	96.47%	74.37%	-
$R^2_{adjusted,2}$	98.59%	90.44%	-
$R^2_{adjusted,3}$	98.51%	84.87%	-

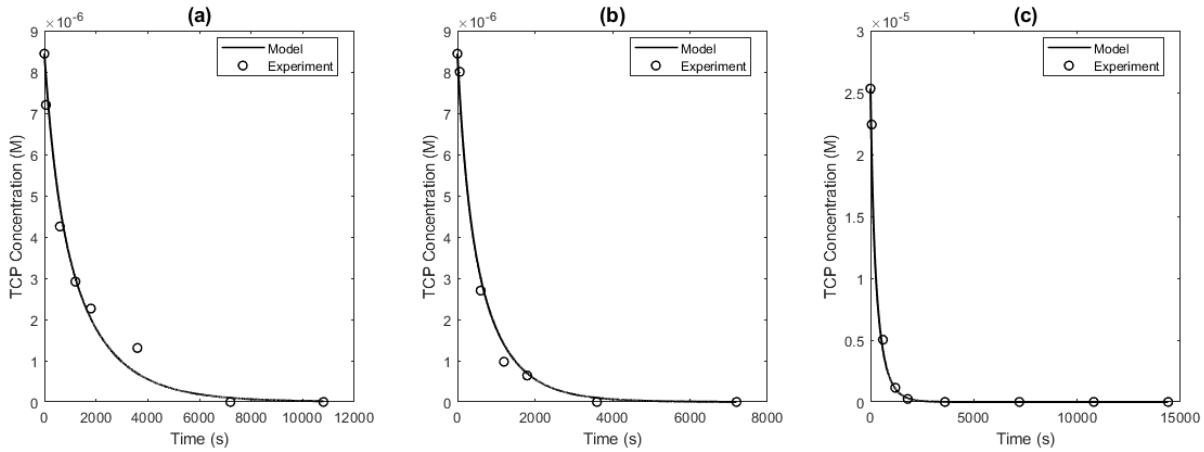

Figure 6.31 – Model prediction of TCP multi-substrate degradation with SBP in batch. SBP concentrations of: (a) 4.39 x 10^{-9} M; (b) 8.77 x 10^{-9} M; (c) 1.75 x 10^{-8} M.

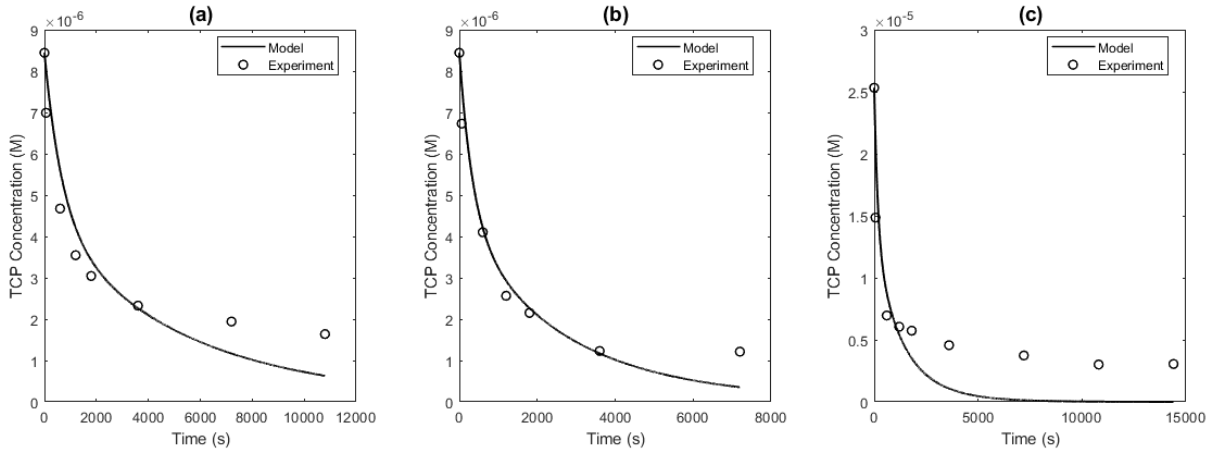

Figure 6.32 – Model prediction of TCP multi-substrate degradation with HRP in batch. HRP concentrations of: (a) 4.39 x 10^{-9} M; (b) 8.77 x 10^{-9} M; (c) 1.75 x 10^{-8} M.

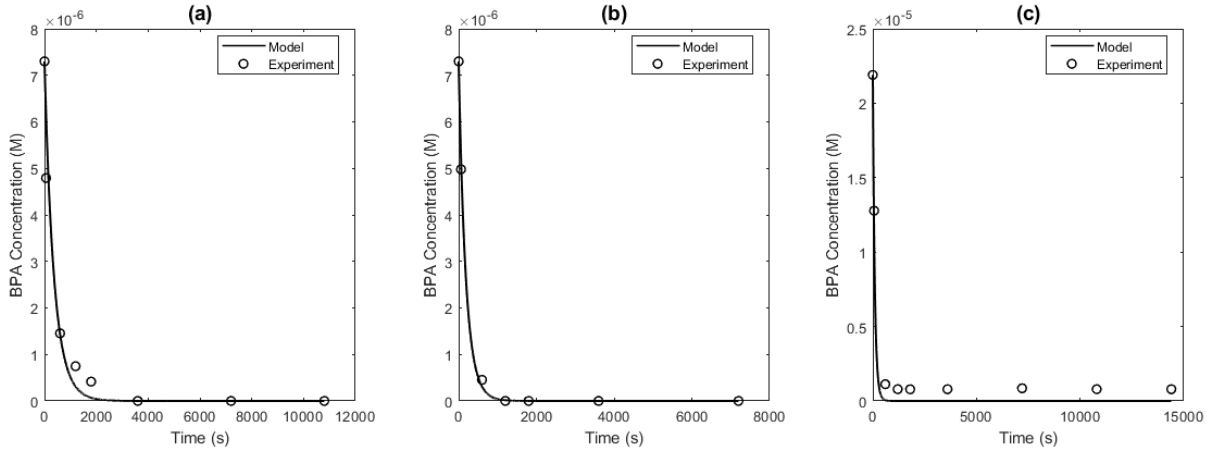

Figure 6.33 – Model prediction of BPA multi-substrate degradation with SBP in batch.

SBP concentrations of: (a) 4.39 x 10^{-9} M; (b) 8.77 x 10^{-9} M; (c) 1.75 x 10^{-8} M.

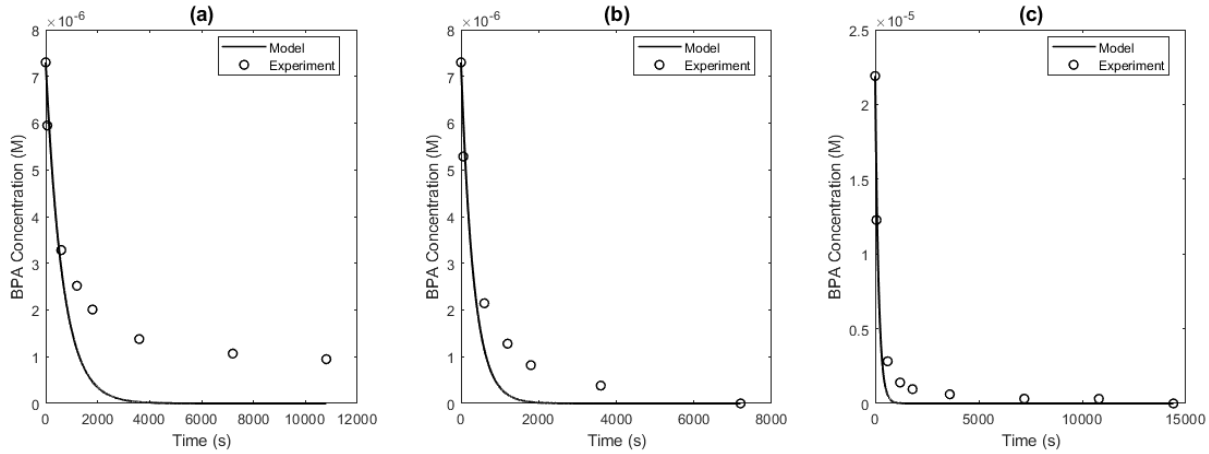

Figure 6.34 – Model prediction of BPA multi-substrate degradation with HRP in batch.

HRP concentrations of: (a) 4.39 x 10^{-9} M; (b) 8.77 x 10^{-9} M; (c) 1.75 x 10^{-8} M.

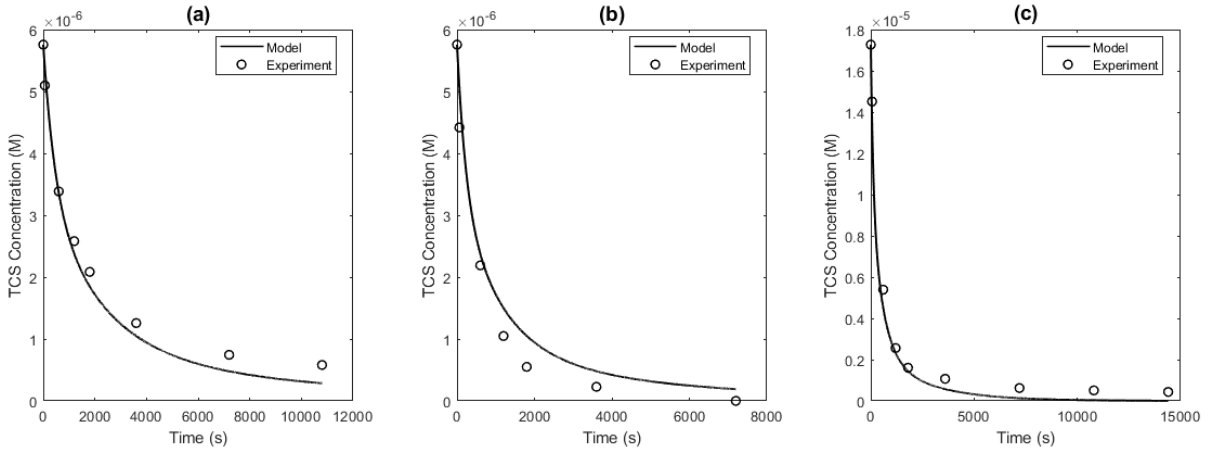

Figure 6.35 – Model prediction of TCS multi-substrate degradation with SBP in batch.

SBP concentrations of: (a) 4.39 x 10^{-9} M; (b) 8.77 x 10^{-9} M; (c) 1.75 x 10^{-8} M.

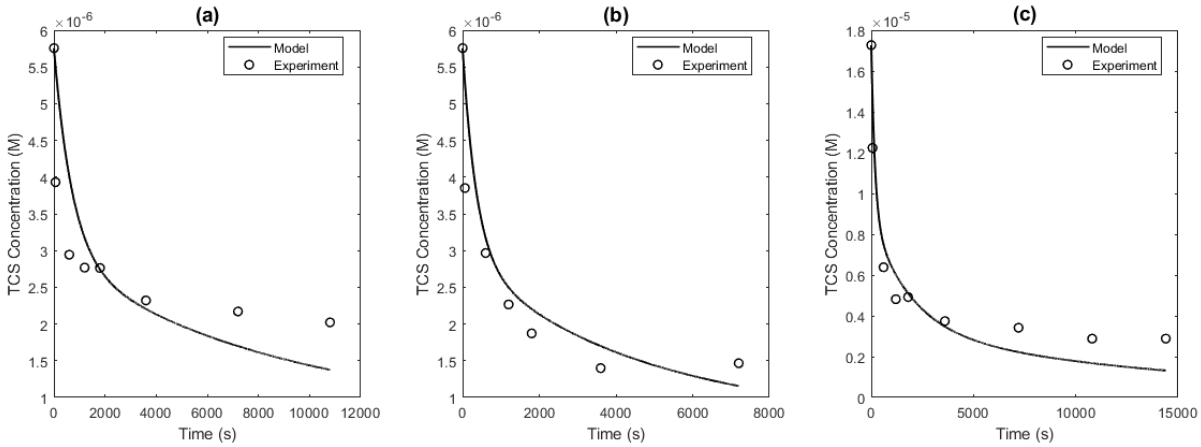

Figure 6.36 – Model prediction of TCS multi-substrate degradation with HRP in batch.
HRP concentrations of: (a) 4.39 x 10^{-9} M; (b) 8.77 x 10^{-9} M; (c) 1.75 x 10^{-8} M.

These results show that the proposed multi-substrate model better represents the substrates degradation data. This conclusion is quite relevant, since the multi-substrate model considering the modified bi-bi ping pong model is proposed in this thesis. It is also worth noting that the degradation data with the SBP enzyme showed a better fit.

CHAPTER 7
CONCLUSIONS AND FUTURE WORKS

7.1 CONCLUSIONS

The studies presented in this work showed the efficiency of the SBP enzyme in degrading harmful compounds, such as the chlorinated phenolic ones, by the degradation reactions catalyzed by SBP in the presence of hydrogen peroxide. SBP is an enzyme that can be extracted from soybean hulls in a sustainable and cost-effective process, being a very promising bioremediation method for wastewater treatment. In this work, SBP was extracted and purified successfully by the soybean seed hulls, with a specific activity of 35 μmol/min, and an RZ value of 0.45, which suggests that the protein obtained is not particularly pure, probably because of an aging factor of the soybean hulls. However, the SBP enzyme obtained showed a good performance in the degradation of pollutants.

TCP degradation with HRP commercial enzyme in the presence of hydrogen peroxide was carried out in the microreactor in the same operational conditions as previously conducted by Costa (2016) with SBP, as well as TCS degradation reactions. The maximum percentage of TCP degradation achieved using SBP was approximately 96%, while for HRP it was approximately 78%. The maximum percentage of TCS degradation achieved with HRP was approximately 70%. Studies were also carried out on the influence of pH, temperature, and concentration in the microreactor, showing a better efficiency at pH between 5 and 6, room temperature, and H_2O_2 concentration of 0.3 mM. The microreactor showed good repeatability and reproducibility of data obtained under these different conditions, as expected.

Batch reactions were also carried out aiming to study the enzymatic degradation reactions in conditions closer to a real application. Compared to the microreactor, the batch reactions were slower, as expected due to mass transport factors included and also due to the controlled conditions of pH, temperature, and pressure in the microreactor. However, 100% of degradation was achieved in batch, but not in the microreactor for the same conditions. Compar-

ing the single-substrate degradation with the multi-substrate degradation, it was observed that a substrate may behave differently depending on the situation, due to a possible competition between the pollutants in the reaction medium. Comparing the performance of the SBP and HRP enzymes, SBP showed a faster and more efficient degradation, as well as in the microreactor.

All experiments were performed in triplicate, with acceptable repeatability. The calibration curves of TCP, TCS, and BPA were obtained with R^2 values close to 100% and could be used to quantify these substrates using HPLC-UV properly. It was possible to observe the formation of two products of the TCP degradation reaction, which is consistent with the literature. For TCS, in turn, several products were formed that could be observed only momentarily, which would probably be the dimers and trimers formed, which are quite unstable. For BPA, it was not possible to observe the reaction products consistently, probably because the wavelength chosen for HPLC-UV analysis was not the most suitable for these specific compounds, or even because they were also degraded in the reaction.

A toxicity test of the mix solution with TCP, BPA and TCS was also performed, both before and after the degradation reaction with the SBP enzyme. It was possible to observe a decrease in the effect of toxicity throughout the reaction, indicating that the increase in the viability of the bacteria is correlated with the removal of the three pollutants.

Regarding the mathematical modeling and simulation of the process, a study was first carried out to develop the modified bi-bi ping-pong model using the experimental data of Costa (2016). Six different hypotheses based on the bi-bi ping pong model were used to match the experimental data. Those assumptions consisted of the enzyme inactivation and the formation of additional intermediate compound CpIII and the $CpI{\cdot}H_2O_2$ complex, which could be considered in the model or not. A parameter estimation procedure was implemented in MATLAB, to obtain the kinetic constants of the reactions. It used the *fmincon* solver, considering the interior point method, and the *ode15s* solver, which solves the DAE systems by the BDF method. The objective function was the weighted least squares between the experimental data set and the values predicted by the respective model. The results were compared based on the OF values, RMSE, and adjusted R^2. A global analysis concluded that considering all the enzyme forms (CpI, CpII, CpIII, and $CpI{\cdot}H_2O_2$), as well as the enzyme inactivation model, provides more consistent results. The 9 kinetic constants of the model were obtained for the degradation of TCP with the enzymes SBP and HRP, and for the degradation of TCS with HRP in the microreactor, as well as the simulation of the concentration profiles of all species of the reactions.

Mathematical modeling of the process was also performed for the batch reactions, which were performed for the comparison of TCP, TCS, and BPA substrates both separately and in a mixture. Besides, the simplest model was considered in this case, with the formation of only compounds I and II, to enable the comparison with the proposed multi-substrate model, in which there is a significant increase in the number of parameters. It was observed that the single-substrate model could not represent well the multi-substrate degradation data, but the proposed multi-substrate model could represent the degradation data quite consistently.

Therefore, all the results presented in this work can serve as a basis for a better understanding of the enzymatic degradation reaction mechanism, which allows a more accurate reactor design and process simulation.

7.2 FUTURE WORKS

Future works can be carried out:

- Considering the SBP enzyme immobilization so that it can be reused in new reaction cycles, which cannot be done with the enzyme in solution as done in this work;
- Performing a more precise experimental analysis to identify the reaction products and possibly the oxidized intermediates of the enzyme (CpI, CpII, and CpIII);
- Doing other degradation experiments considering other chlorinated phenolic compounds and different combinations of these substrates, or even reagents with completely different functional groups to further explore the degradation potential of the SBP enzyme with other types of pollutants;
- Perform new experiments of enzymatic reactions or other kinetics in the microreactor, corroborating the study of fast kinetics.

BIBLIOGRAPHY

ADEDIRAN, A.; LAMBEIR, A. “Kinetics of the reaction of compound I1 of horseradish peroxidase with hydrogen peroxide to form compound III”. ***European Journal of Biochemistry***, v. 186, p. 571–576, 1989.

AI, L.; REN, T.; YAN, Q.; WAN, M.; PENG, Y.; XU, X.; LIU, X. “Degradation efficiencies of 2,4,6-TCP by Fe0-based advanced oxidation processes (AOPs) with common peroxides”. ***PLOS ONE***, Public Library of Science, v. 16, n. 9, p. 1–14, Sept. 2021.

AL-ANSARI, M.; SAHA, B.; MAZLOUM, S.; TAYLOR, K.; BEWTRA, J.; BISWAS, N. “Soybean peroxidase applications in wastewater treatment”. ***Soybeans: Cultivation, Uses and Nutrition***, p. 189–221, 2011.

ALTAHIR, B. M.; AL-ROBAIEY, T. J.; ABBAAS, Z. M.; MASHHADI, N.; VILLEGAS, L. G. C.; TAYLOR, K. E.; BISWAS, N. “Soybean peroxidase catalyzed decoloration of acid azo dyes”. ***Journal of Health and Pollution***, v. 10, n. 25, p. 1–10, 2020.

ANJANEYULU, Y.; CHARY, N. S.; RAJ, D. S. S. “Decolorization of industrial effluents-available methods and emerging technologies: a review”. ***Reviews in Environmental Science and Biotechnology***, v. 4, p. 245–273, 2005.

ARNAO, M.; ACOSTA, M.; RIO, J. del; VARON, R.; GARCIA-CANOVAS, F. “A kinetic study on the suicide inactivation of peroxidase by hydrogen peroxide”. ***Biochimica et Biophysica Acta***, v. 1041, p. 43–47, 1990.

AZIZYAN, R.; GEVORGYAN, A.; ARAKELYAN, V.; GEVORGYAN, E. “Computational modeling of kinetics of the bisubstrate enzymatic reaction with ping-pong mechanism”. ***Biological Journal of Armenia***, v. 2, n. 64, p. 85–93, 2012.

AZIZYAN, R. A.; GEVOGYAN, A. E.; ARAKELYAN, V. B.; GEVORGYAN, E. S. “Mathematical modeling of bi-substrate enzymatic reactions with ping-pong mechanism in the presence of competitive inhibitors”. ***International Scholarly and Scientific Research and Innovation***, v. 7, n. 2, p. 163–165, 2013.

BASSI, A.; Z., G.; GIJZEN, M. “Enzymatic removal of phenol and chlorophenols using soybean seed hulls”. ***Engineering in Life Sciences***, v. 4, p. 125–130, 2004.

BILAL, M.; BARCELó, D.; IQBAL, H. M. N. “Persistence, ecological risks, and oxidoreductases-assisted biocatalytic removal of triclosan from the aquatic environment”. ***Science of the Total Environment***, v. 735, n. 139194, 2020.

BÓDALO, A.; GÓMEZ, J. L.; GÓMEZ, E.; BASTIDA, J.; MÁXIMO, M. F. “Comparison of commercial peroxidases for removing phenol from water solutions”. ***Chemosphere***, v. 63, n. 4, p. 626–632, 2006.

BORZANI, W.; SCHMIDELL, W.; LIMA, U. A.; AQUARONE, E. "***Biotecnologia Industrial: Fundamentos***". São Paulo: Edgard Blücher, 2001. v. 1. 254 p.

BROOKS, S. P. J.; SUELTER, C. H. "Estimating enzyme kinetic parameters: a computer program for linear regression and non-parametric analysis". ***International Journal of Bio-Medical Computing***, v. 19, p. 89–99, 1985.

BUCHANAN, I.; NICELL, J. "Model development for hoseradish peroxidase catalyzed removal of aqueous phenol". ***Biotechnology and Bioengineering***, v. 54,3, p. 251–261, 1997.

CALZA, P.; AVETTA, P.; RUBULOTTA, G.; SANGERMANO, M.; LAURENTI, E. "TiO2-soybean peroxidase composite materials as a new photocatalytic system". ***Chemical Engineering Journal***, Elsevier B.V., v. 239, p. 87–92, 2014.

CALZA, P.; ZACCHIGNA, D.; LAURENTI, E. "Degradation of orange dyes and carbamazepine by soybean peroxidase immobilized on silica monoliths and titanium dioxide". ***Environmental Science and Pollution Research***, v. 23, n. 23, p. 23742–23749, 2016.

CAZA, N.; BEWTRA, J. K.; BISWAS, N.; TAYLOR, K. E. "Removal of phenolic compounds from synthetic wastewater using soybean peroxidase". ***Water Research***, v. 33, n. 13, p. 3012–3018, 1999.

CHERRY, J.; FIDANTSEF, A. "Directed evolution of industrial enzymes: an update". ***Current Opinion in Biotechnology***, v. 14, p. 438–443, 2003.

CLELAND, W. W. "Computer programmes for processing enzyme kinetic data". ***Nature***, n. 4879, p. 463–465, 1963.

CLELAND, W. W. "The kinetics of enzyme catalysed reaction with two or more substrates or products, nomenclature and rate equations". ***Biochimica et Biophysica Acta***, v. 67, p. 104–137, 1963.

CORNISH-BOWDEN, A.; EISENTHAL, R. "Statistical considerations in the estimation of enzyme kinetic parameters by the direct linear plot and other methods". ***Biochemical Journal***, v. 139, p. 721–730, 1974.

COSTA, R. A.; CUNHA, A. S.; PERES, J. C. G.; AZZONI, A. R.; LAURENTI, E.; VIANNA, A. S. "Enzymatic degradation of 2,4,6-trichlorophenol in a microreactor using soybean peroxidase". ***Symmetry***, v. 12, n. 1129, 2020.

COSTA, R. de A. "***Degradação Enzimática de Clorofenol em Microrreator***". Master's Thesis. PEQ-EPUSP, University of São Paulo, São Paulo - SP: [s.n.], 2016.

CUNHA, A. S.; VIANNA, A. S.; LAURENTI, E. "Modeling and simulation of the enzymatic degradation of 2,4,6-trichlorophenol using soybean peroxidase". ***Brazilian Journal of Chemical Engineering***, v. 38, p. 719–730, 2021.

CURRIE, D. J. "Estimating michaelis-menten parameters: Bias, variance and experimental design". ***International Biometric Society***, v. 38, n. 4, p. 907–919, 1982.

DOU, R. N.; WANG, J. H.; CHEN, Y. C.; HU, Y. Y. "The transformation of triclosan by laccase: Effect of humic acid on the reaction kinetics, products and pathway". ***Environmental Pollution***, v. 234, p. 88–95, 2018.

DURRUTY, I.; OKADA, E.; GONZáLEZ, J. F.; MURIALDO, S. E. “Multisubstrate monod kinetic model for simultaneous degradation of chlorophenol mixtures”. ***Biotechnology and Bioprocess Engineering***, v. 16, p. 1–8, 2011.

EMBRAPA. “**Soja em números (safra 2021/22).**” Available in: <https://www.embrapa.br/soja/cultivos/soja1/dados-economicos>, Accessed in: 28 jan. 2023.

ESCALONA, I.; GROOTH, J.; FONT, J.; NIJMEIJER, K. “Removal of BPA by enzyme polymerization using NF membranes”. ***Journal of Membrane Science***, v. 468, p. 192–201, 2015.

FATIBELLO FILHO, O.; VIEIRA, I. C. “Uso analítico de tecidos e de extratos brutos vegetais como fonte enzimática”. ***Química Nova***, v. 25, p. 455–464, 2002.

FERRARI, R. P.; LAURENTI, E.; TROTTA, F. “Oxidative 4-dechlorination of 2,4,6-trichlorophenol catalyzed by horseradish peroxidase”. ***Journal of Biological Inorganic Chemistry***, v. 4, n. 2, p. 232–237, 1999.

FERSHT, A. “***Structure and mechanism in protein science: A guide to enzyme catalysis and protein folding.***” 1st. ed. [S.l.]: W. H. Freeman, 1999. 650 p.

FOGLER, H. S. “***Elements of Chemical Reaction Engineering***”. 5th. ed. [S.l.]: Prentice Hall PTR, 2016. 992 p.

GACCHE, R.; FIRDAUS, Q.; SAGAR, A. “Soybean (Glycine max L.) seed coat peroxidase immobilized on fibrous aromatic polyamide: a strategy for decreasing phenols from industrial wastewater”. ***Journal of Scientific and Industrial Research***, v. 62, p. 1090–1093, 2003.

GARDINER, W. R.; OTTAWAY, J. H. “Observations on programs to estimate the parameters of enzyme kinetics”. ***FEBS Letters***, v. 2, p. 34–38, 1969.

GHAEMMAGHAMI, F.; ALEMZADEH, I.; MOTAMED, S. “Seed coat Soybean peroxidase: extraction and biocatalytic properties determination”. ***Iranian Journal of Chemical Engineering***, v. 7, n. 2, p. 28–38, 2010.

GILLIKIN, J. W.; GRAHAM, J. S. “Purification and Developmental Analysis of the Major Anionic Peroxidase from the Seed Coat of Glycine max”. ***Plant Physiology***, v. 96, n. 1, p. 214–220, 1991.

GOWDA, T.; LOCK, J.; KURTZ, R. “A comprehensive study of risk assessment for a hazardous compound of public health concern”. ***Water, Air & Soil Pollution***, v. 24(2), 1985.

HENRIKSEN, A. “Structure of soybean seed coat peroxidase: A plant peroxidase with unusual stability and haem-apoprotein interactions”. ***Protein Science***, v. 10, n. 1, p. 108–115, 2001.

HONG-MEI, L.; NICELL, J. A. “Biocatalytic oxidation of bisphenol A in a reverse micelle system using horseradish peroxidase”. ***Bioresource Technology***, v. 99, p. 4428–4437, 2008.

HONGMEI, L.; NICELL, J. A. “Optimal Conditions for Oxidative Degradation of Bisphenol A by Horseradish Peroxidase in Aqueous Phase”. ***2011 International Conference on Multimedia Technology***, p. 25442–5446, 2011.

HUANG, Q.; WEBER JR, W. J. “Transformation and removal of bisphenol A from aqueous phase via peroxidase-mediated oxidative coupling reactions: efficacy, products, and pathways.” ***Environmental Science & Technology***, v. 39, p. 6029–6036, 2005.

HUSAIN, Q. “Peroxidase mediated decolorization and remediation of wastewater containing industrial dyes: a review”. ***Reviews in Environmental Science and Biotechnology***, v. 9, p. 117–140, 2010.

JIANG, X.; ZHENG, H. “Removal of Bisphenol A by Soybean Hulls Peroxidase”. ***Asian Journal of Chemistry***, v. 25, n. 11, p. 5887–5890, 2013.

JIMENEZ-HOLGADO, C.; CALZA, P.; FABBRI, D.; DAL BELLO, F.; MEDANA, C.; SAKKAS, V. “Investigation of the aquatic photolytic and photocatalytic degradation of citalopram”. ***Molecules***, v. 26, n. 5331, 2021.

JOB, D.; DUNFORD, H. B. “Substituent effect on the oxidation of phenols and aromatic amines by horseradish peroxidase compound I”. ***European Journal of Biochemistry***, v. 66, p. 607–14, 1976.

KALSOOM, U.; ASHRAF, S.; MEETANI, M.; RAUF, M.; BHATTI, H. “Mechanistic study of a diazo dye degradation by soybean peroxidase”. ***Chemistry Central Journal***, v. 7:93, 2013.

KAMAL, J. K. A.; BEHERE, D. V. “Thermal and conformational stability of seed coat soybean peroxidase”. ***Biochemistry***, v. 41, n. 29, p. 9034–9042, 2002.

KOBAYASHI, S.; UYAMA, H.; USHIWATA, T.; UCHIYAMA, T.; SUGIHARA, J.; KURIOKA, H. “Enzymatic oxidative polymerization of bisphenol-A to a new class of soluble polyphenol”. ***Macromolecular Chemistry and Physics***, v. 199, p. 777–782, 1998.

KONG, M.; ZHANG, Y.; LI, Q.; DONG, R.; GAO, H. “Kinetics of horseradish peroxidase-catalyzed nitration of phenol in a biphasic system”. ***Journal of Microbiology and Biotechnology***, v. 27, n. 2, p. 297–305, 2017.

LAURENTI, E.; GHIBAUDI, E.; ARDISSONE, S.; FERRARI, R. P. “Oxidation of 2,4-dichlorophenol catalyzed by horseradish peroxidase: Characterization of the reaction mechanism by UV-visible spectroscopy and mass spectrometry”. ***Journal of Inorganic Biochemistry***, v. 95, n. 2-3, p. 171–176, 2003.

LAURENTI, E.; GHIBAUDI, E.; TODARO, G.; FERRARI, R. P. “Enzymatic degradation of 2,6-dichlorophenol by horseradish peroxidase”. ***Journal of Inorganic Biochemistry***, v. 92, p. 75–81, 2002.

LAURENTI, E.; VIANNA JR, A. d. S. “Enzymatic microreactors in biocatalysis: history, features, and future perspectives”. ***Biocatalysis***, v. 1, n. 1, 2016.

LEVENSPIEL, O. “***Chemical Reaction Engineering***”. 3rd. ed. [S.l.]: Wiley, 1999.

LI, J.; PENG, J.; ZHANG, Y.; JI, Y.; SHI, H.; MAO, L.; GAO, S. “Removal of triclosan via peroxidases-mediated reactions in water: Reaction kinetics, products and detoxification”. ***Journal of Hazardous Materials***, v. 310, p. 152–160, 2016.

LLORET, L.; EIBES, G.; MOREIRA, M. T.; FEIJOO, G.; LEMA, J. M.; MIYAZAKI, M. “Improving the catalytic performance of laccase using a novel continuous-flow microreactor”. ***Chemical Engineering Journal***, Elsevier B.V., v. 223, p. 497–506, 2013.

MARCHIS, T.; AVETTA, P.; BIANCO-PREVOT, A.; FABBRI, D.; VISCARDI, G.; LAURENTI, E. “Oxidative degradation of Remazol Turquoise Blue G 133 by soybean peroxidase”. ***Journal of Inorganic Biochemistry***, Elsevier Inc., v. 105, n. 2, p. 321–327, 2011.

MELO, C. F.; DEZOTTI, M. “Evaluation of a horseradish peroxidase-catalyzed process for triclosan removal and antibacterial activity reduction”. ***Journal of Chemical Technology and Biotechnology***, v. 88, p. 930–936, 2013.

NAKAJIMA, R.; YAMAZAKI, I. “The mechanism of oxyperoxidase formation from ferry1 peroxidase and hydrogen peroxide”. ***Journal of Biological Chemistry*** , v. 262, p. 2576–2581, 1987.

NGO, T.; LENHOFF, H. “A sensitive and versatile chromogenic assay for peroxidase and peroxidase-coupled reactions”. ***Analytical Biochemistry***, v. 105, p. 389–397, 1980.

NICELL, J.; WRIGHT, H. “A model of peroxidase activity with inhibition by hydrogen peroxide”. ***Enzyme and Microbial Technology***, v. 21, p. 302–310, 1997.

NICELL, J. A. “Kinetics of horseradish peroxidase-catalysed polymerization and precipitation of aqueous 4-chlorophenol”. ***Journal of Chemical Technology & Biotechnology***, v. 60, n. 2, p. 203–215, 1994.

NICELL, J. A.; BEWTRA, J. K.; TAYLOR, K. E.; BISWAS, N.; St. Pierre, C. “Enzyme catalyzed polymerization and precipitation of aromatic compounds from wastewater”. ***Water Science and Technology***, v. 25, n. 3, p. 157–164, 1992.

NISSUM, M.; SCHIODT, C. B.; WELINDER, K. G. “Reactions of soybean peroxidase and hydrogen peroxide pH 2.4-12.0, and veratryl alcohol at pH 2.4”. ***Biochimica et Biophysica Acta***, v. 1545, n. 1-2, p. 339–348, 2001.

PECK, E.; VINING, G.; MONTGOMERY, D. “***Introduction to Linear Regression Analysis***”. 5th. ed. [S.l.]: Wiley Series in Probability and Statistics, 2012. 672 p.

REICH, J. G. “Parameter estimation and enzyme kinetic models”. ***FEBS Letters***, v. 9, n. 5, p. 245–251, 1970.

SAKURADA, J.; SEKIGUCHI, R.; SATO, K.; HOSOYA, T. “Kinetic and molecular orbital studies on the rate of oxidation ofmonosubstituted phenols and anilines by horseradish peroxidase compound II”. ***Biochemistry***, v. 29, p. 4093–4098, 1990.

SARRO, M.; GULE, N. P.; LAURENTI, E.; GAMBERINI, R.; PAGANINI, M. C.; MALLON, P. E.; CALZA, P. “ZnO-based materials and enzymes hybrid systems as highly efficient catalysts for recalcitrant pollutants abatement”. ***Chemical Engineering Journal***, Elsevier, v. 334, n. June 2017, p. 2530–2538, 2018.

SCHMALL, M. “***Cinética e Reatores: Teoria e Exercícios***”. 2nd. ed. [S.l.]: Synergia: COPPE/UFRJ: FAPERJ, 2013. 541 p.

SCHWAAB, M. “***Avaliação de Algoritmos Heurísticos de Otimização em Problemas de Estimação de Parâmetros***”. Master’s Thesis. COPPE/UFRJ, Federal University of Rio de Janeiro, Rio de Janeiro - RJ: [s.n.], 2005.

SCHWAAB, M.; PINTO, J. "***Análise de Dados Experimentais I - Fundamentos de Estatística e Estimação de Parâmetros***". 1st. ed. [S.l.: s.n.], 2007. 462 p.

SHARMA, B.; DANGI, A. K.; SHUKLA, P. "Contemporary enzyme based technologies for bioremediation: A review". ***Journal of Environmental Management***, v. 210, p. 10–22, 2018.

SHINTAKU, M.; MATSUURA, K.; YOSHIOKA, S.; TAKAHASHI, S.; ISHIMORI, K.; MORISHIMA, I. "Absence of a detectable intermediate in the compound I formation of horseradish peroxidase at ambient temperature". ***Journal of Biological Chemistry***, v. 280, n. 49, p. 40934–40938, 2005.

SILVA, M. C.; TORRES, J. A.; Vasconcelos De Sá, L. R.; CHAGAS, P. M. B.; FERREIRA-LEITÃO, V. S.; CORRÊA, A. D. "The use of soybean peroxidase in the decolourization of Remazol Brilliant Blue R and toxicological evaluation of its degradation products". ***Journal of Molecular Catalysis B: Enzymatic***, Elsevier B.V., v. 89, p. 122–129, 2013.

SRINIVASAN, V.; AIKEN, R. C. "Parameter Estimation In Approximate Enzyme Kinetics Models". ***Mathematical Biosciences***, v. 69, p. 235–242, 1984.

STEEVENSZ, A.; CORDOVA VILLEGAS, L. G.; FENG, W.; TAYLOR, K. E.; BEWTRA, J. K.; BISWAS, N. "Soybean peroxidase for industrial wastewater treatment: a mini review". ***Journal of Environmental Engineering and Science***, v. 9, n. 3, p. 181–186, 2014.

STEEVENSZ, A.; MADUR, S.; AL-ANSARI, M. M.; TAYLOR, K. E.; BEWTRA, J. K.; BISWAS, N. "A simple lab-scale extraction of soybean hull peroxidase shows wide variation among cultivars". ***Industrial Crops and Products***, Elsevier B.V., v. 48, p. 13–18, 2013.

SVETOZAREVIć, M.; SEKULJICA, N.; ONJIA, A.; BARAć, N.; MIHAJLOVIć, M.; KNEžEVIć-JUGOVIć, Z.; MIJIN, D. "Biodegradation of synthetic dyes by free and cross-linked peroxidase in microfluidic reactor". ***Environmental Technology and Innovation***, v. 26, n. 102373, 2022.

SYRRIS. "**Asia Flow Chemistry System.**" Available in: <https://syrris.com/product/asia-flow-chemistry/>, Accessed in: 9 jun. 2022.

TAMURA, Y.; YAMAZAKI, I. "Reactions of the oxyform of horseradish peroxidase". ***Journal of Biochemistry***, v. 71, p. 311–319, 1972.

TCHOBANOGLOUS, G.; BURTON, F.; STENSEL, H. "***Wastewater Engineering: Treatment and Resource Recovery***". 5th. ed. [S.l.]: McGraw-Hill, 2014. 1856 p.

TIŠMA, M.; ZELIĆ, B.; VASIĆ-RAČKI, D.; ŽNIDARŠIČ-PLAZL, P.; PLAZL, I. "Modelling of laccase-catalyzed l-DOPA oxidation in a microreactor". ***Chemical Engineering Journal***, v. 149, n. 1-3, p. 383–388, 2009.

TOLARDO, V.; GARCÍA-BALLESTEROS, S.; SANTOS-JUANES, L.; VERCHER, R.; AMAT, A. M.; ARQUES, A.; LAURENTI, E. "Pentachlorophenol Removal from Water by Soybean Peroxidase and Iron(II) Salts Concerted Action". ***Water, Air, and Soil Pollution***, Water, Air, & Soil Pollution, v. 230, n. 6, 2019.

TORRES, E.; AYALA, M. "***Biocatalysis Based on Heme Peroxidases. Peroxidases as Potential Industrial Biocatalysts***". 1st. ed. [S.l.]: Springer, 2010. 371 p.

TUSEK, A.; TISMA, M.; BREGOVI, V.; PTICAR, A.; KURTANJEK, Z.; ZELIC, B. "Enhancement of phenolic compounds oxidation using laccase from trametes versicolor in a microreactor". ***Biotechnology and Bioprocess Engineering***, v. 18, p. 686–696, 2013.

VIANNA JR., A. dos S. "***Equações Diferenciais - Uma visão intuitiva usando exemplos***". [S.l.]: Blucher, 2021.

VOET, D.; VOET, J. "***Biochemistry***". 4th. ed. [S.l.]: Wiley and Sons, 2011. 1515 p.

WATANABE, C.; KASHIWADA, A.; MATSUDA, K.; YAMADA, K. "Soybean peroxidase-catalyzed treatment and removal of bpa and bisphenol derivatives from aqueous solutions". ***Environmental Progress and Sustainable Energy***, v. 30, n. 1, p. 81–91, 2011.

YAMADA, K.; IKEDA, N.; TAKANO, Y.; KASHIWADA, A.; MATSUDA, K.; HIRATA, M. "Determination of optimum process parameters for peroxidase-catalysed treatment of bisphenol A and application to the removal of bisphenol derivatives". ***Environmental Technology***, v. 31, n. 3, p. 243–256, 2010.

YAMAZAKI, I.; NAKAJIMA, R. "Physico-chemical comparison between horseradish peroxidases A and C". *In:* ***Molecular Physiological Aspects of Plant Peroxidases*** *by H. Greppin, C. Penel and T. Gaspar (eds)*, p. 71–84, 1986.

YOSHIDA, J.; NAGAKI, A.; IWASAKI, T.; SUGA, S. "Enhancement of chemical selectivity by microreactors". ***Chemical Engineering & Technology***, v. 28, 3, p. 259—266, 2005.

ZHANG, Y.; LIU, M.; LIU, J.; WANG, X.; WANG, C.; AI, W.; CHEN, S.; WANG, H. "Combined toxicity of triclosan, 2,4-dichlorophenol and 2,4,6-trichlorophenol to zebrafish (Danio rerio)". ***Environmental Toxicology and Pharmacology***, v. 57, p. 9–18, 2018.

ZHENG, W.; COLOSI, L. M. "Peroxidase-mediated removal of endocrine disrupting compound mixtures from water". ***Chemosphere***, v. 85, p. 553–557, 2011.

APPENDIX A - Publications

The research presented in this thesis has resulted in the following publications:

- COSTA, R. A.; CUNHA, A. S.; PERES, J. C. G.; AZZONI, A. R.; LAURENTI, E.; VIANNA, A. S. “Enzymatic degradation of 2,4,6-trichlorophenol in a microreactor using soybean peroxidase”. **Symmetry**, v. 12, n. 1129, 2020.
- CUNHA, A. S.; VIANNA, A. S.; LAURENTI, E. “Modeling and simulation of the enzymatic degradation of 2,4,6-trichlorophenol using soybean peroxidase”. **Brazilian Journal of Chemical Engineering**, v. 38, p. 719–730, 2021.